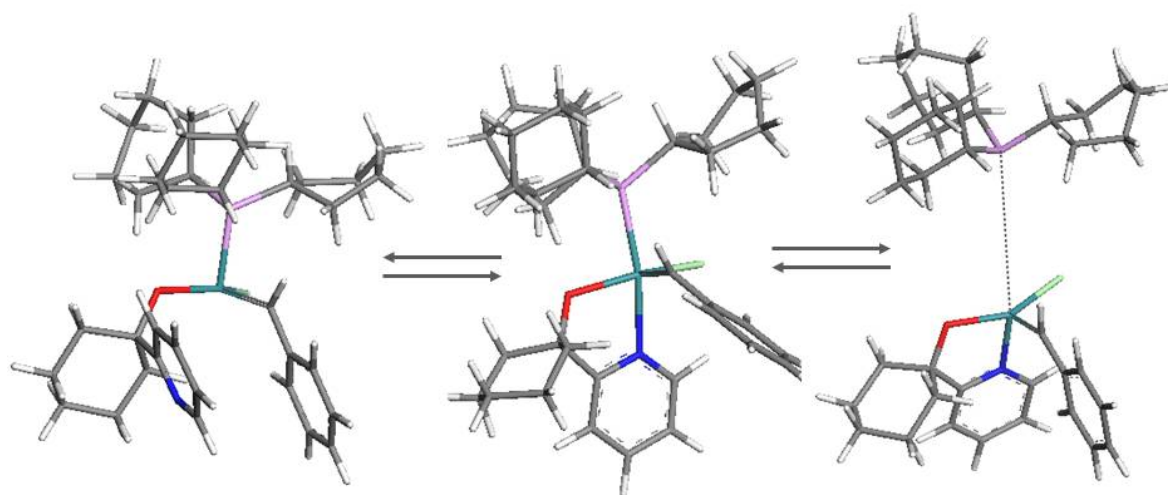


Modelling of Grubbs type precatalysts with bidentate hemilabile ligands



M.F. Raymakers
2012

Modelling of Grubbs type precatalysts with bidentate hemilabile ligands

Fatima Raymakers

BSc (WITS University), Hons Chemistry (UNISA)

Dissertation submitted in partial fulfillment of the requirements for the degree

Magister Scientiae

in

Chemistry

at the North-West University (Potchefstroom campus)

Supervisor: Dr CGCE van Sittert

Co-supervisor: Prof HCM Vosloo

Potchefstroom

November 2012

Acknowledgements

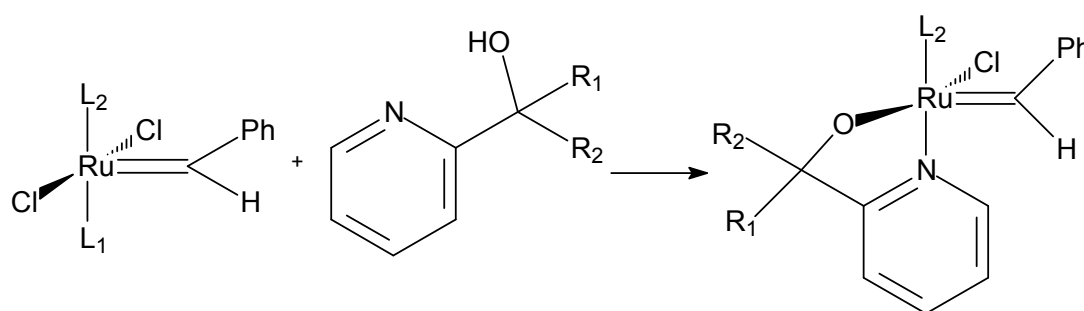
I hereby wish to thank the following people for their assistance and sacrifices during my studies:

- Prof Manie Vosloo for allowing me this opportunity to proceed with this study so far away from the Potchefstroom Campus.
- Dr Cornie van Sittert, my supervisor, for her guidance, friendship and understanding throughout this study.
- My children Nathan and Michaela for bearing with me when I was unable to perform my motherly duties.
- Marc Anthony James for his support and encouragement during the final stretch of this study.
- My colleagues at the School of Education, Vaal Triangle Campus, for offering a shoulder to cry on when I was frustrated with my progress through this study.
- The NRF for their financial support.
- Letsedit for their language editing of this document.

Summary

Keywords: *alkene metathesis, latent Grubbs type precatalysts, mechanism, DFT modelling, hemilabile ligands*

Metathesis is a valuable reaction for the production of new alkenes. In the last 50 years, heterogeneous as well as homogeneous catalysts have been used for this reaction. In the homogeneous category are the very successful catalysts designed by the Grubbs group. The first generation Grubbs precatalyst (Gr1) bearing two phosphine ligands was followed after extensive studies by the more active second generation Grubbs precatalyst (Gr2). In Gr2, one of the phosphine ligands is replaced with an N-heterocyclic carbene. Grubbs type precatalysts bearing pyridynyl-alcoholato chelating ligands are pertinent to this study.



$L_1 = \text{PCy}_3$

$L_2 = \text{PCy}_3$ (Grubbs 1) or NHC (Grubbs 2)

$R_1, R_2 = \text{H, alkyl, aryl}$

Scheme 1: The synthesis of Grubbs type precatalysts bearing a pyridynyl-alcoholato ligand.

In two previous studies, both supported by computational methods, Grubbs type precatalysts with N[^]O chelating ligands were synthesised. These investigations were motivated by the fact that chelating ligands bearing different donor atoms can display hemilability. The loosely bound donor atom can de-coordinate to make available a coordination site to an incoming substrate “on demand”, whilst occupying the site otherwise and hence preventing decomposition via open coordination sites. In the first investigation, the incorporation of an O,N-ligand with both R_1 and R_2 being

phenyl groups into the Gr2 precatalyst, resulted in an increase in activity, selectivity and lifetime of the precatalyst in comparison to Gr2 in the metathesis reaction with 1-octene. In the second study, three synthesised complexes were found to be active for the metathesis of 1-octene.

This computational study sought to better understand the structural differences and thermodynamic properties of these Grubbs type precatalysts with bidentate/hemilabile ligands. A large number of structures were constructed in Materials Studio by varying the R groups of the bidentate/hemilabile ligand attached to both the Gr1 and Gr2 catalysts. The majority of structures were Gr1-type complexes. For each ligand selected, a group of structures consisting of closed precatalyst, open precatalyst, and where applicable a precatalyst less PCy₃, closed metallacycle, open metallacycle and where applicable a metallacycle less PCy₃, was constructed and optimised using DMol³. Bond lengths, bond angles, HOMO and LUMO energies and Hirshfeld charges of structures were compared with one another. PES scans were performed on the metallacycles of four groups. The purpose of the PES scans was to ascertain whether these bidentate ligands were hemilabile and to illuminate the preferred reaction mechanism for these types of precatalysts.

The major finding of this study was that the possibility of an associative mechanism cannot be ruled out for some Gr2-type precatalysts with bidentate ligand. For some precatalysts, hemilability is energetically expensive and possibly not viable. No evidence of a concerted mechanism was found. The dissociative mechanism was found to be the preferred mechanism for most of the structures that were subjected to PES scans.

The HOMO-LUMO energies of a complex can be used, as a predictive tool, to assess the reactivity and stability of a complex, as well as its preference for substrates.

Table of Contents

Acknowledgements	i
Summary	ii
Table of contents	iv
List of abbreviations	vii
 Chapter 1: Introduction and project aims.....	1
1.1 Introduction	1
1.2 Project aims and objectives	8
1.3 References	9
 Chapter 2: Theoretical background of Alkene Metathesis	12
2.1 Introduction	12
2.2 Historical background	13
2.3 Development of the mechanistic pathway.....	13
2.4 Development of some catalytic systems	17
2.5 Factors affecting catalyst initiation and metathesis	21
2.5.1 Influence of Phosphine ligand on initiation of alkene metathesis	21
2.5.2 Influence of halide ligands on catalyst performance.....	22
2.5.3 Solvent effects on catalyst initiation.....	22
2.5.4 The influence that the type of substrate has on catalyst initiation	23
2.5.5 The influence of bidentate chelating ligands present in catalysts on metathesis	23
2.6 References	25
 Chapter 3: Theoretical background of molecular modeling	30
3.1 Introduction	30
3.2 Computable properties.....	31
3.2.1 Geometrical optimised structure.....	31
3.2.2 Energy.....	32
3.2.3 Potential Energy surfaces	33
3.2.4 HOMO/LUMO orbitals and energy	35

3.2.5	Hirshfeld charge Analysis	36
3.3	Computational chemistry of Grubbs type precatalysts	37
3.4	References	44
Chapter 4: Experimental.....		48
4.1	Introduction	48
4.2	Computational methods	51
4.2.1	Hardware.....	51
4.2.2	Software	52
4.3	Method.....	52
4.3.1	Validation of the model used	52
4.3.2	Construction of 'closed' precatalysts	53
4.3.3	Construction of 'open' precatalysts B	55
4.3.4	Construction of 16-electron metallacycles E	56
4.3.5	Construction of phosphine free precatalysts C.....	57
4.3.6	Metallacycles F constructed from the optimised phosphine free structures C	57
4.3.7	Construction of 18-electron metallacycles D	58
4.3.8	Comparing complexes.....	58
4.3.9	Performing PES scans for various reaction pathways.....	59
4.3.10	Confirming the orbitals involved in bonding between precatalyst and substrate	59
4.3.11	Obtaining HOMO-LUMO energy differences for precatalysts and substrates	63
4.3.12	Obtaining HOMO-LUMO gaps for precatalysts	63
4.3.13	Hirshfeld charge analysis	63
4.4	References	63
Chapter 5: Results and Discussion		65
5.1	Calculated properties	65
5.1.1	Bond length and energy calculations.....	65
5.1.2	Conformer searches.....	68
5.1.3	Hirshfeld charges	71
5.1.4	HOMO and LUMO energies	73

5.1.5	Investigation of reaction mechanisms	78
5.1.6	Agostic interactions	95
5.2	References	98
Chapter 6: Conclusions and Recommendations		100
6.1	Introduction	100
6.2	Computational study of Grubbs type precatalyst with hemilabile ligands	100
6.3	Recommendations	101
6.4	References	102
Appendices:		103

List of abbreviations

General abbreviations

ACM	:	Acyclic cross-metathesis
ADMET	:	Acyclic diene metathesis polymerisation
CM	:	Cross-metathesis
DFT	:	Density functional theory
E	:	Electronic energy
GB	:	Gigabyte
GGA	:	Generalised gradient application
HOMO	:	Highest occupied molecular orbital
IP	:	Isomerisation products
L	:	Ligand
LDA	:	Local density approximation
LUMO	:	Lowest unoccupied molecular orbital
M	:	Transition metal atom
NHC	:	N-heterocyclic carbene
NMR	:	Nuclear magnetic resonance
O [^] N	:	Bidentate ligand coordinated to a metal at O and N
PES	:	Potential energy surface
PMP	:	Primary metathesis products
R	:	Hydrogen, aryl or alkyl group
RAM	:	Random access memory
RCM	:	Ring-closing metathesis
ROM	:	Ring-opening metathesis
ROMP	:	Ring-opening metathesis polymerisation
SMP	:	Secondary metathesis products
X	:	Halogen atom
Ψ	:	Wave function

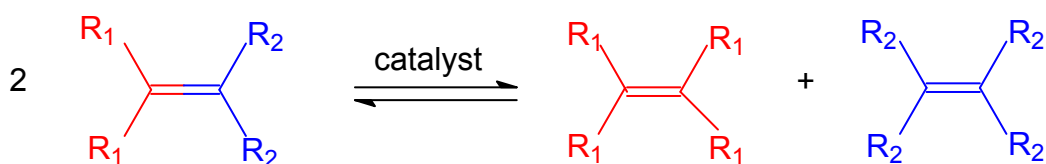
Abbreviations of chemicals

Ad	:	Adamantyl
Cy	:	Cyclohexyl
Et	:	Ethyl
Gr1	:	Grubbs first generation precatalyst
Gr2	:	Grubbs second generation precatalyst
H ₂ IMes	:	1,3-bis-(2,4,6 trimethylphenyl)-2-imidazolidinylidene
Me	:	Methyl
PCy ₃	:	Tricyclohexylphosphine
Ph	:	Phenyl
Py	:	Pyridine

CHAPTER 1: Introduction and project aims

1.1 Introduction

The word metathesis means to ‘change places’, and in chemistry it involves a double decomposition reaction, e.g. in the reaction, $AB + CD \rightarrow AC + BD$, B has changed position with C.¹ In organic chemistry, the alkene metathesis reaction (or olefin metathesis in some texts) involves the cleavage of carbon double bonds followed by a rearrangement of segments and formation of new double bonds to form products that differ from the starting materials.²



Scheme 1.1: The cleavage of double bonds, rearrangement of segments and the formation of new double bonds.²

Catalysts for this reaction can either be placed into the category of heterogeneous catalysts (in a different phase from the reagents) or homogeneous catalysts (in the same phase as the reagents).³ Some of the catalysts that have been employed for alkene metathesis are:

- 1. Heterogeneous catalysts** consisting of a high valent transition metal halide, oxide or oxohalide with an alkylating co-catalyst such as an alkyl zinc or alkyl aluminium. These catalyst systems are placed on an alumina or silica support. Classic examples include $WCl_6/SnMe_4$ and Re_2O_7/Al_2O_3 .^{2,4,5,6} These catalysts are considered “ill-defined” since the oxidation state of the metal and the nature of the ligands were never elucidated.⁷

Although these catalysts are active, they are short-lived and produce side products and do not tolerate functional groups.^{7,8}

2. Homogeneous catalysts

- i. **Fischer-type carbenes as catalysts.** The metal in this complex is in a low oxidation state and the carbene ligand doubly bonded to the metal centre bears a heteroatom (usually O or N).⁷ Although these are excellent metathesis catalysts, they are energetically less favourable.⁹ Reactions with alkenes can result in cyclopropanation.^{10,11} They can be used as a tool for heterocyclic synthesis.¹²
- ii. **Titanium-based catalysts** Example such as Tebbe's reagent $(C_5H_5)_2TiCH_2ClAl(CH_3)_2$. The active species, which is a titanocene methyldiene, is capable of reacting with more sterically hindered carbonyl groups to give alkenes.¹³
- iii. **Schrock tungsten¹⁴, molybdenum^{15,16} and rhenium¹⁷ precatalysts.** The most important of these are the arylimido complexes of molybdenum which have the general formula $(Ar'N)(RO)_2Mo=CHR$. These are exceedingly active. Although these catalysts have a high tolerance for functionality, they are air- and water-sensitive.^{2,18}
- iv. **Grubbs ruthenium precatalysts.** These catalysts are so tolerant of functionality that some of them can metathesize in water on the bench top! Such functional group tolerance comes at the expense of lower metathesis rates than the Schrock catalysts.¹⁹

The first catalysts found to promote alkene metathesis were of the heterogeneous type.^{4,5} The disadvantage of these heterogeneous catalysts is that only a small percentage of the material serves as an active catalyst, and very little is known about the nature of the actual catalytic species.² The catalyst developments by Fischer, Tebbe, Schrock and Grubbs not only broadened the range of precatalysts available for alkene metathesis but also contributed to a better understanding of the alkene metathesis mechanism, and motivated further improvements of these homogenous type catalysts.¹⁹

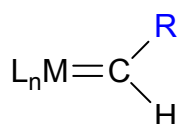
Although different types of catalysts are available, each with their own strength and weaknesses, no single ideal catalyst has been identified or synthesised to date. A catalyst which is,

- active and will produce a high turnover of the desired product,
- stable and not prone to decomposition so that it can be used repeatedly, i.e. high active lifetime,
- able to function in the air and in water,
- selective for a particular substrate,

may be considered ideal.

In the pursuit of such ideal catalysts, much research has been done and continues to be done to modify existing catalysts. Such research has been experimental or theoretical in nature and occasionally a combination of both. Different transition metals were used,^{5-6,14-17,19,20} and varying the ligands^{14,16,17,21-24} on the catalyst was another approach.

Since the first reported “metal carbene” complex in 1964 by Fischer and Maasböl,²⁵ many investigations brought about synthesis of more of these complexes also known as alkylidene complexes (Figure 1.1). These complexes possess a metal-carbon double bond.²⁶ These complexes were added to alkenes and began to be linked to the alkene metathesis reaction and its products.⁷



$\text{R} = \text{H}, \text{alkyl or aryl}$

Figure 1.1: Alkylidene complexes (M = metal atom, L = ligand).

Schrock began isolating alkylidene complexes in the early seventies.²⁷ The breakthrough in improved catalysts was made in the late 1980s by the Schrock group, who developed tungsten and molybdenum alkylidene complexes that contained bulky imido ligands.^{14,15} The alkoxide ligands (Figure 1.2) were introduced by the Schrock group in the mid-eighties, followed by the incorporation of the imido ligand in 1986.^{14,16}

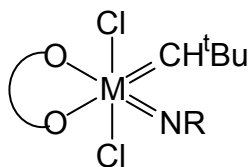
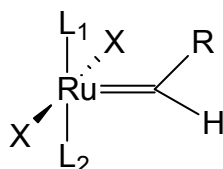


Figure 1.2: Alkylidene complex bearing alkoxide and an imido ligand.^{14,15}

The Grubbs group began with development of their ruthenium catalysts in the early 1990s.^{19,28,29} Their catalyst overcame many problems associated with polymerisation of dicyclopentadiene by heterogeneous catalysts such as intolerance of air, water and impurities.¹⁹ The key to the further improvement of their catalysts was extensive mechanistic studies³⁰ and inquiry into decomposition routes¹⁹ of the catalyst which suggested that ligand exchanges were necessary for catalyst improvement. The Grubbs group also took lessons from the Schrock group and Herrmann *et al.*³¹ to help with the identification of suitable ligands in order to enhance catalyst activity and improve catalyst lifetime. Although there are many variations of the Grubbs catalyst, the basic ligand array remains the same – two *trans* neutral ligands, two halogens and the alkylidene around a ruthenium centre.



R = H, alkyl or aryl

X = halogen

L = ligand

Figure 1.3: Basic structure of Grubbs type catalysts.

The most famous of the Grubbs catalysts are the first generation catalyst (Gr1) which have chlorine for the halogens, a phenyl ring for the alkylidene ligand and phosphorus atoms attached to three cyclohexyl groups for each of L₁ and L₂. The second generation catalyst (Gr2) differs only in that L₁ is an N-heterocyclic mesityl substituted ligand.

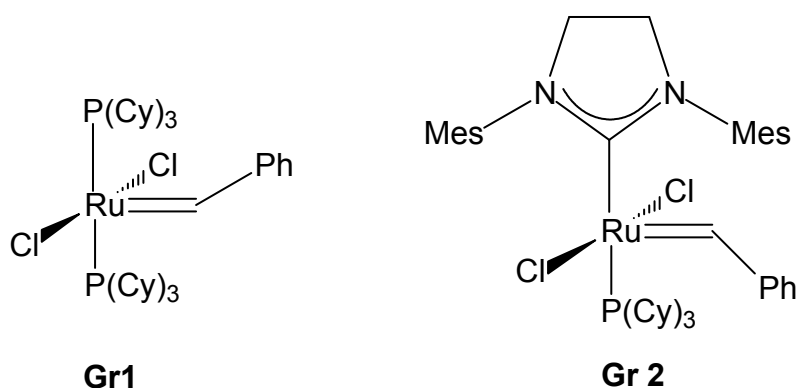
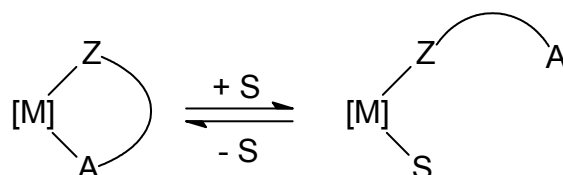


Figure 1.4: Grubbs first and second generation catalysts.

One of the attempts of the Grubbs group to improve on the stability of their catalysts involved the use of bidentate Schiff-base ligands which would simultaneously substitute one of the neutral phosphine and one of the anionic chloride ligands.³² During the metathesis reaction, the softly bound atom of the bidentate Schiff-base would de-coordinate, leaving a vacant site on the metal for coordination to an alkene substrate.³² This inspired Herrmann and co-workers to perform a ligand exchange using a bidentate hemilabile pyridinyl alcoholate ligand on the Grubbs catalyst.³³ This precatalyst exhibited increased activity at elevated temperatures during alkene metathesis.³³

A bidentate ligand has two locations at which lone pair electrons are present for coordination to a metal atom. Bidentate ligands can consist of significantly different chemical donor functions, such as hard and soft donor atoms or groups; these are termed hybrid ligands. The term ‘hemilabile’ ligand was first introduced by Rauchfuss *et al.*³⁴ while investigating phosphine-amine and phosphine-ether ligands. An essential feature of a hemilabile bidentate chelating ligand (Scheme 1.2)³⁵ is the presence of a labile portion of the ligand (A) which will de-coordinate while the tightly bound group (Z) keeps the ligand attached to the metal centre. The labile portion of the ligand (A) remains available for re-coordination. This occupation and releasing of a coordination site on the metal atom should be reversible and have relatively small energy differences between the ‘open’ and ‘closed’ situations.³⁶ The ‘open’ situation leaves an available site on the complex for external substrates to bind while the ‘closed’ situation can stabilise the metal centre by protecting a coordination site. These different functionalities can also result in different interactions with the metal

centre and influence the bonding/reactivity of other ligands bound to the metal.³⁶ This hemilability is believed to increase the thermal stability and activity of the catalytic systems by preventing decomposition via free coordination sites at room temperature.^{33,37}



S = substrate

Z = tightly bound group

A = labile group

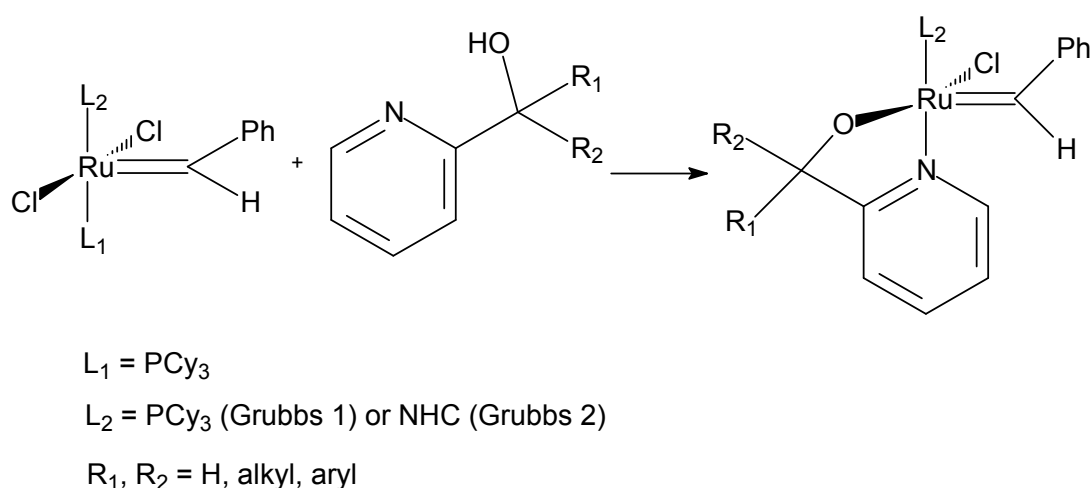
Scheme 1.2: A generalised depiction of a bidentate hemilabile ligand.³⁵

Since this concept was introduced, various combinations of different donors have been studied. Various transition metal complexes with hemilabile $P^{\wedge}N$ -³⁸⁻⁴⁰, $P^{\wedge}O$ -⁴¹⁻⁴⁶, $O^{\wedge}N$ -^{47,48}, and $S^{\wedge}O$ -ligands⁴³ have been synthesised, and a number of them applied to catalytic reactions. Excellent reviews have been published on this subject matter by Slone *et al.*³⁵, Lindner *et al.*³⁷ and Bader *et al.*⁵⁰ Jordaan⁵¹ synthesised various Grubbs type precatalysts with hemilabile bidentate ligands attached (Scheme 1.3) and tested their activity for 1-octene metathesis. The “PUK-Gr2 precatalyst” was the most successful ($R_1 = R_2 = Ph$). It showed an increase in lifetime, stability, activity and selectivity during the metathesis of 1-octene.⁵²

Jordaan also found that the R groups of the $N^{\wedge}O$ hemilabile ligand had a great influence on the activity and lifetime of the modified Grubbs precatalyst. Jordaan, however, could not conclude with certainty whether the precatalysts all displayed hemilability and only considered one type of reaction mechanism namely, the dissociative mechanism.

Huijsmans⁵³ then performed a study involving both computational methods and experiments by varying the R groups on the $N^{\wedge}O$ hemilabile ligand (Scheme 1.3) in an attempt to improve further on PUK-Gr2 precatalyst. After an initial screening of over two hundred ligands using computational methods, Huijsmans determined that

the ligands that were promising were those with two different R groups (Scheme 1.3). From the computational results, Huijsmans selected three ligands, which showed potential for effective ligand exchange with Gr2 to synthesise precatalysts, which had similar characteristics to that of PUK-Gr2. Huijsmans also selected two ligands, which had been identified as having poor potential for ligand exchange with Gr2 for synthesis. These predictions based on computational results were confirmed in all five cases. The three ligands identified as promising resulted in successful synthesis and isolation of bidentate/hemilabile precatalysts while the two ligands, identified as poor potential, did not result in successful synthesis. Isolation of these precatalysts proved to be difficult possibly due to decomposition of the precatalyst as a result of poor ligation.⁵³ The three precatalysts that were isolated were then tested for alkene metathesis activity. One synthesised complex showed a similar selectivity to PUK-Gr2 catalyst. All three complexes, which were successfully synthesised, showed much longer lifetimes and higher turnover numbers than PUK-Gr2. At elevated temperatures and increased catalyst loads, these three catalysts showed an increase in activity but simultaneously a decrease in selectivity. In Huijsmans' study, like that of Jordaan, the focus was on the performance of the catalysts in alkene metathesis.



Scheme 1.3: Grubbs type precatalysts undergoing ligand exchange with hemilabile pyridinyl alcoholate ligand.⁵²

Huijsmans did not extend her investigation to determine whether hemilability is a characteristic of these precatalysts containing bidentate ligands or whether more than one mechanism might be a possibility during metathesis. Although the predictions made by Huijsmans were based on qualitative data, the use of molecular modelling prior to experimentation proved to be a very powerful predictive tool.

The Catalysis and Synthesis Group at the North-West University became more confident in their use of computational chemistry to gain more insight into the Grubbs type precatalysts with bidentate ligands. However, it is important that the type of computational method selected is suitable for the system that is being scrutinised.

In a study involving molecular modelling, du Toit⁵⁴ undertook to determine which functional PW91, BP, or BLYP would be optimal for the study of alkene metathesis catalysts. The use of crystal data and statistical methods concluded that the PW91 functional combined with the DNP basis set currently in use by the Catalysis and Synthesis Group at the North-West University, is the best choice. This functional will be used for this study.

1.2 Project aims and objectives

The purpose of this study is to determine whether hemilability is displayed in all precatalysts bearing pyridinyl-alcoholate ligands and identifying distinguishing features of these bidentate ligands that could result in improved stability, selectivity, lifetime and activity. The dissociative and associative mechanisms will also be investigated, as well as the possibility of a concerted mechanism.

To reach the aim of this study the following objectives are stated:

1. The study will be limited to variations of the pyridinyl-alcoholate ligand as shown in Scheme 1.3.
2. This study will be theoretical in nature using computational methods to design, optimise and gain thermodynamic data on a variety of precatalysts and metallacycles, most of which will consist of theoretical bidentate ligands.

3. Large amounts of quantitative data will be analysed. Data will be scrutinised to identify any factors which could determine the stability, selectivity, lifetime and activity of these catalysts.
4. Energy calculations and PES scans will be used in order to determine whether these precatalysts are either always bidentate, always hemilabile, or whether it differs from precatalyst to precatalyst.
5. All possible intermediates and transition structures in both dissociative and associative mechanisms will be constructed and optimised for a few selected precatalysts. PES scans will be performed on a few selected precatalysts in order to determine whether any mechanism is preferred.

1.3 **References**

- [1] The Free Dictionary. 2010. Metathesis. [Web:]
<http://www.thefreedictionary.com/metathesis> [Date of access: 11/06/2010].
- [2] Toreki, R., 2003, Olefin metathesis. [Web:]
<http://www.ilpi.com/organomet/olmetathesis.html> [Date of access: 24/11/09].
- [3] Lewis, D.W., Designer Catalysts for clean Chemistry. [Web:]
http://www.postgraduate-courses.net/articles/clean_chemistry.htm [Date of access: 07/03/2008].
- [4] Banks, R. L., Bailey, G. C., *Ind., Eng. Chem. Prod. Res. Dev.*, 1964, **3**, 170.
- [5] Eleuterio, H. S., *J.Mol. Catal.*, 1991, **65**, 55.
- [6] Haines, R. L. and Leigh, G. J., *Chem. Soc. Rev.*, 1975, **4**, 155.
- [7] Schrock, R. R., and Hoveyda, A. H., *Angew. Chem. Int. Ed.*, 2003, **42**, 4592.
- [8] Tsuji, J., Hashiguchi, S., *Tetrahedron Lett.*, 1980, **21**, 2955.
- [9] Toreki, R., 2003, Olefin metathesis. [Web:]
<http://www.ilpi.com/organomet/carbene.html> [Date of access: 31/10/2012].
- [10] Casey, C. P., Tuinstra, H. E., and Saeman, M. C., *J. Am. Chem. Soc.*, 1976, **98**, 608.
- [11] Weinand, A., and Reissig, H., *Organometallics*, 1990, **9**, 3133.
- [12] Barluenga, J., *Pure Appl. Chem.*, 2002, **74**, 1317.
- [13] Hartley, R. C., Li, J., Main, C. A., and McKiernan, G. J., *Tetrahedron*, 2007, **63**, 4825.

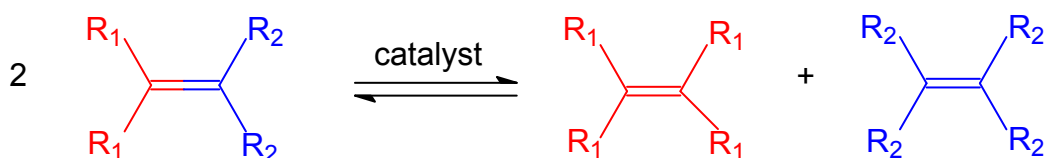
- [14] Schaverien, C.J., Dewan, J.C., Schrock, R.R., *J. Am. Chem. Soc.*, 1986, **108**, 2771.
- [15] Murdzek, J.S., Schrock, R.R., *Organometallics*, 1987, **6**, 1373.
- [16] Schrock, R.R., *J. Mol. Catal. A: Chem.*, 2004, **213**, 21.
- [17] Schrock, R.R., Toreki, R., Homogenous Rhenium Catalysts for Metathesis of Olefins. United States Patent US 5.146.033, 1992.
- [18] Schrock, R.R., *Tetrahedron*, 1999, **55**, 8141.
- [19] Grubbs, R.H., *Tetrahedron*, 2004, **60**, 7117.
- [20] Schrock, R.R., *Acc. Chem. Res.*, 1979, **12**, 98.
- [21] Schrock, R.R., DePue, J.F., Schaverien, C.J., Dewan, J.C., and Liu, A.H., *J. Am. Chem. Soc.*, 1988, **110**, 1423.
- [22] Wallace, K. C., Liu, A. H., Dewan, J. C. and Schrock, R. R., *J. Am. Chem. Soc.*, 1988, **110**, 4964.
- [23] Wu, Z., Nguyen, S. T., Grubbs, R. H. and Ziller, J. W., *J. Am. Chem. Soc.*, 1995, **117**, 5503.
- [24] Nguyen, S. T., R. H. Grubbs, *J. Am. Chem. Soc.*, 1993, **115**, 9858.
- [25] Fischer, E. O., and Maasböl, A., *Angew. Chem.*, 1964, **76**, 645.
- [26] Toreki, R., 2003, Alkylidene Complexes. [Web:] <http://www.ilpi.com/organomet/alkylidene.html> [Date of access: 12/06/2010].
- [27] Schrock, R.R., *J. Am. Chem. Soc.*, 1974, **96**, 6797.
- [28] Trnka, T. M., and Grubbs, R. H. *Acc. Chem. Res.* 2001, **34**, 18.
- [29] Nguyen, S. T., Johnson, L. K., Grubbs, R. H., Ziller, J. W., *J. Am. Chem. Soc.*, 1992, **114**, 3974.
- [30] Dias, E. L., Nguyen, S. T., and Grubbs, R. H., *J. Am. Chem. Soc.*, 1997, **119**, 3887.
- [31] Weskamp, T., Schattenmann, W. C., Spiegler, M., Herrmann, W. A. *Angew. Chem., Int. Ed. Engl.* 1998, **37**, 2490.
- [32] Chang, S., Jones, L., Wang, C., Henling, L.M., Grubbs, R.H., *Organometallics*, 1998, **17**, 3460.
- [33] Denk, K., Fridgen, J., Herrmann, W.A., *Adv. Synth. Catal.*, 2002, **344**, 666.
- [34] Jeffrey, J. C., and Rauchfuss, T., *Inorganic Chemistry*, 1975, **14**, 652.
- [35] Slone, C. S., Weinberger, D. A., and Mirkin, C. A., *Progr. Inorg. Chem.*, 1999, **48**, 233.
- [36] Braunstein, P., and Naud, F., *Angew. Chem.*, 2001, **40**, 680.

- [37] Lindner, E., *Coord. Chem. Rev.*, 1996, **155**, 145.
- [38] Dekker, G.P.C.M., Buijs, A., Elsevier, C. J., and Vrieze, K., *Organometallics*, 1992, **11**, 1937.
- [39] Rulke, R. E., Kaasjager, V. E., Wehman, P., Elsevier, C. J., van Leeuwen, P.W.N.M., and Vrieze, K., *Organometallics*, 1996, **15**, 3022.
- [40] Costella, L., Del Zotto, A., Mezzetti, A., Zangrando, E., and Rigo, P., *J. Chem. Soc. Dalton Trans.*, 1993, 3001.
- [41] Le Gall, I., Laurent, P., Soulier, E., Sasaün, J., and des Abbayes, H., *J. Organomet. Chem.*, 1998, **567**, 13.
- [42] Britovsek, G. J. P., Cavell, K. J., and Keim, W., *J. Mol. Catal. A: Chem.*, 1996, **110**, 77.
- [43] Lindner, E., Wald, J., Eichele, K., and Fawzi, R., *J. Organomet. Chem.*, 2000, **601**, 220.
- [44] Rogers, C. W., and Wolf, M. O., *Chem. Commun.*, 1999, 2297.
- [45] Valls, E., Suades, J., and Mathieu, R., *Organometallics*, 1999, **18**, 5475.
- [46] Lindner, E., Haustein, M., Herrmann, A. M., Gierling, K., Fawzi, R., and Steinmann, M., *Organometallics*, 1995, **14**, 2246.
- [47] Desjardins, S. Y., Cavell, K. J., Jin, W., Skelton, B. W., and White, A. H., *J. Organomet. Chem.*, 1996, **515**, 233.
- [48] Hoare, J. L., Cavell, K. J., Skelton, B. W., and White, A. H., *J. Chem. Soc., Dalton Trans.*, 1996, 2197.
- [49] Meyer, W. H., Brull, R., Raubenheimer, H. G., Thompson, C., and Kruger, G. J., *J. Organomet. Chem.*, 1998, **553**, 83.
- [50] Bader, A., and Lindner, E., *Coord. Chem. Rev.*, 1991, **108**, 27.
- [51] Jordaan, M., ***Experimental and Theoretical investigation of New Grubbs type Catalysts for the metathesis of Alkenes***, PhD-thesis (North-West University), 2007.
- [52] Jordaan, M., and Vosloo, H.C.M., *Adv. Synth. Catal.*, 2007, **349**, 184.
- [53] Huijsmans, C.A.A., ***Modelling and Synthesis of Grubbs type complexes with hemilabile ligands***, MSc-dissertation (North-West University), 2009.
- [54] du Toit, J. I., ***'n Modelleringsondersoek na die meganisme van die homogene alkeenmetatesereaksie***, MSc-dissertation (North-West University), 2009.

CHAPTER 2: Theoretical background of Alkene Metathesis

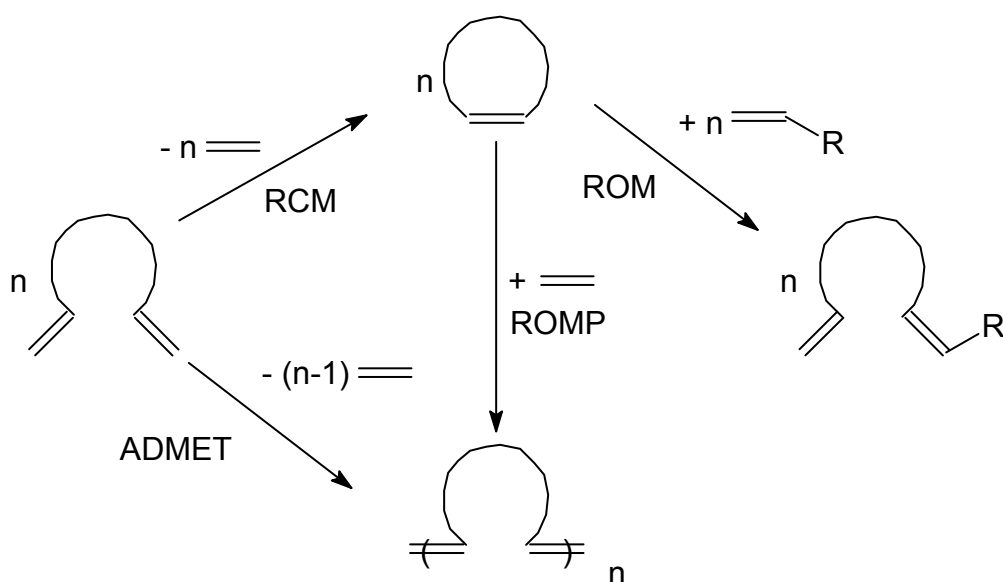
2.1 Introduction

The word metathesis in chemistry entails a double decomposition reaction as is represented in Scheme 2.1.¹



Scheme 2.1: The cleavage of double bonds, rearrangement of segments and formation of new double bonds.²

Apart from the acyclic cross-metathesis (ACM) or cross-metathesis (CM) reactions given in Scheme 2.1, a variety of other types of alkene metathesis reactions exist; examples being ring-closing and ring-opening (RCM/ROM) metathesis, ring-opening metathesis polymerisation (ROMP), and acyclic diene metathesis polymerisation (ADMET).³



Scheme 2.2: Types of alkene metathesis reactions.³

2.2 Historical background

It was Calderon who coined the phrase 'olefin metathesis' in 1967 for this type of reaction⁴, but the non-catalytic reaction was first encountered in 1931, in the form of propene metathesis at high temperature producing butylene and ethylene as products.⁵

The first catalysed metathesis reactions were carried out in the 1950s by industrial chemists. At Du Pont, Eleuterio,⁶ using propylene feed passed over a molybdenum-on-aluminum catalyst, observed a mixture of propylene, ethylene and 1-butene. Chemists at various petrochemical industries were getting the same results. Banks and Bailey presented what they believed to be "A New Catalytic Process" (1964), the 'disproportionation' of linear alkenes by molybdena-alumina catalyst.⁷ The chemists at Du Pont,⁶ and Truett *et al.* (1960)⁸ independently reported the first polymerisation of norbornene. Natta polymerized cyclic alkenes using homogenous catalysts [e.g. tungsten (VI) chloride-triethylaluminium].⁹ In 1967, researchers at the Goodyear Tyre and Rubber company, Calderon and co-workers, used $[\text{WCl}_6]\text{-EtOH-EtAlCl}_2$ as a catalyst mixture, and were the first to recognise that alkene metathesis involves transalkylidenation.⁴ The connection between these reactions was not made initially because different catalysts and conditions were involved.¹⁰

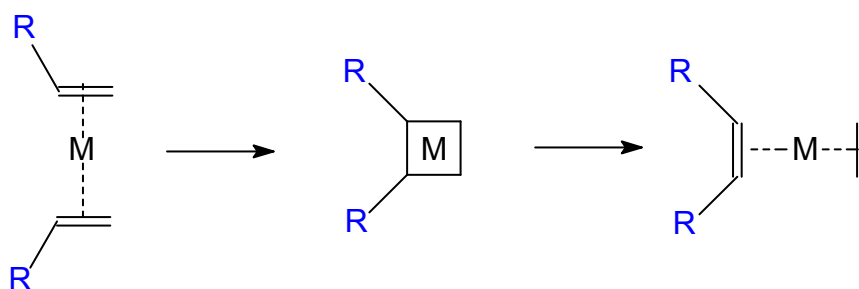
The discovery that heterogeneous and homogenous catalysts could promote the reaction at much lower temperatures with minimum side reactions, unlocked the potential of alkene metathesis.

2.3 Development of the mechanistic pathway

This extraordinary reaction, in which double bonds were cleaved, and segments put back together again, took chemists by surprise.¹⁰ A better understanding of the mechanism was necessary for the development of better catalysts.¹¹

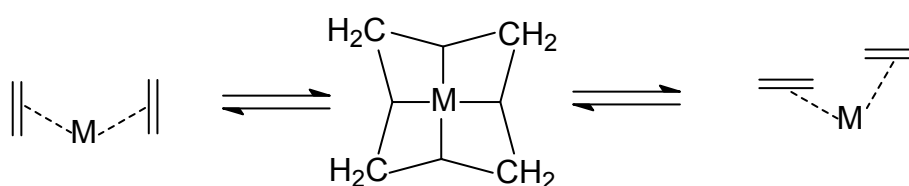
The first proposals were termed pairwise mechanisms in which the metal atom lies in the centre of a four membered carbon ring. Calderon *et al.*⁴ had shown that alkene metathesis involved a transalkylidenation process in which the reaction proceeds via scission of the double bond and redistribution of alkylidene moieties¹² and were in

agreement with the “quasicyclobutane” intermediate proposed by Bradshaw and co-workers.¹³



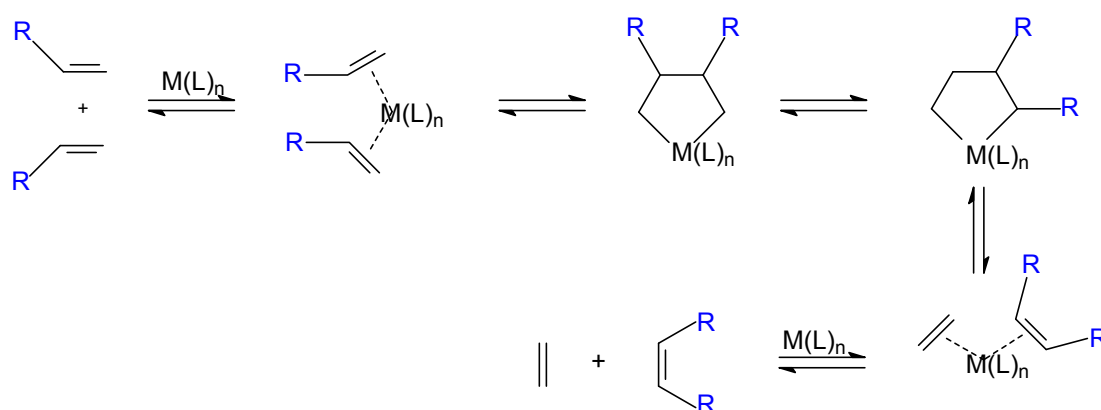
Scheme 2.3: Mechanism with proposed ‘quasicyclobutane’ intermediate.¹³

Since these mechanisms were symmetry forbidden by the Woodward-Hoffmann rules, Petit (1971) proposed a tetramethylene complex to account for the role played by the metal atom.¹⁴



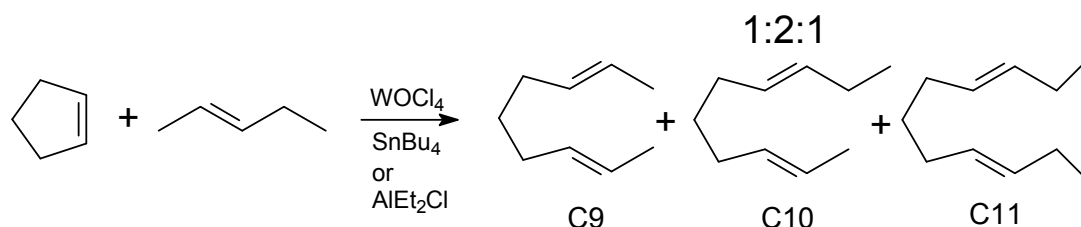
Scheme 2.4: Mechanism with proposed tetramethylene complex.¹⁴

Based on evidence for the presence of a carbon-metal sigma bond, Grubbs followed with a suggestion for a metallocyclopentane intermediate.¹⁵



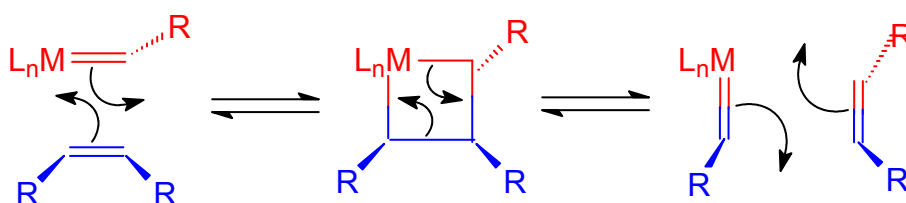
Scheme 2.5: Mechanism with metallocyclopentane intermediate.¹⁵

The proposal by Chauvin in 1971 for a 4-membered metallacycle, was intended to support the observation of the statistical distribution (1:2:1) of products during cross-metathesis experiments.¹⁷



Scheme 2.6: Chauvin's cross-metathesis experiment.¹⁷

Chauvin's mechanism suggested the presence of a transition metal alkylidene complex (metal carbene species) which after a [2+2] cycloaddition, formed a metallacyclobutane intermediate followed by a [2+2] cycloreversion to form products.¹⁸ This was a non-pairwise mechanism since the metal atom forms part of the four-member ring.



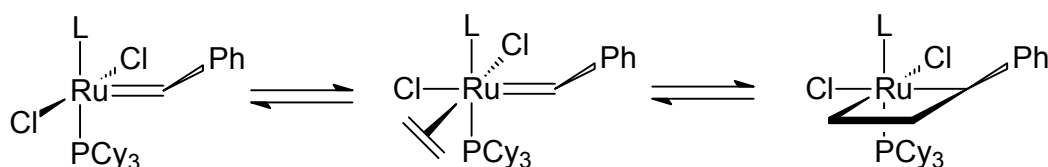
Scheme 2.7: The mechanism proposed by Chauvin involving a metallocyclobutane intermediate.¹⁸

By 1975, enough evidence supported the mechanism of Chauvin and the pairwise mechanisms had been disregarded.^{19,20,21,22} Presently, this mechanism with a metal carbene species is generally accepted as the mechanism for alkene metathesis.

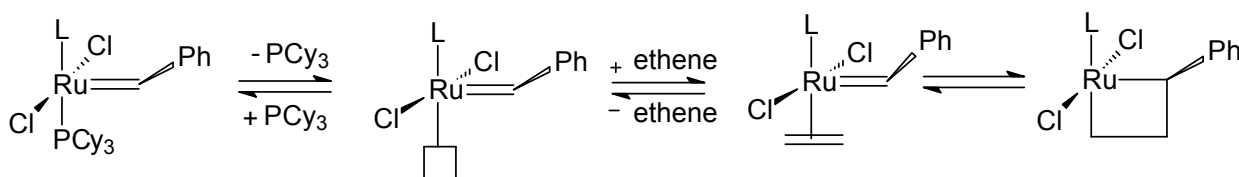
While research was conducted on the metathesis mechanism, progress was also made in the development and isolation of alkylidenes complexes, which contributed more evidence for Chauvin's mechanism.¹¹ (§ 2.4) For example, in a study involving Tebbe complexes, a stable metallacycle was formed whose structure could be determined.²³

In the mid '80s, research that led to the development of ruthenium-based catalysts for alkene metathesis was initiated. In order to maximise the potential of these ruthenium-based catalysts, an understanding of the reaction pathway for catalysis was essential. Detailed studies of the mechanism of metathesis using ruthenium catalysts were, therefore, undertaken and greatly contributed to improvements in ruthenium-based catalysts.¹¹

Initial investigations into the alkene metathesis mechanism with ruthenium carbenes established that the pathway involved substitution of a phosphine from the ruthenium complex for an alkene.²⁴ Whether alkene binding occurred prior to phosphine loss (associative mechanism, Scheme 2.8) or phosphine dissociation preceded alkene coordination (dissociative mechanism, Scheme 2.9) needed to be clarified.²⁵



Scheme 2.8: The associative pathway.



Scheme 2.9: The dissociative pathway.

With time and research, results from multi-technique experiments of Grubbs and co-workers,^{25,26} and Jordaan *et al.*,²⁷ provided evidence to support the dissociative pathway for the Grubbs type precatalysts.^{26,27} Theoretical studies supported the experimental findings.^{28,29}

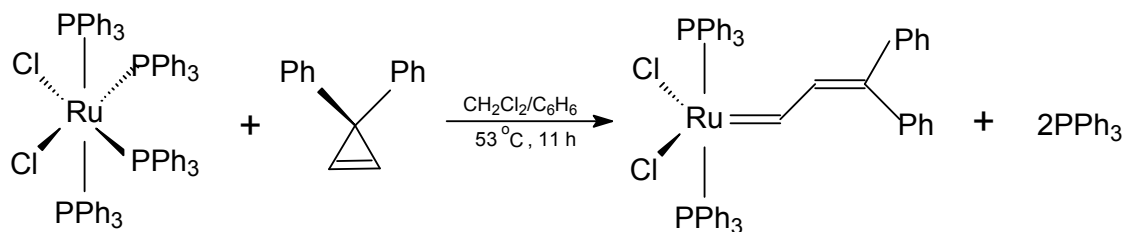
2.4 Development of some catalytic systems

Chauvin's proposal for the mechanism of alkene metathesis in the early 1970s greatly influenced catalyst design.

Before 1970, alkene metathesis was carried out with poorly defined, multi-component homogenous and heterogenous catalyst systems, as can be seen in the work at Du Pont in the mid-1950s⁶ to the early 1980s.³ These systems were comprised of transition metal salts in combination with the main group alkylating agents or various refractory materials, such as alumina or silica, serving as supports.^{3,30} The function of the different components could not be clearly defined.³⁰ The utilisation of these catalysts were limiting due to difficulties with initiation, reaction control and conditions comprising harsh Lewis acids.^{3,30}

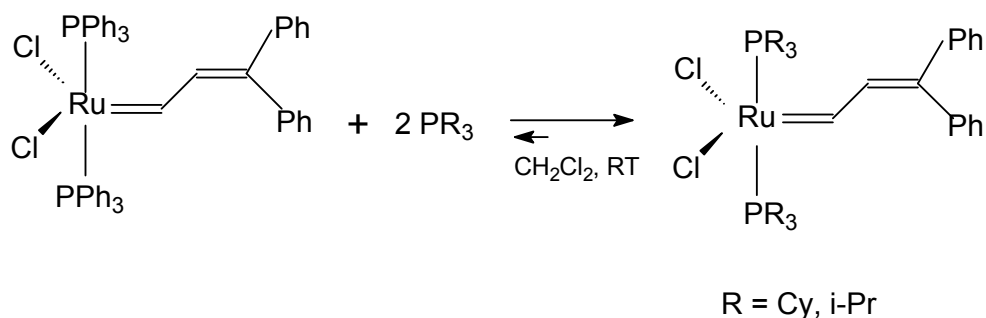
In the early 1970s, after Chauvin's proposal for the mechanism of alkene metathesis, efforts were made to synthesise alkylidene and metallacyclobutane complexes, which led to the discovery of the first single-component homogenous catalysts during the late 1970s and early 1980s.^{31,32,33,34} These catalysts based on the early transition metals provided better initiation and higher activity under milder conditions, but improvements were still necessary. Because of the high oxophilicity of the metal centres, these catalysts suffered extreme sensitivity to oxygen and moisture. In addition, these early metal catalysts were intolerant to functional groups.³

It wasn't till the mid-80s that the development of ruthenium-based catalysts began, when Novak and Grubbs found that ruthenium trichloride polymerized alkenes and would even generate high molecular weight polymers in water.³⁵ Relying on the experience of Johnston with tungsten carbenes,³⁶ Nguyen reacted a ruthenium(II) complex with diphenylcyclopropene.³⁷ This reaction produced a stable 16 electron ruthenium carbene complex. The resulting complex was active towards the polymerisation of norbornene, and in addition, showed stability in the presence of protic solvents.³⁷ These changes led to the first well-defined ruthenium catalyst.



Scheme 2.10: Formation of the first well-defined ruthenium catalyst.³⁷

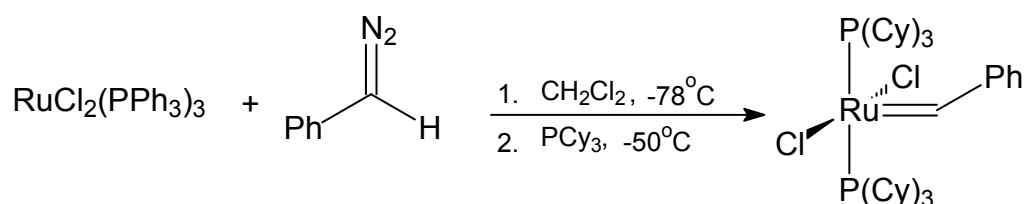
The bis(triphenylphosphine) complex was a good catalyst for the ROMP of highly strained cyclic alkenes but inefficient for the ROMP of low-strain cyclic alkenes and acyclic alkenes.^{3,11} Taking lessons from the Schrock group³⁸, Nguyen replaced the Cl with a variety of electron-withdrawing groups in an attempt to make the metal center more electrophilic but did not obtain the desired metathesis activity.³⁹ The desired activity was only obtained upon substitution of the triphenylphosphine ligands with better σ -donating alkylphosphines which produced the first metathesis of an acyclic alkene by a well-defined ruthenium carbene complex. The influence of phosphine ligands on the activity of the Grubbs type catalysts will be discussed further in section 2.5.1.



Scheme 2.11: Improvement of the ruthenium catalyst by variation of ancillary ligands.⁴⁰

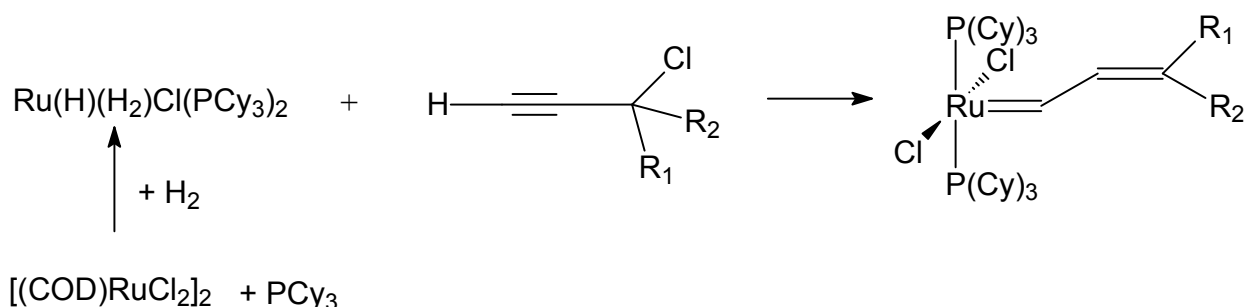
Not only could these ruthenium carbene complexes promote many of the same reactions as the Schrock molybdenum-based alkylidene complexes, but they also showed better functional group tolerance than the Schrock catalysts.⁴¹ In addition, the ruthenium catalysts could be handled in air as solids and reactions performed in standard flasks under nitrogen atmosphere.³

The availability of these complexes was limited by the difficulty of synthesising diphenylcyclopropene. An alternative route for the synthesis of ruthenium complexes was developed by Schwab *et al.*⁴², which involved the reaction of $\text{RuCl}_2(\text{PPh}_3)_3$ with alkyl- or aryldiazoalkane compounds. The result was the preparation of the highly active ruthenium benzylidene complex known as the first generation Grubbs catalyst (Gr1).⁴³



Scheme 2.12: Alternative route for production of the first generation Grubbs catalyst (Gr1).⁴³

However, this route relied on unstable phenyl diazomethane, which is unsuitable for large-scale applications. To meet the demand for these catalysts commercially a better route for synthesis was needed. Amongst several synthetic routes,⁴⁴⁻⁴⁷ the method of choice, initially, was a one-pot procedure developed on the basis of the insertion of alkynes into ruthenium-hydride bonds.⁴⁸ It begins with readily available starting materials and proceeds in high yields.³ This method results in the 3,3-disubstituted vinylcarbene complex which is known to have activity in alkene metathesis.⁴⁸



Scheme 2.13: One-pot procedure to give metathesis-active ruthenium carbenes.^{11, 48}

As the ruthenium catalyst shown in Scheme 2.13 became commercially available, the application of alkene metathesis became widespread, from the synthesis of

pharmaceuticals to polymers.¹¹ Even though, metathesis could be applied successfully in the presence of functional groups, limitations existed. The reacting alkenes needed to be relatively isolated and electronically insulated from functionality. Poor yields were obtained for metathesis reactions of directly (α)-functionalized alkenes, including both electron-rich (enol ethers) and electron-poor (α , β -unsaturated carbonyl) functionality. Sterically, the catalyst was also quite sensitive to the bulk on the alkene substrates.⁴³

The Grubbs group undertook detailed studies of the mechanism of metathesis⁴⁷ as well as the activation pathways of ruthenium alkylidene complexes.²⁴ This led to the realisation that changes in the ligand system were required for the next breakthrough.³ Extensive studies were done on ligand (L) variation^{49,50,51} of the basic (L)(L')X₂Ru=CHR complexes as well as substituents on the functional alkylidene ligand (R)⁵² and the halogen (X).⁴⁹ The most important finding was that the reaction was initiated by the loss of one of the neutral ligands (L) to produce a 14 e⁻ species (Scheme 2.9). Less bulky basic phosphines slowed down the initiation because they coordinated too strongly while phosphines with a larger cone angle than cyclohexylphosphine were too labile to produce a stable complex. It was also hypothesised that the more basic phosphine played a role in the stabilisation of the intermediate metallacycle. The Grubbs group concluded that catalyst activity could be increased by combining a strong donor ligand which would remain coordinated together with a labile ligand (weak donor).³ It was at this point that the Grubbs group became interested in the potential of N-heterocyclic carbenes (NHC).

Herrmann and co-workers had successfully substituted both phosphines in Gr1 with alkyl-substituted NHC's and had demonstrated that they were capable of ROMP and RCM reactions.⁵³ N-heterocyclic carbene ligands are stronger σ donors and much less labile³ thus resulting in catalysts that were less active. This drawback was overcome with the combination of the strongly donating NHC with the labile phosphine creating a complex superior to the alkoxy imido molybdenum complex and the previous Gr1 catalyst.⁵⁴ This new complex represented the "next generation" Grubbs alkene metathesis catalyst (Gr2).³

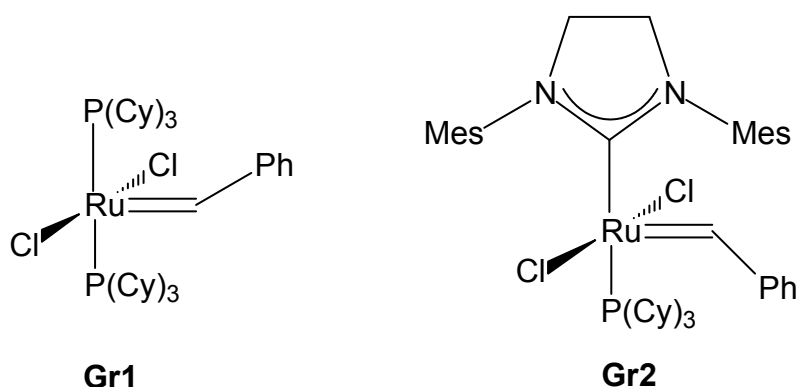


Figure 2.1: The first generation (Gr1) and second generation (Gr2) Grubbs catalysts.

Since ligand variation has had such a remarkable influence on catalyst performance, it was of importance, to study all factors which could improve catalyst function.

2.5 Factors affecting catalyst initiation and metathesis

The understanding of the factors that influence catalyst initiation and alkene metathesis is vital to ligand-design strategies for new catalysts.⁵⁵ In order to design new and improved catalysts, we need to have as much information about the catalyst initiation and metathesis steps as possible.

2.5.1 Influence of Phosphine ligand on initiation of alkene metathesis

The type of phosphine ligand plays an important role in metathesis activity of Gr1 catalysts. Results from experimental investigations suggested that electronic factors were more important than steric effects. The d^6 Ru^{II} metal center requires electron-rich ancillary ligands.⁴⁰ Larger and more electron-donating phosphines produced more active catalysts.⁴⁹ Bulkier phosphines favour phosphine dissociation as a result of less steric crowding around the ruthenium centre. Simultaneously, the greater *trans* influence of more electron donating phosphines favours phosphine dissociation by stabilising the mono-phosphine alkene complex, as well as the electron deficient metallacyclobutane.^{40,56} The substitution of one of the phosphine ligands and chlorine in Gr1 with a chelating ligand will no doubt have a significant effect on the electron distribution around the ruthenium centre and hence the initiation, activity and lifetime of the precatalyst. The question that arises from the addition of chelating ligands is; will phosphine dissociation be easier or will it be hampered? It is also

necessary to determine whether initiation by phosphine dissociation for the Gr1-type catalysts with hemilabile ligands will be in competition with de-coordination of the soft donor atom.

The substitution of one of the phosphine ligands for the IMes ligand in the bis phosphine complex resulted in a huge increase, in the metathesis activity. Although dissociation of the phosphine ligand (and hence, initiation) was slower for Gr2, coordination of the alkene was more facile than for the Gr1 catalyst. Even though both PCy₃ and IMes are large ligands, the distribution of steric bulk is different. NHC ligands are electronically more flexible. They can contribute to stabilising electron rich metals through a $d \rightarrow \pi^*$ back-donation scheme, but they can also stabilize electron deficient metals through a $\pi \rightarrow d$ donation scheme.⁵⁷ It was also determined, experimentally, that the metal centre became more positively charged with NHC ligation.⁵⁸ Replacing the phosphine ligand and a chlorine of Gr2 with a chelating ligand can have an effect on the initiation, lifetime and activity of the precatalyst, as was determined by Jordaan.⁵⁹ Understanding why this is so can help to improve further on this type of precatalyst.

2.5.2 Influence of Halide Ligands on catalyst performance

Studies showed that exchanging chloride ligands for bromide ligands resulted in a decrease in initiation of the alkene metathesis reaction while exchanging with iodide ligands results in an increase in initiation but not an increase in metathesis activity. These differences have been attributed to differences in steric bulk around the ruthenium centre as well as electronic effects.²⁵

Since one of the chloride ligands of the Grubbs catalyst can be replaced with a different atom of a chelating ligand, this should create differences in the electronic environment of ruthenium and changes in the steric bulk. Such changes should affect initiation rates.

2.5.3 Solvent affects on catalyst initiation

It is hypothesised that solvents can play a role in the stabilisation of the electron-deficient intermediate species that are formed after dissociation of a phosphine ligand. In addition, the solvent can stabilise the free phosphine or perhaps trap it and

prevent it from re-coordinating to the intermediate species.²⁵ The type of solvent selected could also determine whether a hemilabile ligand attached to a precatalyst would de-coordinate to produce an open site.⁶⁰ The effect of different solvents on the metathesis reaction with Grubbs type catalysts having hemilabile ligands will not be investigated in this study since solvents were not used in the experimental studies done by Jordaan⁵⁹ with these precatalysts.

2.5.4 The influence that the type of substrate has on catalyst initiation

Chen and co-workers²⁹ investigated Gr1 and Gr2 computationally and found that changing the substrate did not change the reaction pathway for alkene metathesis but only the energy profiles reflecting intermediates, transition states and rate limiting steps of the reaction. The substrate used in this study was propene, but this was not expected to have an influence on the reaction pathways followed by the different precatalysts. The effect of different substrates on the metathesis reaction with Grubbs type catalysts having hemilabile ligands will not be investigated.

2.5.5 The influence of bidentate chelating ligands present in catalysts on metathesis

In the field of polymer chemistry, well-defined single-component homogenous catalysts had become powerful tools. It was believed that polymerisation was initiated by the dissociation of the ligand (e.g. L^2)^{25,49} A need existed for initiators that could be triggered into action by a certain event. Stimuli for the initiation can be irradiation with UV or visible light, treatment with acid, or heat. Most work in this area had been done on thermally switchable initiators⁶¹⁻⁶⁵ following different design concepts (Figure 2.2).⁶⁶

It was hypothesised that the dissociation of L^2 at room temperature had to be minimised. To date, an inert ligand that can take the position of L^2 in motif A has not been accomplished, while motifs B and C take advantage of the chelate effect. Motif D represents Fischer carbenes, where X is O or S, for example. Motif B is based on the Hoveyda-type catalysts^{67,68} where L^2 is attached to the carbene. Motif B and D initiate slowly but propagate faster than motif C.⁶⁶

Grubbs,⁶⁹ Verpoort⁷⁰ and Herrmann⁷¹ utilised motif C using different approaches. Bidentate Schiff base ligands were studied by Grubbs⁶⁹ and later Verpoort⁷⁰ while Herrmann *et al.*⁷¹ combined chelating pyridinyl-alcoholato ligands with an N-heterocyclic carbene ligand. All studies reported reasonable ROMP activity of norbornene and cyclooctene at elevated temperatures.

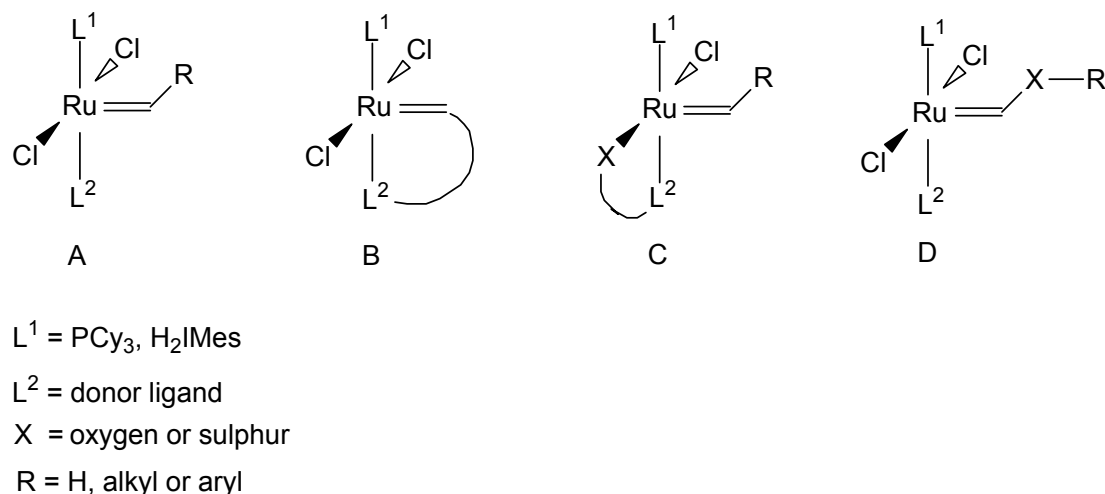
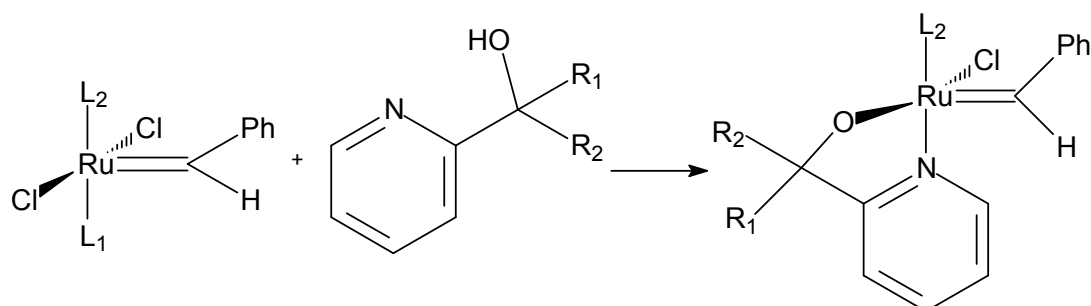


Figure 2.2: Design concepts for thermally switchable initiators.⁶⁶

The Catalysis and Synthesis group of the North-West University conducted a series of studies based on motif C using the pyridinyl-alcoholato ligands and Grubbs 1 and 2 precatalysts. Since the Gr1-type systems with chelating pyridinyl-alcoholato ligand had not been tested for catalytic activity in any metathesis reaction by Herrmann *et al.*⁷¹ Jordaan^{59,72} and Huijsmans⁷³ investigated the metathesis of 1-octene in the presence of the Gr1 and Gr2 precatalysts with a variety of chelating pyridinyl-alcoholato ligands, both experimentally and theoretically. Compared to Gr1, an increase in the primary metathesis product (PMP) formation resulted from the incorporation of the hemilabile ligands, together with a decrease in isomerisation products (IP) (observed at 60°C, 1-octene/Ru=9000, no solvent).^{83,84} Compared to Gr2, not all complexes with the chelating ligand resulted in an increase, in PMP.^{59,73} For both Gr1 and Gr2 complexes with chelating ligands, an increase in the lifetime of the catalysts was observed^{59,72,73} (Scheme 2.15). This group also found that by incorporating the chelating pyridinyl alcoholato ligand into the Gr1 and Gr2-type

precatalysts, the thermal stability, selectivity, and activity of these precatalysts had been improved.⁵⁹



$L_1 = \text{PCy}_3$

$L_2 = \text{PCy}_3$ (Grubbs 1) or NHC (Grubbs 2)

$R_1, R_2 = \text{H, alkyl, aryl}$

Scheme 2.15: The formation of Grubbs type precatalyst with bidentate hemilabile ligand.⁵⁹

Important to these chelating bidentate pyridinyl-alcoholato ligands is the possibility that they can display hemilability.^{59,72} Evidence for hemilability and a dissociative mechanism was obtained for the Gr2-type precatalyst with chelating pyridinyl alcoholato ligand, but the evidence was not conclusive for the Gr1-type catalyst with the bidentate ligand.^{59,72} This will be discussed further in Chapter 3.

2.6 References

- [1] The Free Dictionary. 2010. Metathesis. [Web:] <http://www.thefreedictionary.com/metathesis> [Date of access: 11/06/2010].
- [2] Toreki, R., 2003, Olefin metathesis. [Web:] <http://www.ilpi.com/organomet/olmetathesis.html> [Date of access: 24/11/2009].
- [3] Trnka, T. M., and Grubbs, R. H. *Acc. Chem. Res.* 2001, **34**, 18.
- [4] Calderon, N., *Tetrahedron Lett.*, **1967**, *34*, 3327.
- [5] Schneider, V., and Frolich, F., *Ind. Eng. Chem.*, **1931**, 1405.
- [6] Eleuterio, H. S., *J. Mol. Catal.*, 1991, **65**, 55.
- [7] Lewis, D.W., Designer Catalysts for clean Chemistry. [Web:] http://www.postgraduate-courses.net/articles/clean_chemistry.htm [Date of access: 07/03/2008].

- [8] Truett, W. L., Johnson, D. R., Robinson, I. M., and Montague, B. A., *J. Am. Chem. Soc.*, 1960, **82**, 2337.
- [9] Natta, G., Dall'Asta, G., and Mazzanti, G., *Angew. Chem., Int. Ed.*, 1964, **3**, 723.
- [10] Ivin, K. J., Mol, J. C., ***Olefin Metathesis and Metathesis Polymerisation*** (2nd edition), Academic press, New York, 1997.
- [11] Grubbs, R.H., *Tetrahedron*, 2004, **60**, 7117.
- [12] Calderon, N., Ofstead, E. A., Ward, J. P., Judy, W. A., and Scott, K. W., *J. Am. Chem. Soc.*, 1968, 4134.
- [13] Bradshaw, C. P. C., Owman, E. J., and Turner, L., *J. Catalysis*, 1967, **9**, 269.
- [14] Lewandos, G. S., and Pettit, R., *J. Am. Chem. Soc.*, 1971, **93**, 7087.
- [15] Grubbs, R. H., and Brunck, T.K., *J. Am. Chem. Soc.*, 1972, **94**, 2538.
- [16] Grubbs, R. H., Carr, D. D., Hoppin, and C., Burk, P. L., *J. Am. Chem. Soc.*, 1976, **98**, 3478.
- [17] Unknown, 2009. Olefin metathesis.[Web:]
http://en.wikipedia.org/wiki/Olefin_metathesis. [Date of access: 24/11/09].
- [18] Rouhi, M., *C & EN*, 2002, **80**, 34.
<http://pubs.acs.org/cen/coverstory//8051olefin2.html>
- [19] Casey, C. P., and Burkhard, T. J., *J. Am. Chem. Soc.* 1973, **95**, 5833.
- [20] Schrock, R. R., *J. Am. Chem. Soc.* 1974, **96**, 6796.
- [21] Katz, T. J., and McGinnis, J., *J. Am. Chem. Soc.* 1975, **9**, 1592.
- [22] Grubbs, R. H., Burk, P. L., and Carr, D. D., *J. Am. Chem. Soc.* 1975, **97**, 3265.
- [23] Howard, T. R., Lee, J.B., and Grubbs, R. H., *J. Am. Chem. Soc.* 1980, **102**, 6876.
- [24] Ulman, M., and Grubbs, R. H., *Organometallics.*, 1998, **17**, 2484.
- [25] Sanford, M.S., Love, J.A., and Grubbs, R.H., *J. Am. Chem. Soc.*, 2001, **123**, 6543.
- [26] Sandford, M.S., Ulman, M., and Grubbs, R.H., *J. Am. Chem. Soc.*, 2001, **123**, 749.
- [27] Jordaan, M., van Helden, P., van Sittert, C.G.C.E., and Vosloo, H.C.M., *J. Mol. Catal. A: Chem.*, 2006, **254**, 145.
- [28] Cavallo, L., *J. Am. Chem. Soc.*, 2002, **124**, 8965.
- [29] Adlhart, C., and Chen, P., *J. Am. Chem. Soc.*, 2004, **126**, 3496.

- [30] Haines, R. J., *Chem. Soc. Rev.*, 1975, **4**, 155.
- [31] Grubbs, R. H., and Tumas, W., *Science*, 1989, **243**, 907.
- [32] Wallace, K. C., Liu, A. H., Dewan, J. C. and Schrock, R. R., *J. Am. Chem. Soc.*, 1988, **110**, 4964.
- [33] Kress, J., Osborn, J. A., Greene, R. M. E., Ivin, K. J., and Rooney, J. J., *J. Am. Chem. Soc.*, 1987, **109**, 899.
- [34] Quignard, F., Leconte, M. and Basset, J. M., *J. Chem. Soc., Chem. Commun.*, 1985, 1816.
- [35] Novak, B. M., and Grubbs, R. H., *J. Am. Chem. Soc.*, 1988, **110**, 960.
- [36] Johnson, L. K., Grubbs, R. H., and Ziller, J. W., *J. Am. Chem. Soc.*, 1993, **115**, 8130.
- [37] Nguyen, S. T., Johnson, L. K., Grubbs, R. H., and Ziller, J. W., *J. Am. Chem. Soc.*, 1992, **114**, 3974.
- [38] Schaverien, C. J., Dewan, J. C., and Schrock, R. R., *J. Am. Chem. Soc.*, 1986, **108**, 2771.
- [39] Wu, Z., Nguyen, S. T., Grubbs, R. H. and Ziller, J. W., *J. Am. Chem. Soc.*, 1995, **117**, 5503.
- [40] Nguyen, S. T., and Grubbs, R. H., *J. Am. Chem. Soc.*, 1993, **115**, 9858.
- [41] Fu, G. C., Nguyen, S. T., and Grubbs, R. H., *J. Am. Chem. Soc.*, 1993, **115**, 9856.
- [42] Schwab, P., Grubbs, R. H. and Ziller, J. W., *J. Am. Chem. Soc.*, 1996, **118**, 100.
- [43] Morgan, J. P., ***Ruthenium-based olefin Metathesis Catalysts Coordinated with N-Heterocyclic Carbene Ligands: Synthesis and Applications***, Thesis, (California Institute of Technology), 2002.
- [44] Belderrain, T. R., and Grubbs, R. H. *Organometallics*, 1997, **16**, 4001.
- [45] Wolf, J., Stüer, W., Grünwald, C., Werner, H., Schwab, P., and Schuls, M., *Angew. Chem. Int. Ed.*, 1998, **37**, 1124.
- [46] Van der Schaaf, P. A., Kolly, R., and Hafner, A., *Chem. Commun.*, 2000, 1045.
- [47] Gandelman, M., Rybtchinski, B., Ashkenazi, N., Gauvin, R. N., and Milstein, D., *J. Am. Chem. Soc.*, (Communication), 2001, **123**, 5372.
- [48] Wilhelm, T. E., Belderrain, T. R., Brown, S. N., and Grubbs, R. H., *Organometallics*, 1997, **16**, 3867.

- [49] Dias, E. L., Nguyen, S. T., and Grubbs, R. H., *J. Am. Chem. Soc.*, 1997, **119**, 3887.
- [50] Schwab, P., France, M. B., Grubbs, R. H. and Ziller, J. W, *Angew. Chem. Int. Ed.*, 1995, **34**, 2039.
- [51] Mohr, B., Lynn, D. M., and Grubbs, R.H., *Organometallics*, 1996, **15**, 4317.
- [52] Wu, Z., Nguyen, S.T., and Grubbs, R.H., *J. Am. Chem. Soc.*, 1995, **117**, 5503.
- [53] Weskamp, T., Schattenmann, W. C. Spiegler, M., and Herrmann, W. A., *Angew. Chem. Int. Ed.*, 1998, **37**, 2490.
- [54] Scholl, M., Trnka, T. M., Morgan, J. P., and Grubbs, R. H., *Tetrahedron Lett*, 1999, **40**, 2247.
- [55] Zhao, Y., and Truhlar, D. G., *Organic Letters*, 2007, **9**, 1967.
- [56] Trnka, T.M., and Grubbs, R.H., *Acc. Chem. Res.* 2001, **34**, 18.
- [57] Cavallo, L., Correa, A., Costabile, C., and Jacobsen, H., *J. Organomet. Chem.*, 2005, **690**, 5407.
- [58] Getty, K., Delgado-Jaime, M. U., and Kennepohl, P., *J. Am. Chem. Soc.*, 2007, **129**, 15774.
- [59] Jordaan, M., ***Experimental and theoretical investigation of new Grubbs type catalysts for the metathesis of alkenes*** PhD-thesis, North West University, 2007.
- [60] Meyer, W. H., Brüll, R., Raubenheimer, H. G., Thompson, C., and Kruger, G. J., *J. Organomet. Chem.*, 1988, **553**, 83.
- [61] Kingsbury, J. S., Harriety, J. P. A., Bonitatebus, P. J., and Hoveyda, A. H., *J. Am. Chem. Soc.*, 1999, **121**, 791.
- [62] Van der Schaaf, P. A., Kolly, R., Kirner, H. J., Rime, F., Mühlebach, A., and Hafner, A., *J. Organomet. Chem.*, 2000, **606**, 65.
- [63] Chang, S., Jones II, L., Wang, C., Henling, L. M., and Grubbs, R. H., *Organometallics*, 1998, **17**, 3460.
- [64] de Clercq, B., and Verpoort, F., *Tetrahedron Lett.*, 2002, **43**, 9101
- [65] Louie, J., and Grubbs, R. H., *Organometallics*, 2002, **21**, 2153.
- [66] Slugovc, C., Bartscher, D., Steltzer, F, and Mereiter, K., *Organometallics*, 2005, **24**, 2255.
- [67] Garber, S. B., Kingsbury, J. S., Gray, B. L., and Hoveyda, A. H., *J. Am. Chem. Soc.*, 2000, **122**, 8168.

- [68] Gessler, S., Randl, S., and Blechert, S., *Tetrahedron Lett.*, 2000, **41**, 9973.
- [69] Chang, S., Jones, L.-R., Wang, C., Henling, L. M., and Grubbs, R. H., *Organometallics*, 1998, **17**, 3460.
- [70] de Clercq, B., and Verpoort, F., *J. Mol. Catal. A: Chem.*, 2002, **180**, 67.
- [71] Denk, K., Fridgen, J., and Herrmann, W. A., *Adv. Synth. Catal.*, 2002, **344**, 666.
- [72] Jordaan, M., and Vosloo, H.C.M., *Adv. Syth. Catal.*, 2007, **349**, 184.
- [73] Huijsmans, C.A.A, ***Modelling and Synthesis of Grubbs type complexes with hemilabile ligands***, MSc-dissertation (North-West University), 2009.

CHAPTER 3: Theoretical background of Computational Chemistry

3.1 Introduction

Computational chemistry is a branch of chemistry that makes use of computers to solve chemical problems. It is sometimes called theoretical chemistry or molecular modelling. Advances in computer hardware and user-friendly software have contributed to the wide use of computational chemistry by chemists. It uses the results of theoretical chemistry to develop algorithms and computer programs which can then be implemented, by the chemist, to make predictions about the structure and properties of molecules as well as elucidation of reaction pathways. It has become a powerful approach to chemistry. Computational chemistry is widely used in the design of new drugs and materials.¹⁻⁴

When considering a large group of compounds for a particular application, computational chemistry can rule out a large majority of compounds not suitable for their intended use; saving time, money, labour and, possibly, unnecessary toxic waste.⁵

Chemists can make use of different types of computational methods to perform calculations:

1. Molecular mechanics methods are based on classical physics. Atoms are treated as solid spheres with specific radii. Bonding interactions between spheres are treated as “springs” with an equilibrium distance equal to the experimental or calculated bond length. Molecular mechanics is the method of choice for large molecules such as proteins and segments of DNA.^{1,6}
2. *Ab initio* (Latin for ‘from scratch’) methods are calculations based on the theoretical principles of quantum chemistry. Starting with the Schrödinger equation, calculations are performed in order to obtain a wavefunction that represents the motion of an electron as fully as possible. No use is made of empirical data. Since mathematical approximations have to be made in order to cope with multi-electron systems, a variety of methods are available which

differ in the nature of the approximations that are implemented. *Ab initio* methods are best suited to smaller molecules since it takes enormous amounts of computer CPU time, memory and disc space.^{1,7}

3. Semi-empirical methods make use of quantum chemical calculations but omit or approximate certain pieces, e.g. by considering only valence electrons (core electrons and their interactions are omitted).⁴ Parameters to estimate the omitted values are obtained by fitting the results to experimental data or *ab initio* calculations. These approximations speed up calculation time relative to *ab initio* methods.^{1,5} The method does not, however, produce accurate results when the system being investigated differs from the molecules used in the database for the parameterisation process.
4. Density functional theory (DFT) is based on the calculation of the ground state electron density rather than of a many-electron wavefunction. Using the electron density significantly speeds up the calculation since it avoids solving the Schrödinger equation. In the last few years, DFT has become the theory of choice to study large complexes involving transition metals. This method will, therefore, be used in this investigation involving Grubbs type precatalysts.⁸

The methods discussed above each have their advantages and disadvantages and are each suitable for specific systems.¹ It is important to select a method most suitable to the system being investigated.

3.2 Computable Properties

3.2.1 Geometrical optimised structure

Geometry optimisation is a method used for finding a stable conformation of a molecule. The computational chemist starts with a molecule (existing or theoretical), knowing the atoms that make up the molecule and the connectivity between them and provides this as input to the computational method that he/she has selected. Geometry optimisation starts off with a mathematical relationship correlating the input structure with its energy. The computational method then begins to 'look' for the 'best' structure; 'best' is defined as having the lowest possible energy, from the

starting positions of the atoms chosen by the computational chemist.^{3,9} This is done by searching for stationary points, by calculating the first derivative of the energy with respect to the structures coordinates. If the first derivative is zero, a stationary point was obtained. This procedure brings us only to the nearest stationary point which is not necessarily the minimum structure or global minimum with the lowest energy.

Many optimisation algorithms calculate the second derivative of the energy with respect to the coordinates known as a Hessian. If the second derivatives are all positive, a minimum structure was obtained.^{3,9,10} In this study, many structures will be geometrically optimised. Frequency calculations will be performed on optimised structures in order to confirm that they are minimum structures.

3.2.2 Energy

In order to obtain a mathematical representation of molecules that return their corresponding energies for constructing a potential energy surface (PES), it is important to specify a reference system that is defined as having zero energy. For *ab initio* or DFT methods (used in this study), which model all the electrons in a system, zero energy corresponds to all nuclei and electrons being infinitely far apart. The energy for a particular molecule calculated by a particular method is then relative to the arrangement of atoms corresponding to zero energy.

Even with a particular model, total energy values relative to the method's zero energy are often inaccurate. It is common to find that this inaccuracy is almost always the result of systematic error. For this reason, the most accurate energy values are often relative energies, obtained by subtracting total energies from separate calculations. This is why the difference in energy between conformers and bond dissociation energies can be calculated with accuracy.¹¹ In this study, energy of various complexes resulting from various reaction pathways will be compared to the precatalyst from which they were derived. This will give an indication of which reaction pathways are energetically less expensive.

The method used calculates the electronic energy (E) when everything 'stands still' at 0 K, even though at 0 K molecules do have some vibrational energy (zero point energy).¹² ΔG values includes a vibrational correction. These corrections are important since enthalpic and entropic effects are not reflected by electronic

energies. Such effects may be critical in steps involving a change in molecularity.^{13,14} This study considers both relative electronic energies and some vibrational corrected energies at 298 K.

3.2.3 Potential Energy Surfaces (PES)

Computational methods can calculate the PES. The PES represents the potential energy of a collection of atoms over all possible atomic arrangements. They are usually represented by three-dimensional plots, which are slices through the multi-dimensional PES involving only two coordinates.³ It can describe:

- Either a molecule or collection of molecules having constant atom composition.
- A system where a chemical reaction takes place.
- Relative energies for conformers.¹⁵

Points of interest on a PES include:

1. Local Maxima: These are high values on the PES which correspond to the structures of transition states. In this case, the first derivative of the energy with respect to the structure's coordinates is zero and the second derivative is negative in one direction and positive in all other directions. The Hessian matrix must have only a single negative eigenvalue (imaginary frequency). The imaginary frequency will typically be in the range of 400-2000 cm^{-1} , similar in magnitude to real (positive) vibrational frequencies. It is critical to confirm that the normal coordinate corresponding to the imaginary frequency connects reactants and products. This can be done by 'animating' the normal coordinate corresponding to the imaginary frequency and observing that the vibration is along the correct reaction coordinates.⁴ This vibration appears as a lengthening and shortening of the particular bonds in question.
2. Local Minima: These are low values on the PES which correspond to stable molecules. The first derivative of the energy with respect to the structure's coordinates is zero and the second derivatives are positive. The Hessian will contain only positive vibrational frequencies (as discussed in 3.2.1).

3. Global minimum: This represents the most stable conformation of the molecule and corresponds to the lowest energy arrangement of atoms. In this case, the first derivative of the energy with respect to the structure's coordinates is zero and the second derivatives are positive (as discussed in 3.2.1). The Hessian will contain only positive vibrational frequencies.¹²

Such plots provide essential connections between important chemical observables – structure, stability, reactivity and selectivity as well as energy. An example of a PES and some interpretations thereof are given below:

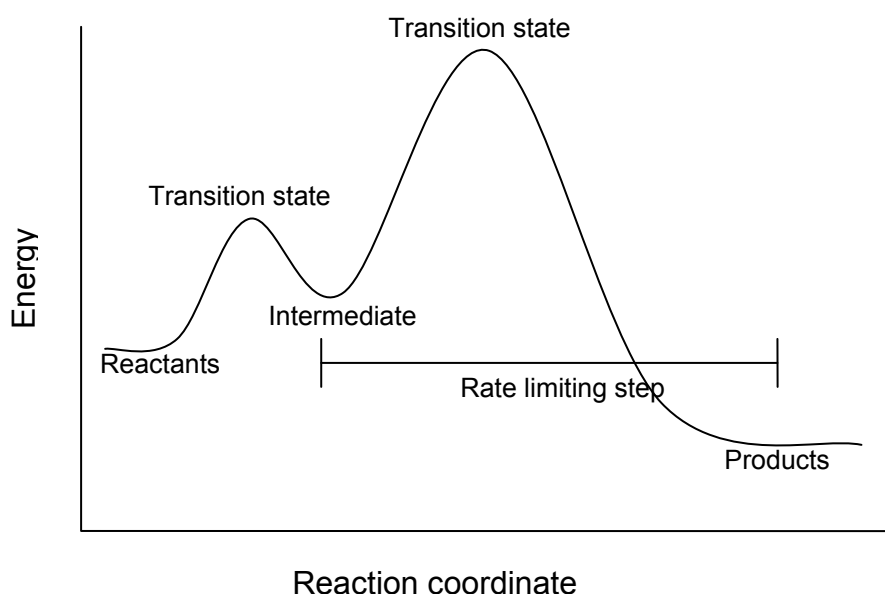


Figure 3.1: A two-dimensional potential energy surface for a system where a chemical reaction takes place.

The starting and ending points on the diagram correspond to the 'reactants' and 'products' respectively, and are energy minima. From this PES, it can be seen that the products are lower in energy than the reactants, this kind of reaction is said to be exothermic. Thermodynamics tells us that in time, and depending on temperature, the amount of products will be greater than the reactants. This reaction involves several distinct steps. Moving along the reaction coordinates two energy maximums are observed corresponding to transition states. The position on the PES having the highest energy is called the global maximum and corresponds to the rate-limiting step of the reaction.^{4,10}

In this study, the focus will be on exploring different possible reaction pathways for the alkene metathesis of propene using hemilabile Grubbs type catalysts and comparing their energy barriers. The mechanism can be determined from computation by comparing the energy barriers of the different reaction pathways and selecting the sequence with the lowest-energy transition state.⁴

3.2.4 HOMO/LUMO orbitals and energy

The highest occupied molecular orbital, HOMO, and the lowest unoccupied molecular orbital, LUMO, of a molecule are called frontier orbitals. The HOMO and LUMO play an important role in chemical reactions. This was first noticed by Fukui.¹⁶ Investigations have revealed that the energy gap between the HOMO and LUMO in a molecule can be an indication of stability.¹⁷⁻¹⁹ A large gap is correlated to high stability or low reactivity, and a small gap is correlated to poor stability and high reactivity.²⁰ If these HOMO-LUMO gaps are determined for each of the various precatalysts, the stability or reactivity of these precatalysts can be compared with each other. To determine these gaps, the HOMO and the LUMO energies of the precatalysts will be calculated.

If a reaction occurs between molecules, there is an overlap between the HOMO of the one molecule and the LUMO of the other molecule. The electrons from the HOMO orbital (nucleophile) are shifted to the LUMO (electrophile). Bonding interaction between the molecules is improved when the energy gap between the reacting HOMO and LUMO is small. This interaction leads to a large drop in energy from the reactants to the products.²¹

Previously, it was shown by du Toit²², that the HOMO of the substrate (1-pentene) interacted with the LUMO of the Gr2 complex and that it was energetically more favoured than the overlap of the LUMO orbital of the substrate and the HOMO orbital of the Gr2 complex.²² In this study, the HOMO-LUMO interactions of a couple of the Grubbs type hemilabile complexes with the propene substrate, will be studied to determine the most favourable orbital overlaps. The HOMO and LUMO energies of propene as well as those of the precatalysts will be obtained by computational methods to confirm which interactions will be more energetically favoured.

Comparisons of HOMO-LUMO energy gaps, between propene and ruthenium 16-

and 14-electron complexes, will be made to assess reactivity towards propene of various precatalysts relative to one another. These computational results will be compared with reactivity that has been observed experimentally.

3.2.5 Hirshfeld Charge Analysis

When two neutral atoms A and B interact and form a chemical bond, the atomic charge of A as a result of bond formation with B, depends on the amount of electron density gained from or lost to B. If the bond between A and B were ionic, there would be a complete transfer of electronic charge from one atom to the other, i.e. one atom gains -1 charge. In an ideal covalent bond, electrons would be shared equally, and charges on A and B would still be zero. However, most molecules are not ideal cases, and a method was needed to quantify the atomic charge.

Various methods have become available to quantify atomic charge in molecules. The Hirshfeld method is based directly on the electron density as a function of space. It makes use of the electronic density of the molecule and of a fictitious pro-molecule constructed from neutral atoms. The pro-molecule refers to a reference electron density model prior to molecule formation.²³ The Hirshfeld method partitions the electron density among the atoms of the molecule by the appropriate weighting. The weight factor $w_A(r)$ is defined as the ratio of the isolated atom electron density of A, $\rho_A^0(r)$, and the density constructed from superimposing the isolated electron densities of the atoms present at their position in the molecule (the pro-molecule density).

The charge q_A of an atom A in a molecule

$$q_A = Z_A - \int \rho_A(r) dr$$

where Z_A is the atomic number of A and $\rho_A(r)$ the electron density of A in the molecule considered. This atomic electron density is obtained by multiplying the molecular electron density $\rho(r)$ with the weight factor.²⁴ From the equation, we see that the Hirshfeld scheme accounts in a natural way for the fact that each atom has a characteristic size dependent on the nuclear charge Z_A .

In order to obtain an indication of electron-poor regions in a structure, which will be

vulnerable to nucleophilic attack and, to identify regions which are likely to attract electrophiles, a quantitative description of molecular charge distribution like Hirshfeld charge values is useful.

Hirshfeld charges are reliable since the procedure to obtain these values is not basis set dependent like that of Mulliken charges. Hirshfeld charges are chemically meaningful since they are consistent with electronegativity values of elements and a good indicator for the nature of chemical bonds. Mulliken charges do not take into account the difference in electronegativity between two atoms. The atoms in molecules (AIM) approach yields values that suggest much ionic character even in the case of covalent bonds.²⁵

In this study, the Hirshfeld charges of various atoms around the ruthenium centre of the studied precatalysts will be computed. The Hirshfeld charges obtained in this study of precatalysts that have been previously investigated experimentally by Jordaan²⁶ and Huijsmans²⁷, will be compared with one another in order to determine if a correlation exists between charge distribution in the precatalyst determined computationally and the activity, selectivity and lifetime of the catalysts that has been observed experimentally.

3.3 Computational Chemistry of Grubbs type precatalysts

Given the huge interest in the metathesis process, it is not surprising that numerous computational studies of Grubbs type precatalysts have appeared in the last decade. These investigations were driven by the need to obtain a better understanding of the metathesis reaction, since certain aspects and mechanistic steps had not been elucidated by experiments such as:

- The structure of the active species.
- The rate limiting steps for first and second generation Grubbs catalysts.
- The coordination of the alkene. Did the incoming alkene coordinate to Ru metal centre in a *cis* or *trans* orientation with respect to the remaining ligand?
- The nature of the metallacyclobutane. Is it an intermediate or a transition state?

Many of these studies used models of the catalyst system $(L)_2Cl_2Ru=CHR$, e.g. with $L = PH_3$ ^{28,29,30,31} or PMe_3 ^{28,29,30,31} and model substrates such as ethene^{18,28,29,32,30,31} to save on calculation time. However, these model systems do not accurately portray steric and electronic influences of real ligands and substrates¹⁴ and, therefore, in some studies the task of using the 'real' systems $(PCy_3)_2Cl_2Ru=CHPh$ and $(PCy_3)(H_2IMes)Cl_2Ru=CHPh$ were undertaken in order to reduce gaps between theory and experiment.^{18,28,27,31,32,34,35}

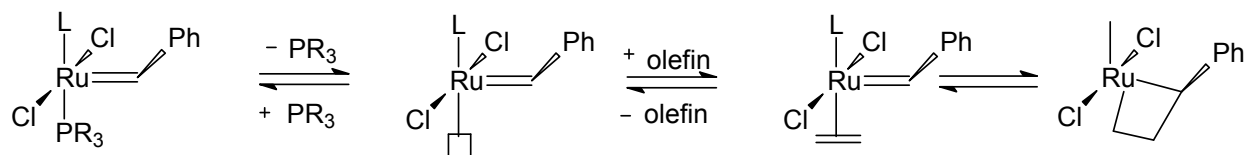
Some of these computational studies were done in tandem with experiments³⁶ or used published experimental data for comparison with their theoretical results.^{18,30,35} Some experimental studies compared their results with values obtained by theory.³⁷ This exercise in synergy between theory and experiment helped to gain a deeper mechanistic insight with regard to issues that had not been resolved experimentally.

These computational studies contributed to a better understanding of the following:

1. The alkene metathesis reaction and different possible pathways^{28,29,38,39}, as well as decomposition routes for the catalysts,³³ formation of the ruthenium carbene,³⁶ the intermediates,¹⁸ transition states^{18,34,40,41} and rate limiting steps.³²
2. New and better precatalysts.^{33,39,42,43}
3. Strengths and weaknesses of various computational methods.^{18,30,35}
4. Orbital interactions in the ruthenium alkene metathesis catalysts.⁴³

Much-needed details about the entire metathesis reaction were obtained. Firstly, it was confirmed by DFT studies that the starting active species in the alkene metathesis reaction is a metal carbene $(PR_3)_2Cl_2Ru=CH_2$ and not a carbenoid complex $(PR_3)_2ClRu-CH_2Cl$.⁴⁵ Computational studies converged with experimental studies on the dissociative mechanism being the most probable for alkene metathesis with Grubbs type catalysts (Scheme 3.1).^{28,39,45} The reaction initiates with the loss of the phosphine ligand for both Gr1 and Gr2 forming a 14-electron species.²⁸ The resulting monophosphine complex is then the active catalytic species (identified experimentally by Adlhart *et al*.⁴⁰) in the metathesis reaction of Gr1, and the phosphine free complex is the active catalytic species for Gr2.³⁹ Mechanistic studies found that phosphine dissociation is an essential step for catalyst initiation.^{46,47} The formation of the catalytically active species is also the rate-limiting

step for the second generation catalysts.²⁸

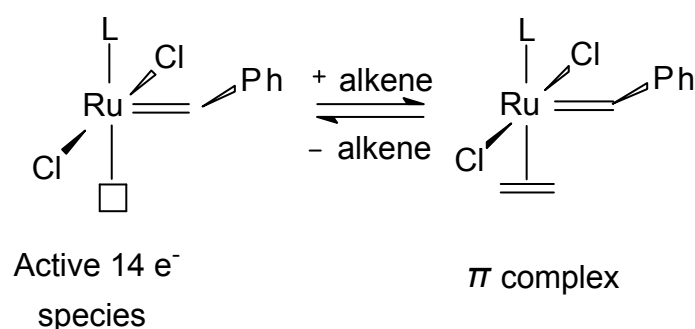


Scheme 3.1: Representation of dissociative pathway for Grubbs type ruthenium carbene complexes.

Recent results of thermochemical data of phosphine binding energies in Gr1 and Gr2 of 33.4 and 36.9 kcal/mol, respectively, have been reported by Torker *et al.*³⁷ These values were obtained by tandem ESI-MS involving collision-induced dissociation (CID) of electrosprayed complexes. These experimental values obtained in the gas phase are noticeably higher than the dissociation energies of 23.6 and 27 kcal/mol reported by Grubbs⁴⁷ for the same process in the solution phase reaction. The reason for this difference is the absence of solvent interactions as was reported by Grubbs in the same study and supported by Jensen *et al.*³⁵ theoretically. Previously, many phosphine dissociation energies that were calculated were compared to the experimental results obtained for metathesis in the solution phase reaction.^{40,41} These comparisons seemed to indicate that the calculation method for phosphine dissociation was producing accurate results, but these results should have been closer to those obtained experimentally in the gas phase but were far from it. Investigations involving the testing of a large range of DFT functionals on phosphine dissociation energies were undertaken recently.^{30,35} In these computational studies, it was shown that many of the functionals previously used to model Grubbs type catalysts, grossly underestimate the phosphine dissociation energies for the gas phase. The application by Torker *et al.*³⁷ of the newly developed MO6-L density functional⁴⁴ specifically suited to organometallic thermochemistry, resulted in calculated phosphine dissociation energies, in good agreement with their experimental values. Zhao and Truhlar³⁰ extended their computational calculations to the real Gr2 catalysts. They took the experimental value obtained by Torker *et al.*³⁷ and removed zero-point vibrational energy and thermal vibrational rotational energy to obtain a phosphine bond dissociation energy of 40.2 kcal/mol. These studies show that it is important to select the correct functional for the system you wish to study.

This value of 40.2 kcal/mol obtained computationally will then be compared with modelled phosphine dissociation energies of Gr2 in this study since solvent interactions are not considered in this study.

Once a 14-electron species is formed, a substrate molecule can attach at the open coordination site (Scheme 3.1). Calculations performed with ethene as substrate and model systems, showed that *trans* alkene coordination, whereby the alkene approaches on the opposite side to the ligand (L) is favoured and barrierless.^{29,34}



Scheme 3.2: *Trans* addition of alkene to active species.

Once the substrate has attached, the metallacycle complex is formed (Scheme 3.1). Cavallo⁴¹ investigated both Gr1 and Gr2 structures together with substrates ethene, 1-butene and norbornene using pure BP86 density functional calculations and determined that the metallacyclic structures are not transition structures but minimum intermediates. Using the same level of theory, precatalysts and similar substrates as Cavallo, Adlhart and Chen²⁸, in addition, it is found that the formation of the metallacyclobutane is the rate-limiting step for the first generation catalysts.

A computational study by Koga *et al.*³⁴ indicated the presence of agostic interactions in the ruthenacyclobutane complex of Gr1. Agostic interaction is a term generally used in organometallic chemistry for the interaction of a coordinately-unsaturated transition metal with a C-H bond. An empty d orbital of the transition metal accommodates two electrons involved in the C-H bond. The stabilisation arising from an agostic interaction has been estimated, by experimental and computational studies, to be 10-15 kcal/mol. This makes agostic interactions stronger than most hydrogen bonds.⁴⁸ Their computational study revealed deviations in the bond angles of the ruthenacyclobutane relative to cyclobutane and deviations in CC bond lengths. These structural features suggested that the CCC component of the four-membered

ring interacted strongly with the Ru atom via one of the vacant d orbitals of Ru (Figure 3.2). This interaction is equivalent to two α -CC agostic interactions. This type of interaction could make the CC bond cleavage facile. In this study, the presence of agostic interactions in 16-electron and 18-electron metallacycles will be investigated to determine whether such interactions will correlate with catalyst activity or the mechanism preferred.

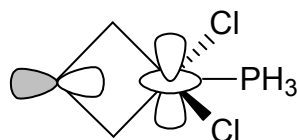


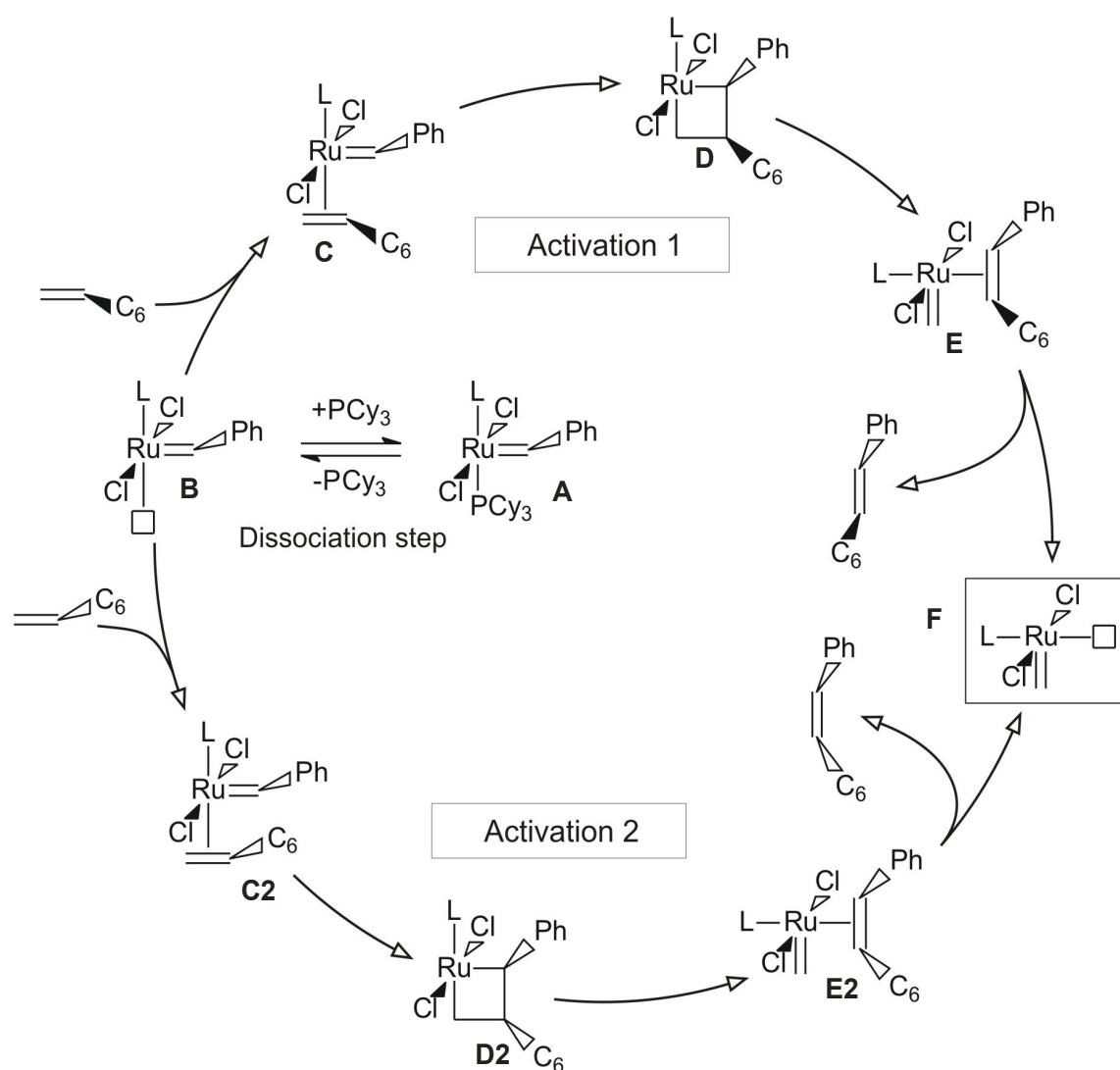
Figure 3.2: The middle carbon interacting with vacant d orbital on ruthenium.

Jordaan *et al.*⁴⁹ investigated the 1-octene metathesis with the first generation Grubbs complex both experimentally and theoretically to gain better insight into the complete mechanism (Scheme 3.3). Using density functional theory at the GGA/PW91/DNP level, it was found that the formation of the catalytically active heptylidene was both kinetically and thermodynamically favoured. Experimental results obtained with NMR and GC/MSD experiments revealed the formation of styrene isomers and the presence of unbound PCy_3 , which is consistent with the dissociative metal carbene mechanism. Two activation steps are possible depending on the spatial orientation of the incoming substrate.

From the above discussion, it can be concluded that computational studies have provided a better understanding of the metathesis mechanism using Gr1 and Gr2 as catalysts.^{28,37,49} Many computational studies have been in agreement even though the same model systems and substrates were not used.^{14,32,41} Given the amount of information obtained thus far on alkene metathesis using computational studies, it is clearly a worthwhile route to travel in pursuit of catalysts tailor-made for specific applications.

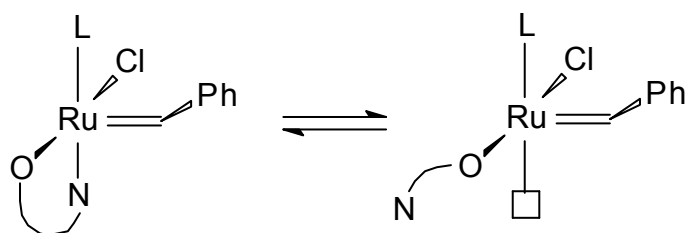
Understanding the value of computational methods for the search of improved precatalysts, Jordaan *et al.*⁵⁰ also undertook an experimental and a DFT computational investigation of a Grubbs type precatalyst bearing a chelating pyridinyl alcoholate ligand, $[\text{RuCl}(\text{L})(\text{O}^{\wedge}\text{N})(=\text{CHPh})]$ ($\text{L}=\text{H}_2\text{IMes}$ or PCy_3 , $\text{O}^{\wedge}\text{N} = 1-(2'$ -

pyridinyl)cyclohexan-1-olate)). The aim was to improve on the Gr1 and Gr2 catalyst. Since it had been confirmed that alkene metathesis with Gr1 and Gr2 proceeded with the dissociative mechanism, Jordaan chose to explore only the dissociative mechanism for these catalysts computationally. The two possible initiation routes of these bidentate/hemilabile precatalysts considered were the dissociation of the labile N-atom as well as the dissociation of the ligand L as shown in Figure 3.3.



Scheme 3.3: Dissociation (A-B) and activation (B-F) steps in the mechanism of productive 1-octene metathesis using $\text{RuCl}_2(\text{PCy}_3)_2(=\text{CHPh})$ ⁴²

a) Dissociation of labile N-atom



b) Dissociation of ligand L

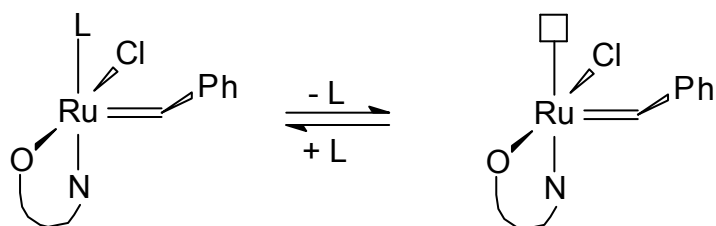


Figure 3.3: Two possible initiation routes for a Grubbs type precatalyst containing a bidentate ligand.⁵⁰

The metathesis of 1-octene in the presence of $[\text{RuCl}(\text{H}_2\text{IMes})(\text{O}^*\text{N})(=\text{CHPh})]$ with ^1H NMR at 50°C in CDCl_3 , showed the presence of five carbene species (Figure 3.4) which might relate to the open and coordinated chelating complexes.⁵¹ The computational results obtained by Jordaan were in agreement with the experimental results obtained with the NMR study of the second-generation chelating complexes, namely that dissociation of the labile N-atom occurred.⁵⁰

However, the metathesis of 1-octene in the presence of $[\text{RuCl}(\text{PCy}_3)(\text{O}^*\text{N})(=\text{CHPh})]$ with ^1H NMR at 50°C in CDCl_3 , showed the presence of only three carbene species (Figure 3.5) which might relate to the coordinated chelating complexes.⁵¹ The computational results suggested that both hemilability and phosphine ligand dissociation could play a role in the metathesis of 1-octene with the Gr1-type precatalyst with bidentate/hemilabile ligand.⁵⁰

In Jordaan's study, free PCy_3 ligand was observed experimentally with GC/FID throughout the 1-octene metathesis investigation in the presence of the first-generation hemilabile complex.⁵¹ This was further motivation to consider only the dissociative mechanism. What was not investigated was the possibility of an associative/dissociative mechanism whereby the alkene could attach to the ruthenium centre to form an $18e^-$ complex after which the PCy_3 ligand detaches to

form the 16e⁻ complex. Jordaan's study could not conclude with certainty that all of these precatalysts always display hemilability. These uncertainties about hemilability and reaction mechanism for Grubbs type precatalysts with bidentate/hemilabile ligands served as motivation for this study.

3.4 References

- [1] Young, D., 1998. Introduction to Computational Chemistry. [Web]
<http://www.ccl.net/cca/documents/dyoung/topics-orig/compchem.html> [Date of access: 18/01/2012].
- [2] Wikipedia, 2008. Computational Chemistry. [Web]
http://en.wikipedia.org/wiki/Computational_chemistry [Date of access: 21/11/2009].
- [3] Cramer, C. J., ***Essentials of Computational Chemistry***, Second Edition, Wiley, England, 2004.
- [4] Hehre, J. H., ***A Guide to Molecular Mechanics and Quantum Chemical Calculations***, Wavefunction, Inc., USA, 2003.
- [5] Young, D., ***Computational Chemistry***, Wiley, USA, 2001.
- [6] Wikipedia, 2012, Molecular mechanics. [Web]
http://en.wikipedia.org/wiki/Molecular_mechanics [Date of access: 2012/01/11].
- [7] Chemviz, 2010, Overview of Computational Chemistry. [Web]
<http://www.shodor.org/chemviz/overview/ccbasics.html> [Date of access 01/06/2010].
- [8] Wikipedia, 2010, Density Functional Theory. [Web]
http://en.wikipedia.org/wiki/Density_functional_theory [Date of access: 01/06/2010].
- [9] Chemviz, 2010, Geometry Optimisation. [Web]
<http://www.shodor.org/chemviz/optimization/teachers/background.html> [date of access: 01/06/2010].
- [10] Jensen, F., ***Introduction to Computational Chemistry***, 2nd ED, John Wiley & Sons, Great Britain, 2007.
- [11] Leach, A. R., ***Molecular Modelling Principles and Applications***, Addison Wesley Longman Limited, England, 1996.

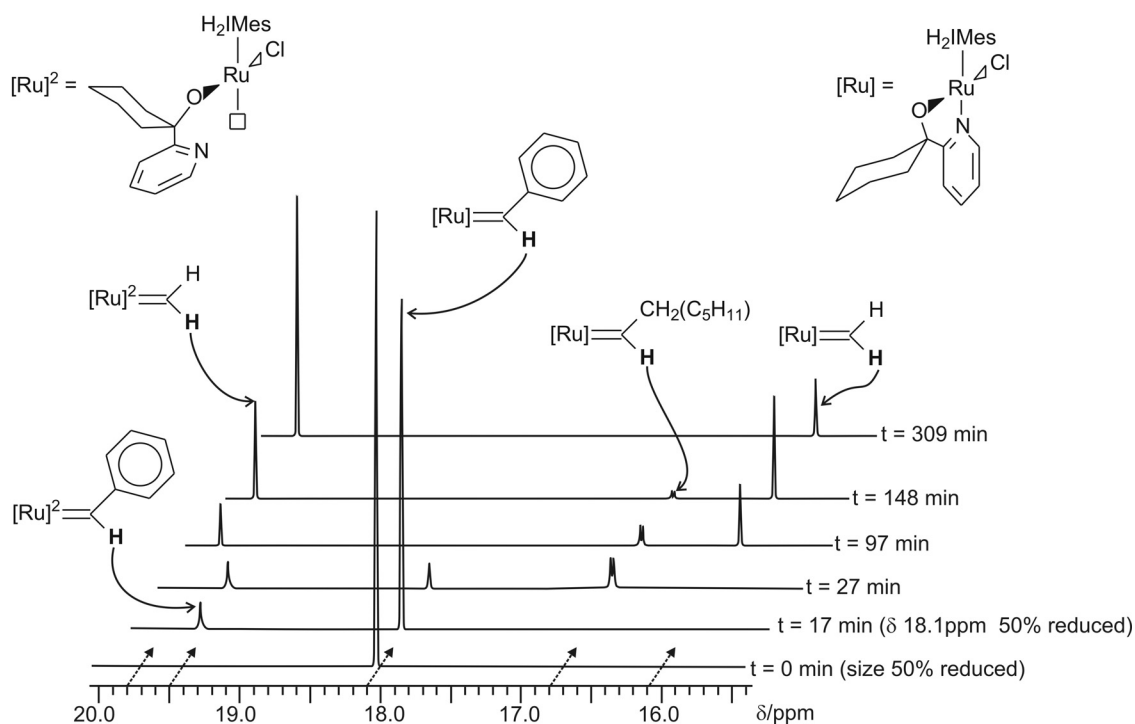


Figure 3.4: ^1H NMR spectra of the carbene proton region at different time intervals of a 1-octene $/[\text{RuCl}(\text{H}_2\text{IMes})(\text{O}^{\wedge}\text{N})(=\text{CHPh})]$ reaction mixture at 50°C in CDCl_3 .⁵¹

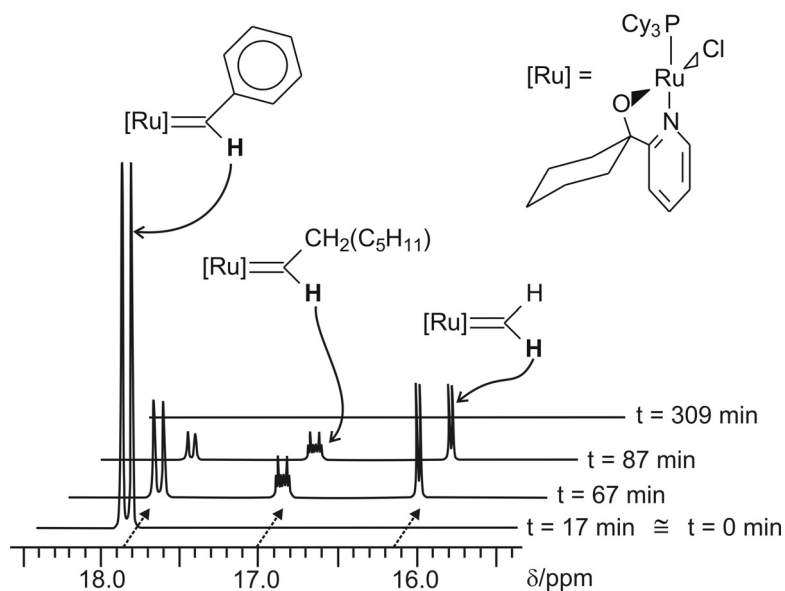


Figure 3.5: ^1H NMR spectra of the carbene proton region at different time intervals of a 1-octene $/[\text{RuCl}(\text{PCy}_3)(\text{O}^{\wedge}\text{N})(=\text{CHPh})]$ reaction mixture at 50°C in CDCl_3 .⁵¹

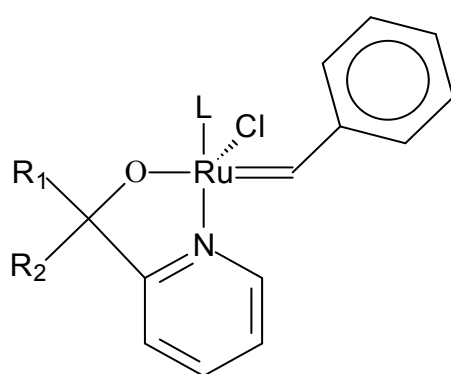
- [12] Lewars, E. G., **Computational Chemistry**, DOI 10.1007/978-90-481-3862-3_2, © Springer Science+Business Media B. V. 2011.
- [13] Goodman, J. M., **Chemical Applications of Molecular Modelling**, Royal Society of Chemistry, UK, 1998.
- [14] Sabbagh, I. T., and Kaye, P. T., *J. Mol. Struct.: THEOCHEM*, 2006, **763**, 37.
- [15] Cremer, D., Kraka, E., Joo, H., Stearns, J. A., and Zweir, T. S., *Phys. Chem. Chem. Phys.*, 2006, **8**, 5304.
- [16] Fukui, K., Yonezawa, T., and Shingu, H., *J. Chem. Phys.*, 1952, **20**, 722.
- [17] Pearson, R. G., *J. Org. Chem.*, 1989, **54**, 1423.
- [18] Zhou, Z., and Parr, R. G., *J. Am. Chem. Soc.*, 1990, **112**, 5720.
- [19] Faust, W. L., *Science*, 1989, **245**, 37.
- [20] Dulal, C. G., and Jibanananda, J. [Web] http://cs-test.ias.ac.in/cs/Downloads/article_id_076_04_0570_0573_0.pdf [Date of access 30/10/2012].
- [21] Fleming, I., **Frontier orbitals and organic Chemical Reactions**, John Wiley & Sons, Great Britain, 1976.
- [22] du Toit, J. I., '**n Modelleringsonderzoek na die meganisme van die homogene alkeenmetatesereaksie**', MSc-dissertation (North-West University), 2009.
- [23] Spackman, M. A., and Maslen, E. N., *J. Phys. Chem.*, 1986, **90**, 2020.
- [24] Boon, G., Van Alsenoy, C., De Proft, F., Bultinck, P., and Geerlings, P., *J. Phys. Chem.*, 2003, **107**, 11120.
- [25] Guerra, C. F., Handgraaf, J., Baerands, E. V., and Bickelhaupt, F. M., *Journal of Computational Chemistry*, 2003, **25**, 189.
- [26] Jordaan, M., **Experimental and Theoretical investigation of New Grubbs type Catalysts for the metathesis of Alkenes**, PhD-thesis (North-West University), 2007.
- [27] Huijsmans, C.A.A., **Modelling and Synthesis of Grubbs type complexes with hemilabile ligands**, MSc-dissertation (North-West University), 2009.
- [28] Adlhart, C., and Chen, P., *J. Am. Chem. Soc.*, 2004, **126**, 3496.
- [29] Vyboishchikov, S. F., Bühl, M., and Thiel, W., *Chem. Eur. J.*, 2002, **8**, 3962.
- [30] Zhao, Y., and Truhlar, D. G., *J. Chem. Theory Comput.*, 2009, **5**, 324.
- [31] Tsipis, A.C., Orpen, A. G., and Harvey, J. N., *Dalton Trans.*, 2005, 2849.
- [32] Zhao, Y., and Truhlar, D. G., *Organic Letters*, 2007, **9**, 1967.

- [33] Janse van Rensburg, W., Steynberg, P. J., Meyer, W.H., Kirk, M. M., and Forman, G. S., *J. Am. Chem. Soc.*, 2004, **126**, 14332.
- [34] Aagaard, O.M., Meier, R.J., and Buda, F., *J. Am. Chem. Soc.*, 1998, **120**, 7174.
- [35] Minenkov, Y., Occhipinti, G., and Jensen, V. R., *J. Phys. Chem. A*, 2009, **113**, 11833.
- [36] Dolker, N., and Frenking, G., *J. Organomet. Chem.*, 2001, **617-618**, 225.
- [37] Torker, S., Merki, D., and Chen, P., *J. Am. Chem. Soc.*, 2008, **130**, 4808.
- [38] Meier, R.J., Aagaard, O.M, and Buda, F., *J. Mol. Catal. A: Chem.*, 2000, **160**, 189
- [39] Fomine, S., Vargas, S. M., and Tlenkopatchev, M. A., *Organometallics*, 2003, **22**, 93.
- [40] Adlhart, C., Hinderling, C., Baumann, H., and Chen, P., *J. Am. Chem. Eur. J.*, 2002, **8**, 3962.
- [41] Cavallo, L., *J. Am. Chem. Soc.*, 2002, **124**, 8965.
- [42] Wescamp, T., Kohl, F., Hieringer, W., Gleich, D., and Herrmann, W. A., *Angew. Chem. Int. Ed.* 1999, **38**, 2416.
- [43] Schoeller, W. W., Schroeder, D., and Rozhenko, A. B., *J.Organomet. Chem.*, 2005, **690**, 6079.
- [44] Suresh, C. H., and Koga, N., *Organometallics*, 2004, **23**, 76.
- [45] Bernardi, F., Bottoni, A., and Miscione, G. P., *Organometallics*, 2003, **22**, 940.
- [46] Dias, E.L., Nguyen, S.T., and Grubbs, R.H., *J. Am. Chem. Soc.*, 1997, **119**, 3887.
- [47] Sanford, M.S., Love, J.A., and Grubbs, R.H., *J. Am. Chem. Soc.*, 2001, **123**, 6543.
- [48] von Frantzius, G., Streubel, R., Brandhorst, K., and Grunenberg, J., *Organometallics*, 2006, **25**, 118.
- [49] Jordaan, M., van Helden, P., van Sittert, C.G.C.E., and Vosloo, H.C.M., *Journal of Molecular Catalysis A: Chemical*, 2006, **254**, 145.
- [50] Jordaan, M., and Vosloo, H. C. M., *Molecular Simulation*, 2008, **34**, 997.
- [51] Jordaan, M., and Vosloo, H. C. M., *Adv. Syth. Catal.*, 2007, **349**, 184.

CHAPTER 4: Experimental

4.1 Introduction

Previous evidence obtained by Jordaan^{1,2}, suggested that two different reaction pathways may be involved in the metathesis of 1-octene by Grubbs type precatalysts with bidentate/hemilabile ligands. In this study, many such bidentate/hemilabile Gr1 and Gr2-type precatalysts will be investigated. These precatalysts will be constructed by varying the R groups on the pyridinyl alcoholato ligand as illustrated in Figure 4.1. This will be explained in more detail in paragraph 4.3.2.



L = PCy₃ or IMes

R₁ and R₂ = H, alkyl, aryl or form part of a ring structure

Figure 4.1: Template for catalyst design.

In Jordaan's^{1,2} study, an associative pathway was never considered in the computational calculations since evidence exists that Gr1 and Gr2 follow the dissociative pathway. This study will investigate the viability of an associative pathway.

The outcomes of Jordaan's^{1,2} and Huijman's³ experimental studies also indicated that the R groups have an influence on the activity, selectivity and lifetime of the precatalysts. Various computable properties of these catalysts will be investigated in an attempt to correlate structure and electronic properties to activity and reaction pathway. Structural, electronic and thermodynamic data of all complexes illustrated in Figure 4.2 will be gathered, in order to identify how these R groups affect the performance of the precatalyst.

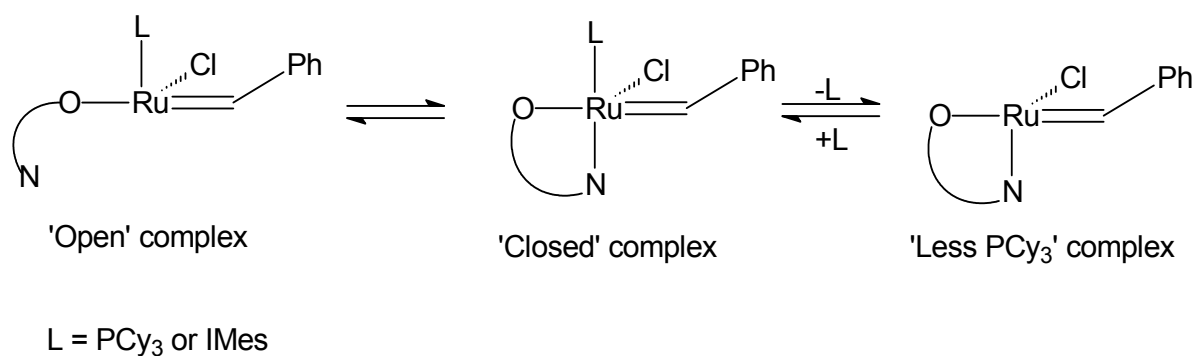


Figure 4.2: Simplified diagram illustrating different forms of precatalysts studied.

There is no certainty whether all the precatalysts having pyridinyl alcoholato ligands will exhibit hemilability. The de-coordination of a softly bound atom will result in an 'open' complex as illustrated in Figure 4.2. The type of reaction pathway favoured could be dependent on the presence of hemilability in the complex with the pyridinyl-alcoholato ligand. The hemilability could be dependent on the R groups attached to the pyridinyl-alcoholato ligand. In this study, the researcher expects to see some precatalysts exhibiting hemilability and others that do not. Where L is a phosphine ligand (Figure 4.2), dissociation of PCy₃ will also be considered. The complex resulting from the dissociation of phosphine will be named 'less PCy₃'.

Possible reaction pathways are illustrated in Figure 4.3. Hemilability is represented between structure A and B, as well as E and D, A and D being named the 'closed' complex. The process between A and B can also be referred to as the de-coordination of the softly bound labile N-atom resulting in a 14-electron species (B).

When a coordination site is unoccupied as in structure B, the substrate propene can coordinate and result in the formation of the metallacycle (E). In order to determine the viability of the pathway between A and E, structures corresponding to A, B and E had to be constructed and optimised. It was assumed in this study that no significant energy barrier would exist between structures A and B and transition structure searches were not performed for this step. Transition structure searches were performed using structure E by lengthening either the bond between ruthenium and C₁ atom originating from the propene or the former carbene carbon of the precatalyst to C₂ atom in the 4-membered ring (Figure 4.4). This calculation separates the

propene (shown in green) from the metallacycle. This calculation would give the energy barrier between B and E.

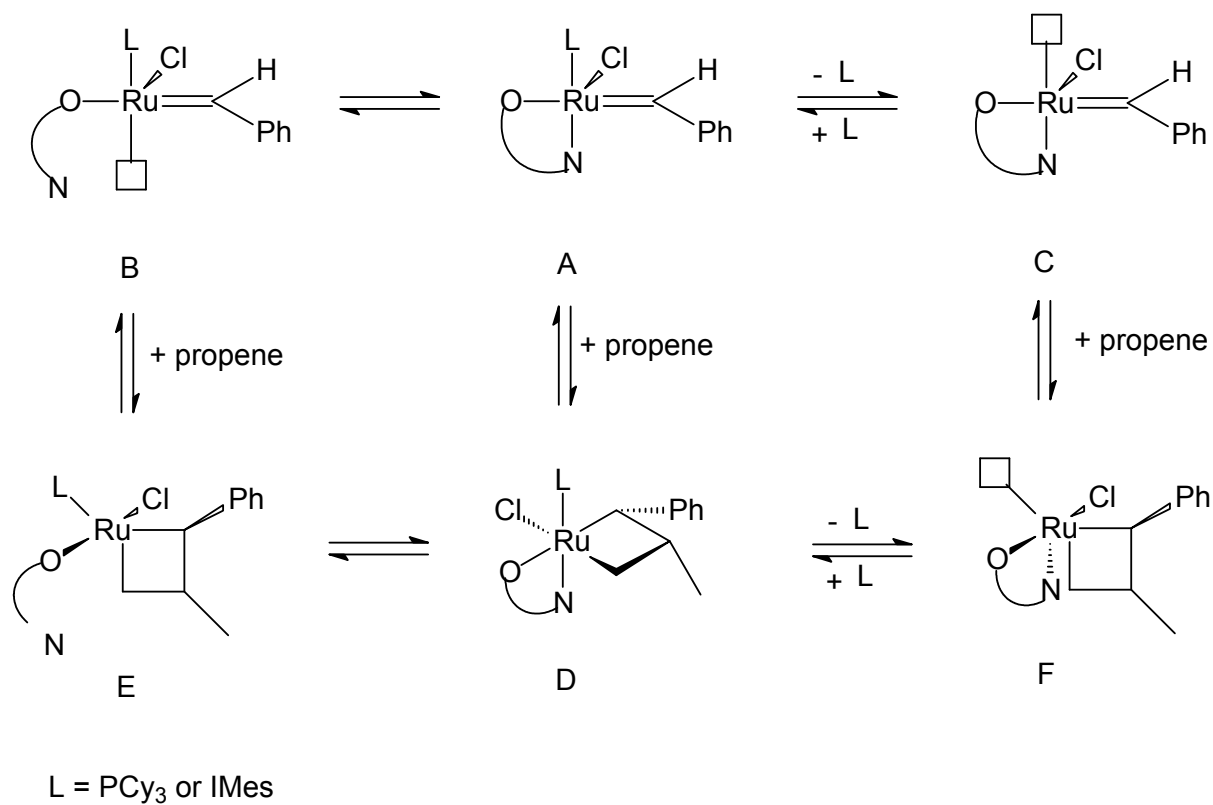


Figure 4.3: Possible reaction pathways for Grubbs-type catalysts with hemilabile ligands.

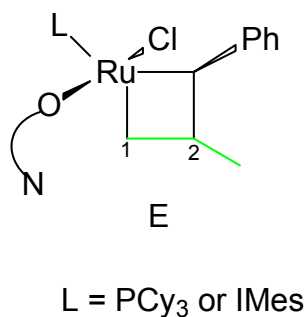


Figure 4.4: Starting structure for PES scan.

The process between A and C is the dissociation of the phosphine ligand, where Gr1 was used, to obtain the 14-electron species (C). Calculations performed by Jordaan² indicated that dissociation of the phosphine ligand can be in competition with de-coordination of the nitrogen since the two processes require nearly equal amounts of energy. Due to results obtained by Jordaan² showing that the dissociation of the H₂IMes is unfavourable to the dissociation of the labile N-atom by 45 kcal/mol, the process between A and C was not investigated for Gr2-type precatalysts with pyridinyl- alcoholato ligands. When a coordination site is unoccupied as in structure C, the substrate propene can become coordinated, and the formation of the metallacycle can result (F). In order to determine the viability of the pathway between A and F, structures corresponding to A, C and F had to be constructed and optimised. It was assumed in this study that no significant energy barrier would exist between structures A and C since this step involves only dissociation and, therefore, transition structure searches were not performed for this step. Transition structure searches were performed using structure F in the same manner as for structure E.

The route from A to D is an associative pathway (not previously investigated) and structure D is an 18-electron metallacycle complex. In order to determine the viability of the pathway between A and D, structures corresponding to A and D had to be constructed and optimised. To obtain the energy barrier for this route, a transition state search was performed using structure D, in a similar manner as for structure E previously. The PES scans obtained for these transition state searches were animated to determine the possibility of a concerted mechanism.

The electronic energies of the three types of metallacycles, E, D and F (Figure 4.3), were compared with one another after being mass balanced.

4.2 Computational methods

4.2.1 Hardware

Two types of hardware were used:

- A personal computer with one CPU was used for conformer search calculations with the following specifications:
Operating system : Microsoft Windows XP Professional (with service pack 2)
Processor : Intel Core 2 Quad 2.66 GHz

Memory : 3.46 GB of RAM

- **HPC cluster:**⁴ (The production HPC currently has 41 nodes and 336 cores reaching more or less 4.2 teraflops)
336 CPU Cluster
1 x Master Node: HP BL460C G6 - 2 Quad Core 2.93 GHz, 16GB RAM,
2 146 GB HDD
40 X Compute Nodes :HP BL460C G6 - 2 Quad Core 2.93 GHz, 16GB RAM,
2 146 GB HDD, ProLiant BL2x220c G5, HP BL460C G1
1 x HP EVA 4400 SAN 3TB
1X Storage Server : HP BL460C G6
Operating system on compute nodes: Scientific Linux SL release 5.3
Cluster operating system : Rocks 5.2 - Scientific Linux SL release 5.3

4.2.2 Software

All computational results in this study were calculated by using the DMol³ DFT (Density Functional Theory) code as implemented in Accelrys Materials Studio 4.2 and 5.0. DFT was used since it usually gives realistic geometries, relative energies and vibrational frequencies for transition metal compounds. The non-local generalised gradient approximation (GGA) functional by Perdew and Wang (PW91)⁵ was used for all geometry optimisations along with the following specifications:

- A medium quality of convergence tolerance using 2×10^{-5} Ha (energy), 0.004 Ha/Å (Max. force) and 0.005 Å (Max. displacement).
- A medium self-consistent field (SCF) of 1×10^{-5} Ha using a maximum of 1000 SCF cycles and octupole multipolar expansion.
- In this study, a polarised split valence basis set, termed double numeric polarised (DNP) basis set was used. In Materials Studio 5.0, the 3.5 basis file was used.

4.3 Method

4.3.1 Validation of the model used

The Gr1 precatalyst was sketched and geometrically optimised in Materials Studio 5.0 using the settings mentioned in paragraph 4.2.2. Comparisons of a few selected

bond lengths, bond angles and dihedral angles around the Ru centre were made with crystallographic data obtained by Nguyen *et al.*⁶ Bond lengths are overestimated, but an acceptable correlation is made.

Table 4.1: Crystallographic and theoretical values of key bond lengths and angles of Gr1

	Nguyen ⁵	Calculated ^a
Bond lengths (Å)		
Ru=C	1.838(2)	1.880
Ru-Cl _{avg}	2.390(1)	2.459
Ru-P _{avg}	2.416(1)	2.475
Bond angles (°)		
Cl-Ru-Cl	168.21(2)	169.93
P(1)-Ru-P(2)	161.90(2)	159.31
Ru=C-R	136.70(2)	137.54

^a DMol³ GGA/PW91/DNP – full DFT calculation of geometries.

4.3.2 Construction of ‘closed’ precatalysts A

Using the template illustrated in Figure 4.1 with PCy₃ as ligand L, thirty different ruthenium complexes, with a chelating pyridinyl-alcoholato ligand, were sketched by varying the groups R₁ and R₂ as shown in Table A.1, in Appendix. Table A.2 represents structures in which a single ring structure is incorporated into the pyridinyl-alcoholato ligand. A few Gr2-type catalysts with the bidentate ligand were also constructed as shown in Table A.3. These complexes were all geometrically optimised in Materials Studio 4.2 using the settings as shown in paragraph 4.2.2. Frequency calculations were performed in order to confirm if the optimised structures were minimum structures by verifying that they had no imaginary frequencies. Structures, which had imaginary frequencies, were altered very slightly by changing some bond or dihedral angle and re-optimised. These steps were followed until all structures had only positive frequencies. The electronic energies of these optimised precatalysts were used to determine the relative energies of all possible complexes resulting from the various pathways illustrated in Figure 4.3.

A few of these precatalysts were re-optimised in Materials Studio 5.0. A comparison of a few selected bond lengths, angles and dihedral angles were made between the optimised structures of Materials Studio 4.2 and 5.0 (See Table 4.2), and no significant differences were found to warrant recalculation of all precatalysts in Materials Studio 5.0.

Table 4.2: Comparison of a few selected bond lengths and angles of a structure having $R_1 = H$, $R_2 = \text{adamantane}$ and $L = \text{PCy}_3$ (Figure 4.1). Optimised in Materials Studio 4.2 and then in Materials Studio 5.0.

	$R_1 = H$; $R_2 = \text{adamantane}$ (closed structure)	
	MS 4.2 ^a	MS 5.0 ^a
Bond lengths (Å)		
Ru=C	1.88	1.88
Ru-Cl	2.41	2.40
Ru-P	2.41	2.41
Bond angles (°)		
P-Ru-Cl	88.79	88.95
P-Ru-O	98.65	98.45
N-Ru=C	99.21	99.25
	$R_1 = H$; $R_2 = \text{adamantane}$ (metallacycle)	
	MS 4.2	MS 5.0
Bond lengths (Å)		
Ru-O	1.94	1.94
Ru-Cl	2.31	2.31
Ru-P	2.73	2.73
Bond angles (°)		
P-Ru-Cl	89.45	89.62
P-Ru-O	99.71	99.62
O-Ru-Cl	119.57	120.25

^a DMol³ GGA/PW91/DNP – full DFT calculation of geometries

4.3.3 Construction of 'open' precatalysts B

For all 30 optimised 'closed' precatalysts A, the nitrogen to ruthenium bond was deleted to produce 'open' complexes B and conformer searches were performed using DFT. The cyclohexyl rings of the phosphine ligand were 'frozen' during conformer searches (Figure 4.5).

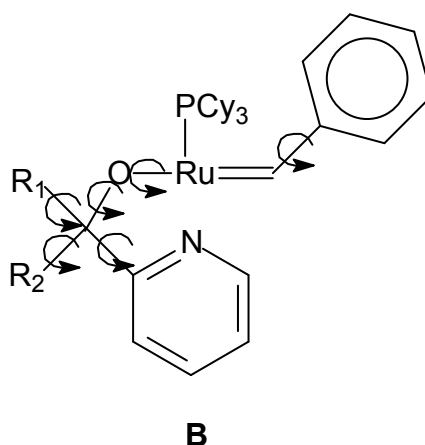


Figure 4.5: Curved arrows show bonds around which rotation occurred during conformation searches.

The number of conformer calculations varied according to R_1 and R_2 groups attached to pyridinyl-alcoholato ligands. The systematic grid scan was used as a search method with a study table and trajectory as output. The following parameters were selected:

- scale van der Waals radii to 40%
- scale vicinal radii to 40%
- scale H-bond radii to 40%
- restraint force constant 1000 kcal/mol/rad²
- perturb reference structure

From the 'open' conformers obtained, structures having a low relative energy combined with a spatial arrangement that would allow access to the active site by the substrate, were chosen. Optimisation of the 'open' conformer was performed in Materials Studio 5.0.

In cases where the nitrogen moved back to a position under the ruthenium after optimisation, the torsion was altered to open the coordination site and the altered structure was re-optimised. This process was continued until an optimised open structure was obtained.

Five structures that were investigated theoretically and experimentally by Huijsmans³ and three structures investigated by Jordaan⁷ (See Table A.3 in Appendix) were also drawn and optimised both in the closed and open forms. These structures consist of Gr2 precatalysts with chelating pyridinyl-alcoholato ligands as shown in Figure 4.1 with L = IMes.

An article by Braunstein *et al.*⁸ states that there should be small energy differences between the ‘open’ and ‘closed’ situations of the bidentate hemilabile ligand, therefore, a comparison of the total energies in kcal/mol of the ‘closed’ precatalysts and the ‘open’ precatalysts was made (Table A.4 in Appendix). Such comparisons are possible since the structures differ only in the absence of a nitrogen-ruthenium bond and their spatial orientations. Unfortunately, Braunstein *et al.*⁸ did not give a quantitative indication as to what a ‘small’ energy difference would be. The results from this study can, therefore, not be compared quantitatively with the limitation on hemilability which they have imposed. The energy differences between the ‘open’ and ‘closed’ structures were used as an indication of the viability of hemilability.

4.3.4 Construction of 16-electron metallacycles E

From the geometrically optimised ‘open’ precatalysts B, metallacycle intermediates, E was constructed using propene as a substrate. All of these structures were optimised in Materials Studio 5.0.

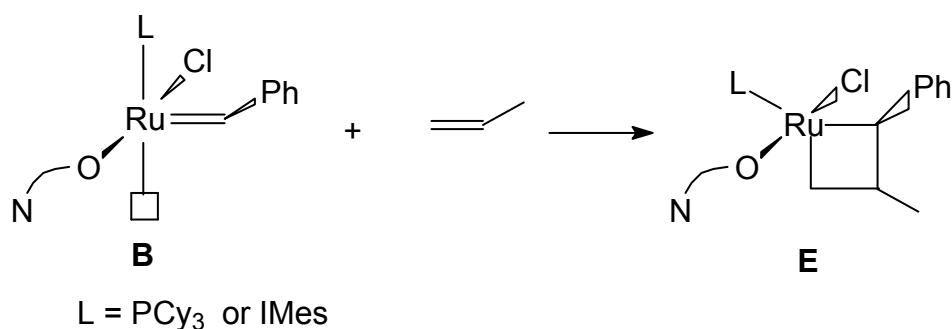


Figure 4.6: Construction of metallacycles E from minimised ‘open’ precatalysts B

4.3.5 Construction of phosphine free precatalysts C

The geometrically optimised 'closed' Gr1-type precatalysts A was altered by removing the PCy₃ ligand and the resulting 14-electron species C was geometrically optimised (Fig 4.7). The total electronic energy for the optimised phosphine ligand and optimised 14-electron ruthenium species C combined can then be compared to the 'closed' (A) and 'open' structures B since the number of electrons are the same. These energy differences can assist in ascertaining if phosphine dissociation is more viable than de-coordination of the soft atom of the bidentate ligand.

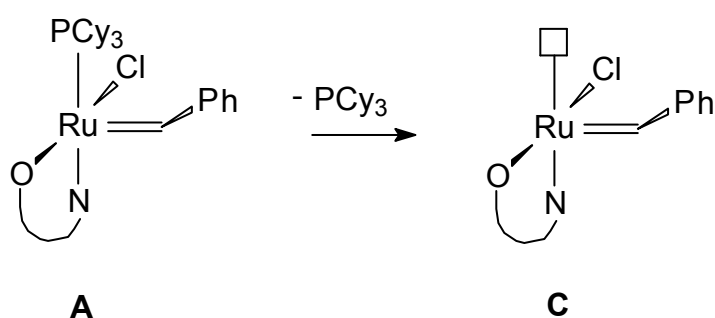


Figure 4.7: Removal of phosphine ligand from Grubbs 1 type precatalysts with hemilabile ligands

The Gr1 and Gr2 structures were also altered by removing the PCy₃ ligand. This was performed twice for Gr1, once for each phosphine ligand. Each altered precatalyst was optimised.

4.3.6 Metallacycles F constructed from the optimised phosphine free structures C

Since it has been established that alkene metathesis proceeds via the dissociation of the phosphine ligand for the first generation Grubbs catalysts, this mechanism was also considered for the Gr1-type catalysts having hemilabile ligands. From the optimised phosphine free precatalysts C, metallacycle intermediates F were constructed using propene as a substrate (Fig 4.8). All of these structures were optimised in Materials Studio 5.0.

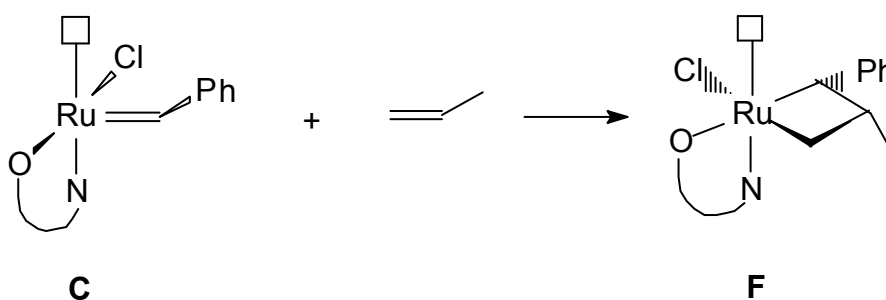


Figure 4.8: Construction of metallacycles from phosphine free structures.

4.3.7 Construction of 18-electron metallacycles D

Since an associative mechanism with hemilabile catalysts has not been investigated in previous studies, metallacycle structures with both the nitrogen and the ligand group coordinated was constructed (Fig 4.9). The resulting 18-electron metallacycles D would be the product of an associative mechanism. These structures were optimised in Materials Studio 5.0.

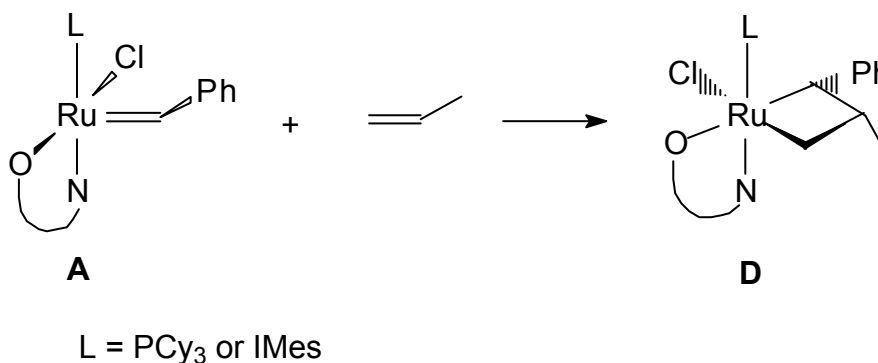


Figure 4.9: Construction of 18-electron metallacycles D.

4.3.8 Comparing complexes

A selection of bond lengths and bond angles around the ruthenium centre were obtained in order to make comparisons between all constructed complexes. Bond lengths were used as an indication of the relative strengths of bonds between the metal centre and ligands and changes in bond order. Bond angles around the ruthenium centre were used to determine whether the 5 coordinated complexes was a trigonal bipyramidal shape or square pyramidal.

4.3.9 Performing PES scans for various reaction pathways

In order to compare the energy differences between different pathways, PES scans were performed on a few selected 16- and 18-electron metallacycles D, E and F in order to obtain transition state structures for each pathway. Transition state structures having only one imaginary frequency were identified. The energy barriers associated with the transition state structures can be an indication of which reaction pathways are likely to be followed.

From the PES scans animations, graphics of a few selected structures were studied in order to follow the approach of propene to the complexes and to observe any event of a concerted mechanism.

4.3.10 Confirming the orbitals involved in bonding between precatalyst and substrate

In a previous study, du Toit⁹ determined that the interaction of the substrate HOMO and the Grubbs catalyst LUMO was favourable over the interaction of the substrate LUMO and Grubbs catalyst HOMO. In order to confirm whether these are the interactions to consider for the hemilabile Grubbs type precatalysts, a few selected structures were obtained from the frames of a few selected PES scans in order to perform calculations that will make it possible to obtain the graphics for the HOMO and LUMO orbitals of the precatalyst and substrate.

In Figure 4.10 below, the HOMO and the LUMO of the precatalyst as the propene approaches is shown. The main contributor to the LUMO (Figure 4.10(a)) is the metal orbitals. This is expected since there are vacant d orbitals on the metal atom. It is also observed that LUMO lobes appearing on the propene at this distance, already contribute to the complex LUMO likely due to a vacant p_z orbital of the carbon atom. On the graphic (b), a HOMO orbital on the propene is directed towards the metal centre. A strong interaction between the metal centre and the phosphine ligand is also observed.

In Figure 4.11(a), the part of the LUMO orbitals which are visible on the metal centre of the precatalyst is due to the contribution of the empty d orbitals of the metal atom to the LUMO. The contribution to the LUMO by the propene is insignificant compared

to the contribution of the precatalyst to the LUMO. The graphic (b) shows the HOMO orbital of the propene directed towards the metal centre.

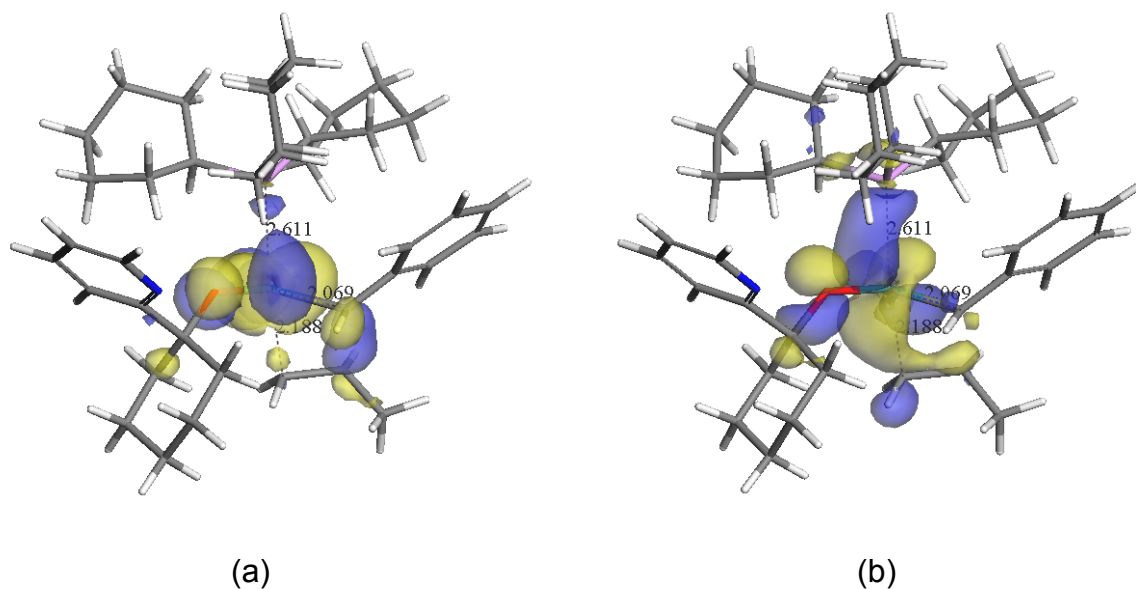


Figure 4.10: LUMO (a) and HOMO (b) graphics for an open cyclohexyl Gr1-type precatalyst with hemilabile ligand and incoming propene.

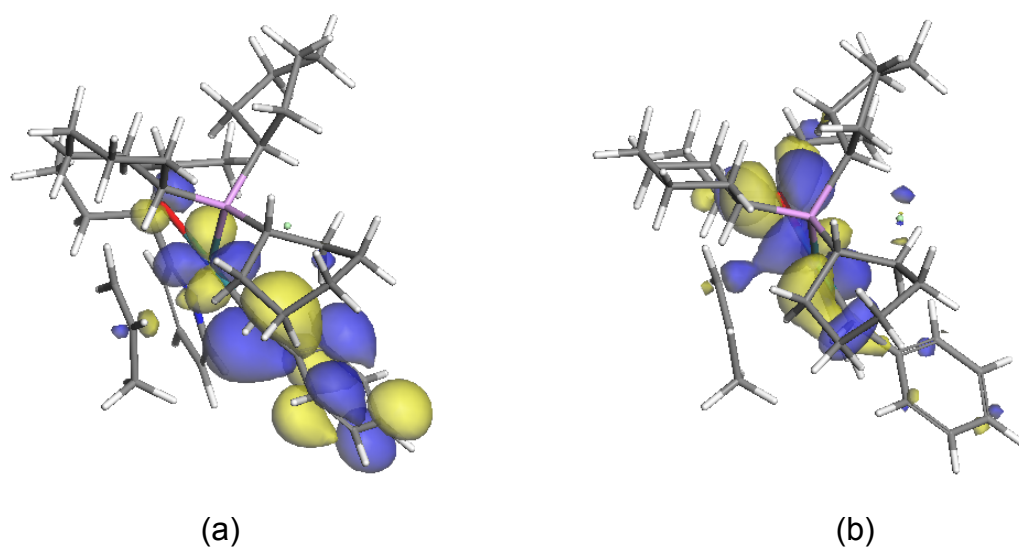


Figure 4.11: LUMO (a) and HOMO (b) graphics for a closed cyclohexyl Gr1-type precatalyst with hemilabile ligand with incoming propene (viewed from phosphine ligand end).

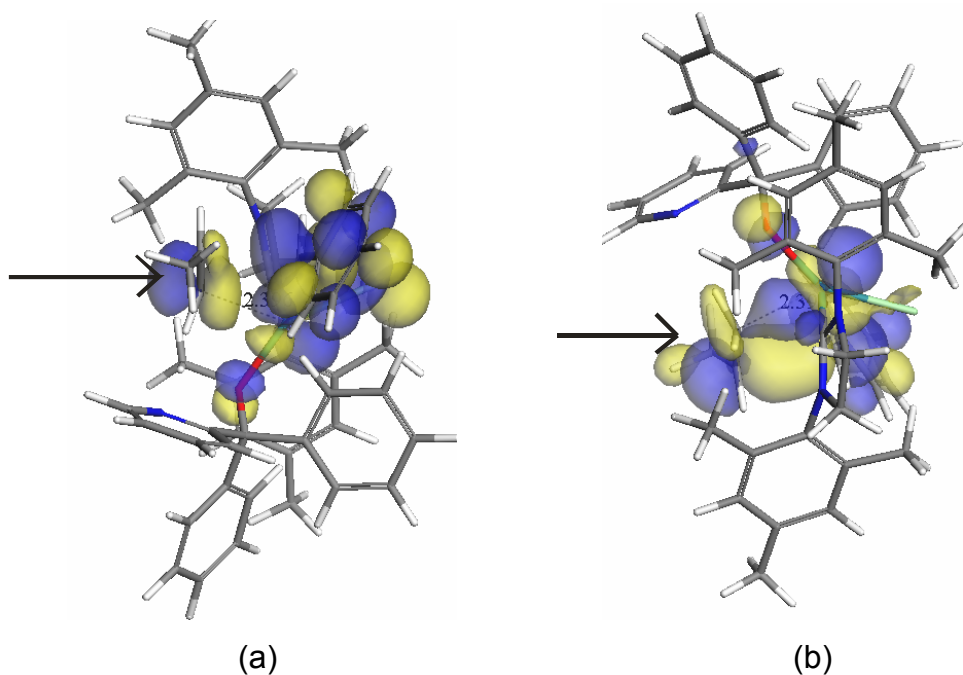


Figure 4.12: LUMO (a) and HOMO (b) graphics for an open Gr2-type precatalyst with hemilabile ligand and approaching propene.

The LUMO orbitals are made up of a contribution from the propene (indicated on the left of graphic (a) in Figure 4.12), and is due to π^* antibonding orbital, and the LUMO contribution of the precatalyst is concentrated around the metal centre. In graphic (b) HOMO orbitals are present between the propene and precatalyst and are directed towards the metal centre and carbene carbon. This is indicative of four atoms interacting simultaneously in a metallacycle.

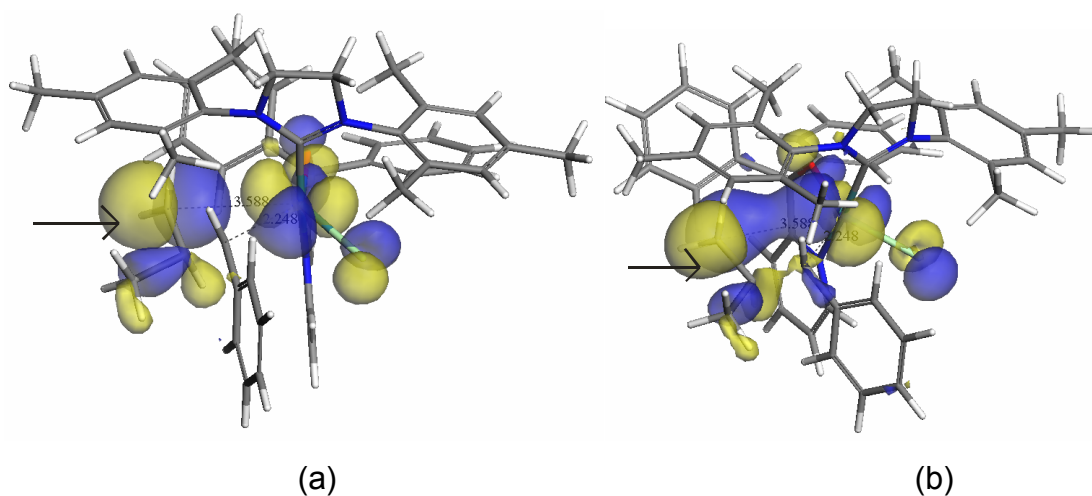


Figure 4.13 LUMO (a) and HOMO (b) graphics for a closed Gr2-type precatalyst with hemilabile with approaching propene.

From graphic (a) in Figure 4.13, we can observe that the d orbitals of the metal atom contribute to the LUMO lobes located on the precatalyst. The LUMO lobes located on the propene indicated to the left of graphic (a) seem larger than in previous graphics possibly due to the absence of a double bond in the propene. In graphic (b), we see the HOMO lobes located between the propene indicated on the left and the metal centre, even at a distance of 3.58 Å from the ruthenium atom, indicative of a good interaction between substrate and precatalyst metal centre.

From these selected graphics, we can conclude that the propene interacts with the metal centre of the precatalyst whether the precatalyst is in the open or closed form. These interactions remain the same regardless of the approach of the propene. These graphics agree with the observations made by du Toit.⁹ For further confirmation, the HOMO and LUMO energies of some precatalysts were calculated and compared with the HOMO and LUMO energies of propene. The comparisons are tabulated in Table 4.3.

Table 4.3: Comparison of a few HOMO and LUMO energies and the difference in energies between a few precatalysts and propene

	LUMO energy (eV)	HOMO energy (eV)	$ \text{LUMO}_{\text{propene}} - \text{HOMO}_{\text{precatalyst}} $	$ \text{LUMO}_{\text{precatalyst}} - \text{HOMO}_{\text{propene}} $
Propene	0.253	5.949		
Precatalysts: $R_1 = R_2$				
Ethyl (Gr 1)	2.513	4.250	3.997	3.436
Phenyl (Gr 2) closed	2.433	3.962	3.709	3.516
Phenyl (Gr 2) open	2.565	4.452	4.199	3.384

From the last two columns in Table 4.3, it can be seen that the HOMO-LUMO gap is smaller when the HOMO of the propene interacts with the LUMO of the precatalyst. This supports what is observed in the graphics, that the LUMO orbital of the precatalyst will interact with the HOMO of the propene during bond forming. In this study, only the LUMO energies of all other optimised precatalysts will be compared

with the HOMO energies of the propene to assess and compare the reactivities of various precatalysts with propene as substrate.

4.3.11 Obtaining HOMO-LUMO energy differences for precatalysts and substrates

The HOMO energies of optimised propene and free phosphine were calculated. These were compared with the LUMO energies calculated for precatalysts. These energy differences will indicate if competition exists between coordination of the alkene and re-coordination of the phosphine ligand.

4.3.12 Obtaining HOMO-LUMO gaps for precatalysts

The HOMO and LUMO energies for numerous optimised 'open', 'closed' and 'less PCy₃' precatalysts were calculated. The differences in these energies were determined to obtain the HOMO-LUMO gap of each precatalyst. These energy differences within a structure give an indication of its stability. The gaps of various precatalysts can then be compared, and predictions can be made regarding their relative reactivity.

4.3.13 Hirshfeld charge analysis

Hirshfeld charge analysis was done on ruthenium and surrounding atoms in all precatalysts in order to assess how electron distribution changes from complex to complex. These charges can be used to assess electron-donating abilities of the different ligands attached to the metal centre.

4.4 References:

- [1] Jordaan, M., and Vosloo, H. C. M., *Adv. Syth. Catal.*, 2007, **349**, 184.
- [2] Jordaan, M., and Vosloo, H. C. M., *Molecular Simulation*, 2008, **34**, 997.
- [3] Huijsmans, C.A.A, ***Modelling and Synthesis of Grubbs type complexes with hemilabile ligands***, MSc-dissertation (North-West University), 2009.
- [4] Author : North-West University High Performance Computer Centre
<http://efundi.nwu.ac.za/access/wiki/site/4ba488f2-2b27-43be-b5f4-f1d97148ec98/home.html>. Year 2010 [Date of access: Aug 2010].
- [5] Perdew, J. P. and Wang, Y., *Phys. Rev.*, 1992, **B45**, 13244.

- [6] Nguyen, S.T. and Trnka, T.M. in ***Handbook of Metathesis***, Grubbs, R.H., Ed., *The Discovery and Development of Well-Defined, Ruthenium-Based Olefin Metathesis Catalysts*, Vol. 1, Wiley, 2003, p. 61.
- [7] M. Jordaan, ***Experimental and theoretical investigation of new Grubbs type catalysts for the metathesis of alkenes*** PhD-thesis, North-West University, 2007.
- [8] Braunstein, P., and Naud, F., *Angew. Chem.*, 2001, **40**, 680.
- [9] du Toit, J. I., ***'n Modelleringsondersoek na die meganisme van die homogene alkeenmetatesereaksie***, MSc-dissertation (North-West University), 2009.

CHAPTER 5: Results

The results gathered in this study were used to try and determine if Grubbs type bidentate/hemilabile catalysts would follow the same route as Gr1 and Gr2 catalysts and initiate metathesis via the dissociative mechanism. The three main questions that needed to be answered about these Grubbs type bidentate/hemilabile catalysts were:

1. Are these precatalysts hemilabile? Is hemilability an essential step in the dissociative mechanism?
2. Does phosphine dissociate in the Gr1-type catalysts with bidentate/hemilabile ligands? If it does, at what stage during the mechanism does it dissociate?
3. Is there a possibility that another mechanism other than the dissociative mechanism might be viable?

Upon completion of the construction and optimisation of many precatalysts and metallacycles, frequency calculations, PES scans and various property calculations were performed. These calculations were necessary in order to help answer the above questions and to try correlate structure and electronic properties of the precatalyst with activity and stability assessed in previous studies.

5.1 Calculated Properties

5.1.1 Bond lengths and Energy calculations

Bond length was used as a quantitative measure of the quality of interaction between atoms. Since energy is always required to break bonds, the energy required to break a bond is indicative of the strength of the bond. Poor orbital overlap between atoms results in a weaker interaction between atoms and is reflected by a long bond length, which would require less energy to break.

The comparison between the total electronic energies of the 'open' and 'closed' precatalysts having the same hemilabile ligand indicated relatively large differences in energy for most structures. The energy of the 'open' precatalyst was always higher than the 'closed' precatalyst. These energy differences between the open and closed structures show that energy is required to de-coordinate the nitrogen from the

ruthenium centre. (Table 5.1 and Table A-4) It cannot be said with certainty that this observation does not agree with the limitation imposed by Braunstein *et al.*¹ for hemilability as discussed in Chapter 1. It only takes 4.5 kcal/mol of energy to break the hydrogen bonds between water molecules, which is significantly lower than the energy required to de-coordinate the nitrogen in this study.

The amount of energy required to de-coordinate the pyridine ring varies depending on the groups attached to the hemilabile ligand. The Gibbs free energy values for de-coordination of nitrogen ranges from 11.7 to 32.6 kcal/mol. (Table 5.1) The difference between the lowest and the highest value could not be correlated to other calculated properties such as Hirshfeld charges, bond angles, bond lengths or HOMO-LUMO energy gaps. The only explanation that can be given with the current information for the differences in energy required for de-coordination of the pyridine ring in the Gr2-type precatalysts is the steric bulk of the groups R_1 and R_2 . As the R_1 and R_2 groups become bulky the energy required to de-coordinate the pyridine ring becomes less. The researcher's hypothesis that hemilability will exist in some complexes and not in others for a particular temperature is supported to a degree by these results. Where very little energy is required to de-coordinate the nitrogen, hemilability should be viable.

Jordaan² calculated the electronic energies required for de-coordination of nitrogen for cyclohexyl Gr1 and Gr2 precatalysts to be 20.3 and 16.1 kcal/mol, respectively. These values correspond well with those obtained in this study. (Table 5.1) The small differences can be attributed to the fact that many conformers can exist for the 'open' structure, and those structures optimised by Jordaan, might not be identical conformers to those obtained in this study.

One particular Gr2-type precatalyst with hemilabile ligand investigated by Huijsmans³ experimentally (R_1 = Ph, R_2 = isopropyl) was found to have a long lifetime. This study calculated that this particular precatalyst required an electronic energy of 34.6 kcal/mol to 'open'. This was the highest value (Table 5.1) obtained for all precatalysts investigated computationally. This observation implies that the more energy that is required to 'open' the structure the longer the lifetime of the catalyst will be. Since the nitrogen does not de-coordinate easily in some cases, coordination sites remain protected, and the catalyst will be less prone to degradation. This result

also means that higher temperatures might be required to initiate metathesis. This was, in fact, one of the goals of Denk *et al.*⁴; their aim was to design a precatalyst with a chelating ligand that would open up a coordination site at elevated temperatures but remain 'closed' at room temperatures to keep the precatalyst stabilised. Longer catalyst lifetimes are sought after since catalysts can be expensive to replace.

For the Gr1-type precatalysts with bidentate ligands, a comparison of the total electronic energy of the 'closed' structure with that of the closed structure without phosphine, revealed that a larger amount of energy is required to dissociate the phosphine ligand than to de-coordinate the nitrogen. (Table 5.1 and Table A-4) Removal of the phosphine ligand from the Gr1 bidentate complexes requires more energy than for Gr1 and Gr2. (Table 5.1) Based on these results, it is, therefore, inconceivable that the phosphine ligand will dissociate in preference to de-coordination of the pyridine ring. The de-coordination of the pyridine ring is a better option than the dissociation of the phosphine ligand since it has been shown that free phosphine contributes to the decomposition of the Grubbs type catalysts.⁵ De-coordination of the nitrogen can also lead to an entropy increase of the system if many conformers of the same or similar energy are possible, which could explain why this route would be more favourable than phosphine dissociation.⁶

A comparison of bond lengths in precatalysts having the bidentate/hemilabile ligand showed that the Ru-P bond length is always longer than the Ru-N bond and that the Ru-O bond is the shortest of the three. (Table 5.2 and Table A.6) This is to be expected since oxygen and nitrogen atoms being smaller than the phosphorus atom can approach the ruthenium atom better when electrons are shared between them. This result would suggest that the phosphine ligand would de-coordinate from the ruthenium rather than the nitrogen. However, a comparison of Ru-P bond lengths with the Gr1 catalyst shows that the Ru-P bond, in the complex, with a bidentate/hemilabile ligand is always shorter than the Ru-P bonds in Gr1. This shorter bond length between ruthenium and phosphorus implies a strong interaction and explains why relatively large amounts of energy is required to dissociate the phosphine ligand from the bidentate precatalyst. From these results, it can be inferred that the phosphine ligand in these Gr1-type hemilabile complexes plays a

larger electron donating role than in Gr1. The fact that the Ru-N bond is shorter than the Ru-P bond could simply be because nitrogen is a smaller atom than phosphorus and can approach ruthenium more closely and not because its electron donation to the ruthenium is better. The nitrogen is a more electronegative element than phosphorus and will hold onto its electrons. The very short Ru-O bond length tells us that the oxygen atom will not de-coordinate from the complex but will play the anchoring role of this bidentate/hemilabile ligand.

Table 5.3 shows the bond lengths of closed metallacycles that would result from the associative mechanism. No significant changes occur in the Ru-O and Ru-N bonds. A lengthening of the Ru-L bond occurs probably due to the steric hindrance around the coordinately saturated metal centre. The Ru-P bond also lengthens in most of the open metallacycles as can be seen from Table A.6. Unfortunately, insufficient data was obtained on the metallacycles' 'less PCy₃' to determine if they are lower in energy than the 'closed' and 'open' metallacycles.

5.1.2 Conformer searches

A closer look at some of the optimised 'open' structures revealed that these conformers, after optimisation, have nitrogen placed very close to ruthenium. These structures indicated no bond between ruthenium and nitrogen, but the distance between the two atoms fell within the range for a single bond. (Figure 5.1) These structures were not regarded as 'open' and although they were altered by rotating the pyridine ring away from the ruthenium centre, the search proved to be difficult in some cases and optimised 'open' structures were not obtained for all complexes. The reason for these difficulties in obtaining an optimised open structure could be as a result of the optimisation procedure. Optimisation procedures search for a minimum and many 'open' conformers lie on the potential energy surface, and since the closed structure is lower in energy than the open structures, the optimisation procedure settles on a 'conformer' where the nitrogen lies below the ruthenium as in the 'closed' structure. These cases were limited to structures where R₁ and R₂ were bulky ligands.

Table 5.1: Electronic energies in kcal/mol of Grubbs type catalysts for the dissociative mechanism. ΔG_{298K} values in brackets.

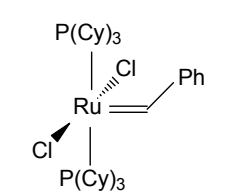
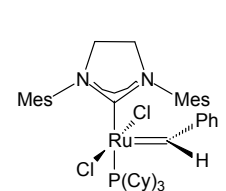
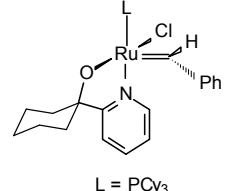
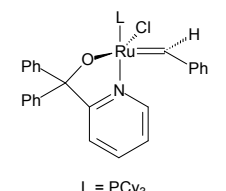
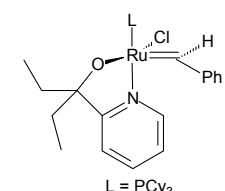
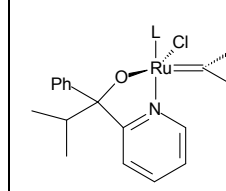
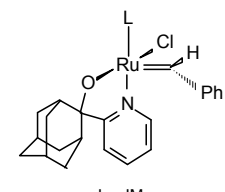
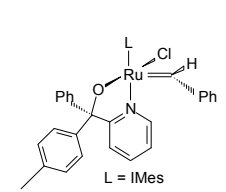
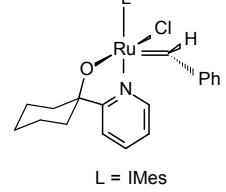
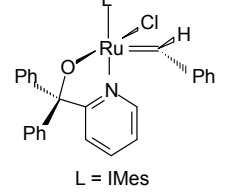
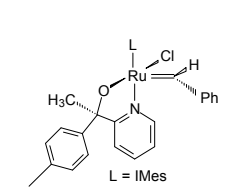
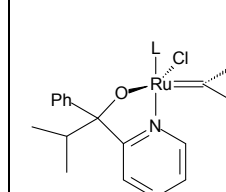
	 <p>Gr1</p>	 <p>Gr2</p>	 <p>Cy-Gr1 L = PCy₃</p>	 <p>PUK-Gr1 L = PCy₃</p>	 <p>diEt-Gr1 L = PCy₃</p>	 <p>L = PCy₃</p>
Loss of PCy ₃	37.82 (24.4)	37.64 (19.91)	42.23 (27.39)	42.37 (30.02)	42.07 (26.75)	42.80 (27.85)
De-co-ordination of Nitrogen	NA	NA	17.95 (16.07)	value not determined	21.42 (18.22)	21.24 (19.84)
	 <p>L = IMes</p>	 <p>L = IMes</p>	 <p>Cy-Gr2 L = IMes</p>	 <p>PUK-Gr2 L = IMes</p>	 <p>L = IMes</p>	 <p>L = IMes</p>
De-co-ordination of Nitrogen	17.89 (14.77)	14.93 (11.71)	17.53 (16.17)	24.36 (19.39)	20.59 (19.94)	34.59 (32.61)

Table 5.2: Bond lengths around ruthenium centre for the dissociative pathway involving hemilability measured in Å.

Structure		Ru-L	Ru=C	Ru-N	Ru-O	Ru-Cl
Gr1	Precatalyst	2.45	1.88	NA	NA	2.46
	Less PCy ₃	2.30	1.87	NA	NA	2.33
	Metallacycle	2.34	2.18	NA	NA	2.38
Gr2	Precatalyst	2.13	1.88	NA	NA	2.45
	Less PCy ₃	1.99	1.87	NA	NA	2.35
	Metallacycle	2.07	2.03	NA	NA	2.42
Cy-Gr1	Precatalyst	2.40	1.88	2.19	2.00	2.40
	Open complex	2.30	1.88	NA	2.00	2.35
	Metallacycle [‡]	2.68	2.14	NA	1.93	2.31
Cy-Gr2	Precatalyst	2.09	1.88	2.18	2.03	2.43
	Open complex	2.00	1.88	NA	2.00	2.38
	Metallacycle [‡]	2.02	2.25	NA	1.97	2.41
diEt-Gr1	Precatalyst	2.40	1.88	2.18	2.01	2.40
	Open complex	2.29	1.88	NA	2.00	2.35
	Metallacycle [‡]	2.72	2.12	NA	1.93	2.31
PUK-Gr2	Precatalyst	2.09	1.88	2.18	2.04	2.43
	Open complex	2.00	1.88	NA	2.03	2.38
	Metallacycle [‡]	2.08	2.28	NA	2.05	2.44
[‡] refers to 16-electron species with N de-coordinated L = PCy ₃ or IMes						

Table 5.3: Bond lengths around ruthenium centre for the associative pathway measured in Å.

Structure		Ru-L	Ru to C(carbene)	Ru-N	Ru-O	Ru-Cl
Gr1	Precatalyst	2.45	1.88	NA	NA	2.46
	Metallacycle	2.84 (top)	2.30	NA	NA	2.40
Gr2	Precatalyst	2.13	1.88	NA	NA	2.45
	Metallacycle	2.42 (top)	2.25	NA	NA	2.42
Cy-Gr1	Precatalyst	2.40	1.88	2.19	2.00	2.40
	Metallacycle [‡]	2.47	2.15	2.16	1.95	2.66
Cy-Gr2	Precatalyst	2.09	1.88	2.18	2.03	2.43
	Metallacycle [‡]	2.18	2.12	2.17	1.96	2.69
diEt-Gr1	Precatalyst	2.40	1.88	2.18	2.01	2.40
	Metallacycle [‡]	2.47	2.13	2.19	1.97	2.66
PUK-Gr2	Precatalyst	2.09	1.88	2.18	2.04	2.43
	Metallacycle [‡]	2.15	2.34	2.15	2.00	2.37
		[‡] refers to 18-electron species with N coordinated L = PCy ₃ or IMes				

5.1.3 Hirshfeld Charges

The positive Hirshfeld charges for ruthenium is in agreement with the relative electrophilic nature of ruthenium, since transition metals act as Lewis acids.⁷ The negative charges on the carbene carbon, chlorine, oxygen and nitrogen, suggest a nucleophilic character. This confirms that Grubbs type precatalysts with bidentate/hemilabile ligands are Schrock carbenes, which have nucleophilic carbene carbon atoms and that these catalysts will produce products of metathesis. (Table 5.4 and Table A.7) The electrophilic nature (positive charge) of the ruthenium is enhanced when a phosphine group of Gr1 is replaced with the pyridinyl-alcoholate ligand while the nucleophilic nature of the carbene carbon is enhanced. This is as a result of the electronic environment changing completely. One of the phosphine

ligands is replaced by a pyridine ring, and one of the chlorine atoms is replaced by an oxygen atom. Oxygen and nitrogen are very small electronegative elements compared to phosphorus and chlorine and will hold onto their electrons more tightly.

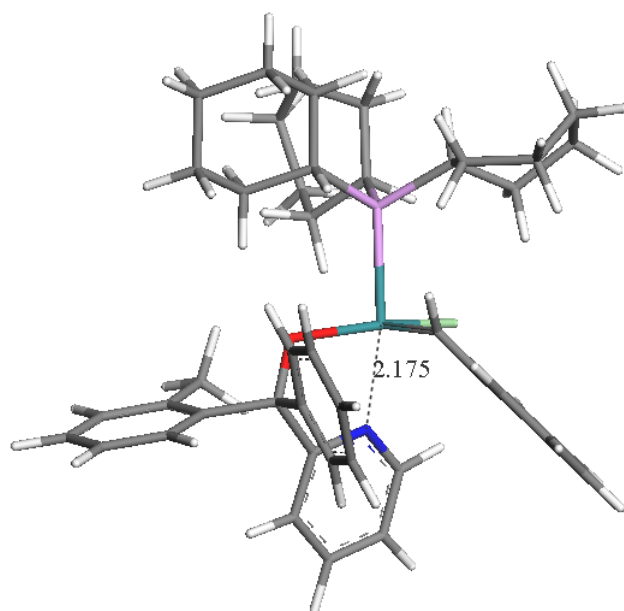


Figure 5.1: An open conformer reverting back to the ‘closed’ structure after optimisation.

Phosphine ligands are known to be good electron donors.⁸ It can be seen from Table 5.4 that the Hirshfeld charge of the phosphorus atom is much more positive than the carbon atom of the IMes ligand indicating that the phosphine ligand donates electrons far better than the IMes ligand. The poorer electron donating ability of the IMes ligand has been shown in a previous study.⁹ The charge on the Ru atom is also seen to be more positive when bound to the IMes ligand. Upon de-coordination of the phosphine group from the ‘closed’ hemilabile precatalyst, the electrophilic nature of the Ru and the nucleophilic nature of the carbene carbon are further enhanced due to the absence of electrons around the ruthenium centre. The electrophilic nature of the Ru is enhanced to a lesser degree when the nitrogen is de-coordinated to form the ‘open’ complex. This is an indication that the nitrogen is not as strong an electron donor as phosphorus, since its de-coordination does not result in a much more positive charge on the ruthenium.

The few Gr2 precatalysts with hemilabile ligands investigated, also revealed an enhancement of electrophilic character of the Ru upon de-coordination of the nitrogen. The Hirshfeld charges on Ru after pyridine de-coordination are more positive when Ru is bound to the IMes ligand. (Table A-6)

The nucleophilic nature of the carbene carbon upon de-coordination of the nitrogen is enhanced in some cases but not in all. In a few cases, the carbene carbon charge became less negative but never positive. These cases were restricted to complexes where the phosphine group was de-coordinated and in other cases where the nitrogen was de-coordinated. The electrophilic nature of a carbene carbon will activate it for reaction with an alkene substrate but will result in cyclopropanation and not produce products of metathesis. Amongst the Gr2 precatalysts with hemilabile ligands studied, only one showed a decrease in the negative charge of the carbene carbon. This precatalyst had R1 and R2 groups of phenyl and isopropyl and was found experimentally to have the longest lifetime.

From Table 5.4, it can be seen that when the nitrogen de-coordinates, the atom of the ligand L bonded to ruthenium becomes more positive indicating a movement of electrons away from the atom probably in the direction of ruthenium to compensate for the loss of electrons as a result of the de-coordination of nitrogen from the ruthenium. The electrons from the chlorine similarly flow away from the chlorine in the 'open' structure of the Gr1-type catalyst with hemilabile ligand.

5.1.4 HOMO and LUMO energies

To obtain an indication of whether the interaction between the precatalyst and the substrate will be favourable, we compare the HOMO energy of the substrate with that of the LUMO energy of the 16-electron and 14-electron precatalysts. In the case of precatalyst less PCy₃, free phosphine competes with propene as substrate.⁸ The smaller the HOMO-LUMO energy gap, the better the chances of there being a reaction between the precatalyst and substrate. From Table 5.5, it can be seen that the HOMO-LUMO energy gap is much smaller for the Gr1 and Gr2 precatalysts than that with hemilabile ligands. Upon dissociation of phosphine ligand from Gr1 and Gr2, the HOMO-LUMO energy gap in the precatalyst less PCy₃ is reduced relative to the closed precatalyst and more significantly for Gr2 than for Gr1. This could explain

Table 5.4: Hirshfeld charges of Ruthenium and atoms around ruthenium centre in Grubbs type catalysts.

Structure		Ru	Carbene C	O	Cl	N	R ₁ CR ₂	Ligand*
Gr1	Precatalyst	0.2095	-0.0696	NA	-0.2514	NA	NA	
	Less PCy ₃	0.2805	-0.0942	NA	-0.2446	NA	NA	0.2900
Gr2	Precatalyst	0.2348	-0.0685	NA	-0.243	NA	NA	0.0292
	Less PCy ₃	0.3103	-0.0849	NA	-0.2476	NA	NA	0.0383
Cy-Gr1	Precatalyst	0.3404	-0.0849	-0.1817	-0.3187	-0.0608	0.0742	0.2777
	Open	0.3304	-0.1137	-0.2212	-0.2634	-0.1278	0.0671	0.2938
	Less PCy ₃	0.391	-0.1134	-0.2518	-0.326	-0.0438	-0.0042	NA
Cy-Gr2	Precatalyst	0.3178	-0.0921	-0.2469	-0.2568	-0.0736	0.0666	0.0228
	Open	0.3549	-0.1053	-0.2368	-0.2564	-0.1329	0.0651	0.0399
*The Hirshfeld charge of the ligand refers to the phosphorus atom of the phosphine ligand or the carbon atom of the IMes ligand.								

the experimental observation that Gr2 has a higher affinity for substrate than Gr1.⁸ Determining the HOMO–LUMO energy gap between the precatalyst less PCy₃ and free phosphine ligand supports another experimental observation that Gr1 has a higher affinity for free phosphine than Gr2.⁸ The HOMO–LUMO energy gap of the precatalysts with hemilabile ligands is also reduced when the phosphine dissociates or the nitrogen de-coordinates. From the table, it can be seen that for the bidentate/hemilabile precatalysts, phosphine also competes with propene for the free co-ordination site. The HOMO-LUMO gap is much smaller for the coordination of the phosphine. (See also Table A-11) These results favour the dissociative mechanism for the Grubbs type catalysts with bidentate/hemilabile ligands.

As mentioned before, the HOMO–LUMO energy gap within the same molecule is an important stability index. A large energy gap implies high stability and a small energy gap implies low stability. A high stability is associated with low chemical reactivity, and low stability indicates high chemical reactivity.¹⁰ These energy differences are indicated in Table 5.6. It can be seen from the HOMO–LUMO energy gaps, that the Gr1 and Gr2 precatalysts are more reactive than the hemilabile complexes both in the form of the 16-electron complexes as well as the 14-electron complexes. These differences in stability/reactivity might explain why Jordaan¹¹ observed that the initiation of the hemilabile complexes was slower than that of the Grubbs catalysts at 60°C. The 16-electron Gr1 precatalyst has a smaller HOMO–LUMO energy gap than the equivalent Gr2. However, the 14-electron complex of Gr2 has a smaller HOMO–LUMO energy gap than the equivalent Gr1. Studies have shown that initiation of Gr2 precatalysts is slower than that of Gr1, but once phosphine has been dissociated, the Gr2 complex is more reactive towards the alkene.⁸ The HOMO-LUMO energy gaps on precatalysts support these observations. The Gr2-type precatalysts with hemilabile ligands are more reactive than their Gr1 counterparts in the ‘closed’ and ‘open’ forms. This follows the trend of Gr1 and Gr2 where Gr2 outperforms Gr1 in alkene metathesis. (See also Table A-12)

Table 5.5: LUMO energies of Grubbs type catalysts in eV and calculated HOMO–LUMO energy gaps between precatalysts and substrate.

	Gr1	Gr2	Cy-Gr1	Cy-Gr2	diEt-Gr1	PUK-Gr2
LUMO energy of precatalyst (eV)	-2.908	-2.697	-2.490	-2.415	-2.513	-2.433
$ E_{\text{LUMO}} - E_{\text{HOMO}}^* $	3.041	3.252	3.459	3.534	3.436	3.516
LUMO energy of precatalyst less PCy_3 (eV)	-2.919	-2.890	-2.838	NA	-2.871	NA
$ E_{\text{LUMO}} - E_{\text{HOMO}}^* $	3.03	3.059	3.111	NA	3.078	NA
$ E_{\text{LUMO}} - E_{\text{HOMO}}^{\ddagger} $	1.871	1.900	1.952	NA	1.919	NA
LUMO energy of open precatalyst	NA	NA	-2.694	-2.487	-2.567	-2.565
$ E_{\text{LUMO}} - E_{\text{HOMO}}^* $	NA	NA	3.255	3.462	3.382	3.384
E_{HOMO}^* for propene (substrate in this study) is -5.949 eV $E_{\text{HOMO}}^{\ddagger}$ for phosphine is -4.790 eV and competes with the substrate						

Table 5.6: HOMO–LUMO energy gaps within precatalysts.

	Gr1	Gr2	Cy-Gr1	Cy-Gr2	diEt-Gr1	PUK-Gr2
Precatalyst $ E_{\text{LUMO}} - E_{\text{HOMO}} $	1.384	1.449	1.780	1.456	1.737	1.529
Precatalyst less PCy ₃ $ E_{\text{LUMO}} - E_{\text{HOMO}} $	1.861	1.744	2.101	NA	2.11	NA
Open precatalyst $ E_{\text{LUMO}} - E_{\text{HOMO}} $	NA	NA	1.922	1.792	1.918	1.887

5.1.5 Investigation of reaction mechanisms

From the PES scans, transition state structures obtained and their electronic energies were compared with the precatalyst energies and used to assess the viability of different reaction routes for the first and second generation Grubbs precatalysts. Although many studies, both experimental¹² and computational,¹³ have previously confirmed that the dissociative mechanism is the mechanism of choice for the first and second generation Grubbs catalysts, applying the researcher's method of investigating various mechanisms to these catalysts was valuable for comparison purposes.

From Figure 5.2, we can see that the electronic energy difference between the 16-electron precatalyst (1) plus propene and the 14-electron species of Gr1 (2) after phosphine dissociation plus propene obtained in this study, agrees with the thermochemical data for phosphine binding energy obtained in the gas phase by Torker *et al.*¹⁴ of 33.4 kcal/mol.

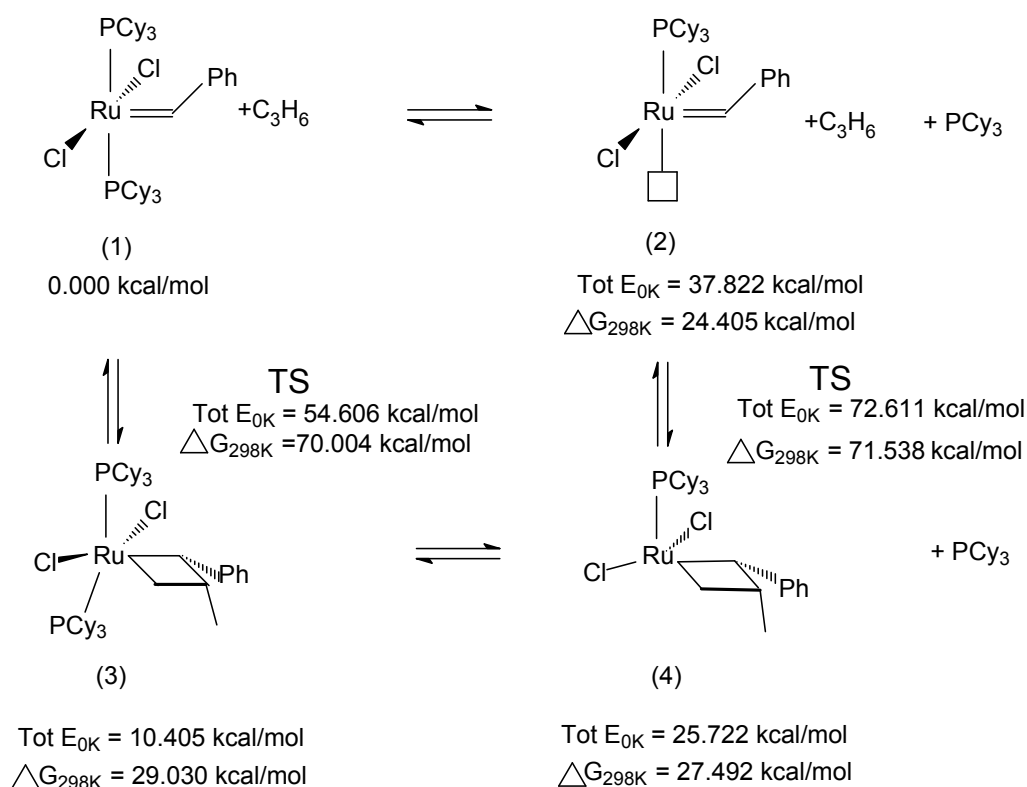


Figure 5.2: Associative and dissociative mechanisms for propene metathesis with Gr1.

Attempts were made to find a transition structure between complex (1) and (2) but energy simply increased as the ruthenium phosphine distance was increased. Previous studies have not calculated transition structures for the dissociation of phosphine since it was assumed that the dissociation of the ligand would not result in considerable rearrangement of the complex.

As can be seen from Figure 5.2, an associative mechanism for Gr1 to produce an 18-electron complex (3), involves an energy barrier of $\Delta G_{298K} = 70.004$ kcal/mol which is relatively larger than the removal of the phosphine ligand of 24.405 kcal/mol. This large difference could certainly favour the dissociative mechanism with phosphine loss being the initiation step. It has been experimentally determined by Grubbs *et al.*¹⁵ that the 14-electron species (2) are more reactive than the 16-electron species (1) and this was confirmed by a Quantum Molecular Dynamics study done by Aagaard *et al.*¹⁶ Aagaard confirmed the experimental findings of Grubbs that less than 5% of unbound phosphine is present in the reaction mixtures and suggested that the dissociation of the phosphine would provide space around the metal centre and could positively influence the electronic structure of the Ru centre. The energy barrier obtained after substrate binding to the 14-electron (2) species is slightly higher than the energy barrier for the 18-electron species (3) which results from the associative mechanism. This together with the energy required to dissociate the phosphine ligand makes the dissociative pathway more energetically expensive than the associative pathway. Other factors which are not included in energy calculations are geometric factors such as effective collisions between species. A large gap in the monophosphine complex would allow the incoming substrate to approach the metal centre with ease and facilitate the correct alignment of the incoming propene. This indicates that more factors other than just the energy involved in various steps of the mechanism must be taken into account when studying reaction mechanisms.

When comparing the Gibbs free energies of the two possible metallacycles, it can be seen that loss of phosphine from the 18-electron metallacycle (3) is exothermic. The loss of phosphine from the 18-electron metallacycle could be for steric relief around the metal centre. It would also result in an increase in entropy. In the event that a 16-electron precatalyst (1) and a substrate molecule collide with the correct orientation

and have enough energy (species in the high-end tail of the Maxwell-Boltzmann velocity distribution) to follow the associative route, the phosphine would probably be lost very quickly after metallacycle formation.

Similarly, results obtained for Gr2 (Figure 5.3) show that energetically, phosphine dissociation is more favourable than an associative mechanism. The energy required for dissociation of the phosphine ligand and the energy barrier associated with the formation of the metallacycle in total is less than the energy barrier encountered in the associative mechanism. The 16-electron metallacycle (4) is also lower in energy than the 18-electron metallacycle (3). The dissociative mechanism will be the route favoured and followed as has been observed experimentally.¹⁵

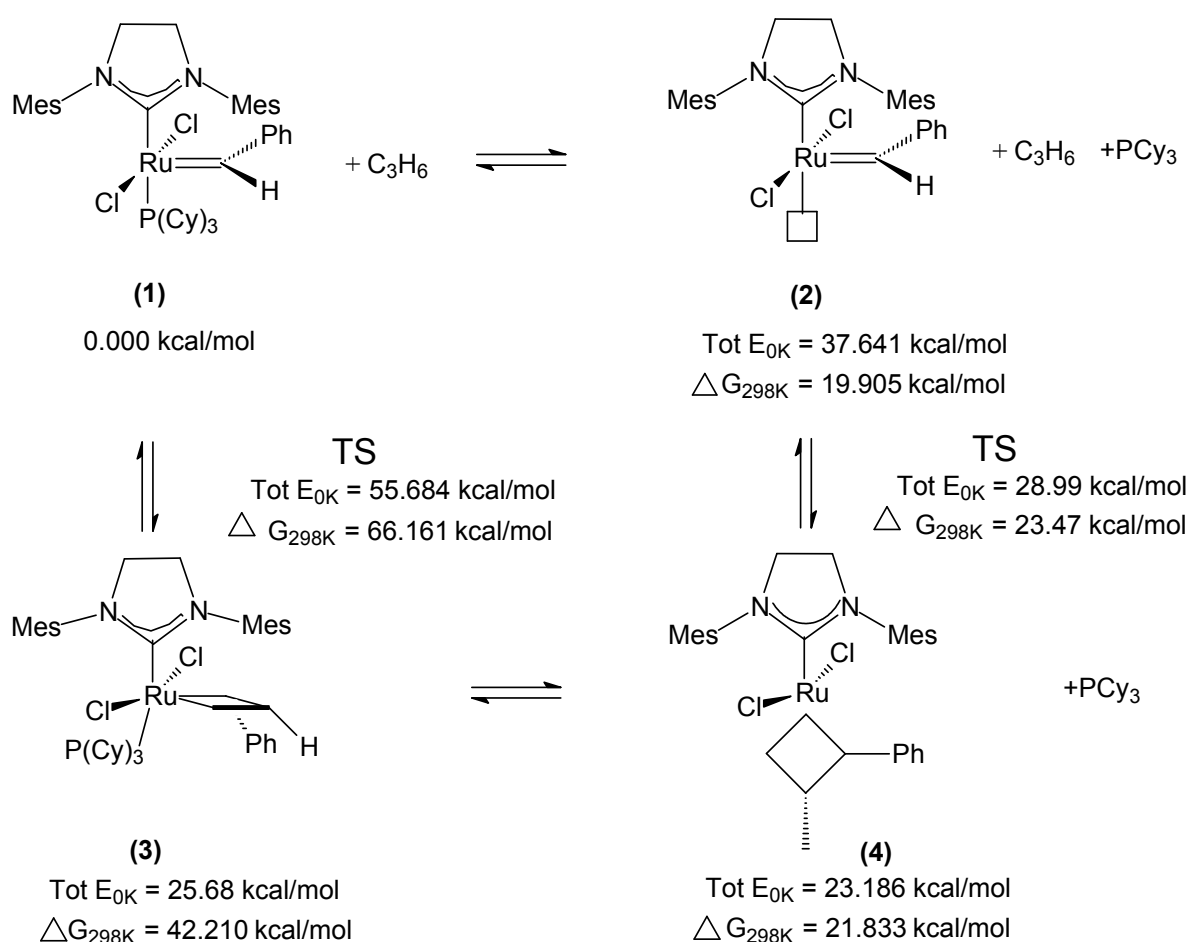


Figure 5.3: Associative and dissociative mechanisms for propene metathesis with Gr2.

The PES scans performed on a few selected Grubbs type catalysts with bidentate/hemilabile ligands were scrutinised to learn more about their mechanisms.

One of the observations made while studying reaction mechanisms of Grubbs type catalysts with bidentate/hemilabile ligands was the changing in length of two bond lengths around the ruthenium centre. These appear shortened in the 14-electron species relative to the 16-electron precatalyst (Figure 5.4 (b)). This indicates that ligands remaining in the 14-electron species increase their electron donation to the metal centre due to the absence of electrons after the opening of a coordination site and hence the bonds around ruthenium shorten. This electron donation by ligands could help to stabilise the 14-electron complex, therefore, making the dissociative pathway more viable. When propene coordinates to the metal centre, it donates electrons from its π bond to ruthenium.⁷ This results in an increase in the electron density around ruthenium and a significant lengthening of some of the bonds around the ruthenium centre, which depends on the approach of the propene (Figure 5.4 (c)).

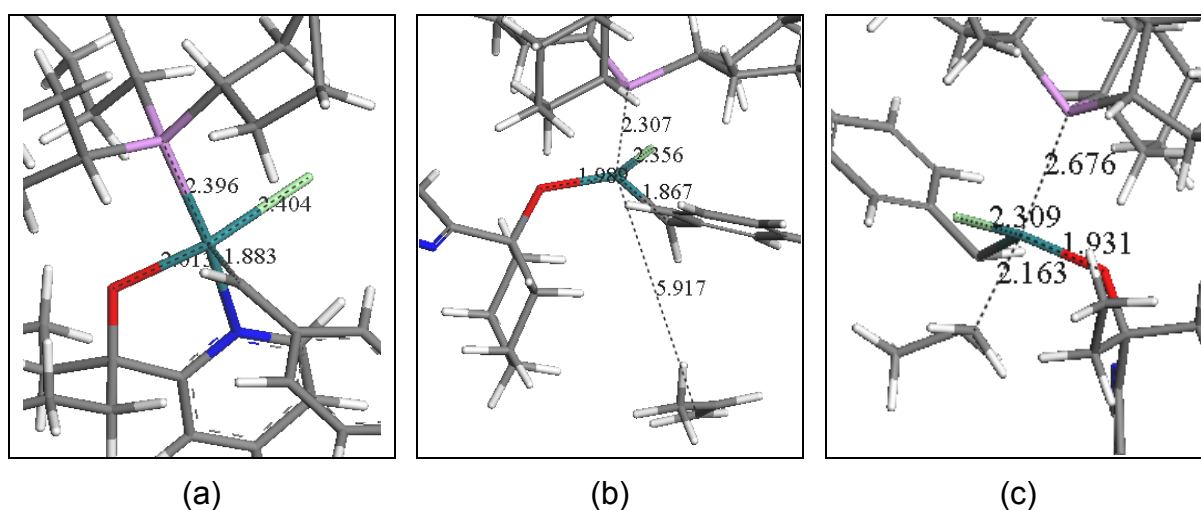


Figure 5.4: A series of diagrams depicting the changes in bond lengths around the metal centre in precatalysts of Gr1-type with bidentate/hemilabile ligands. Structure (a) is the closed precatalyst. Structure (b) depicts the precatalyst after the nitrogen de-coordinates and (c) depicts the propene approaching the open precatalyst *trans* to the phosphine ligand.

For the Cy-Gr1 ‘open’ structure, the propene approach was *trans* to the phosphine ligand. (Figure 5.5 a) This attachment of propene results in a considerable lengthening of the ruthenium phosphine bond. (Figure 5.5 (b)) The possibility exists

that the phosphine ligand could de-coordinate at the time that the propene moves in to react with the metal centre. (See for example, structures 3,4,5 and 6 in Table A-4) The same approach was observed for diethyl Gr1 precatalyst with the hemilabile ligand studied.

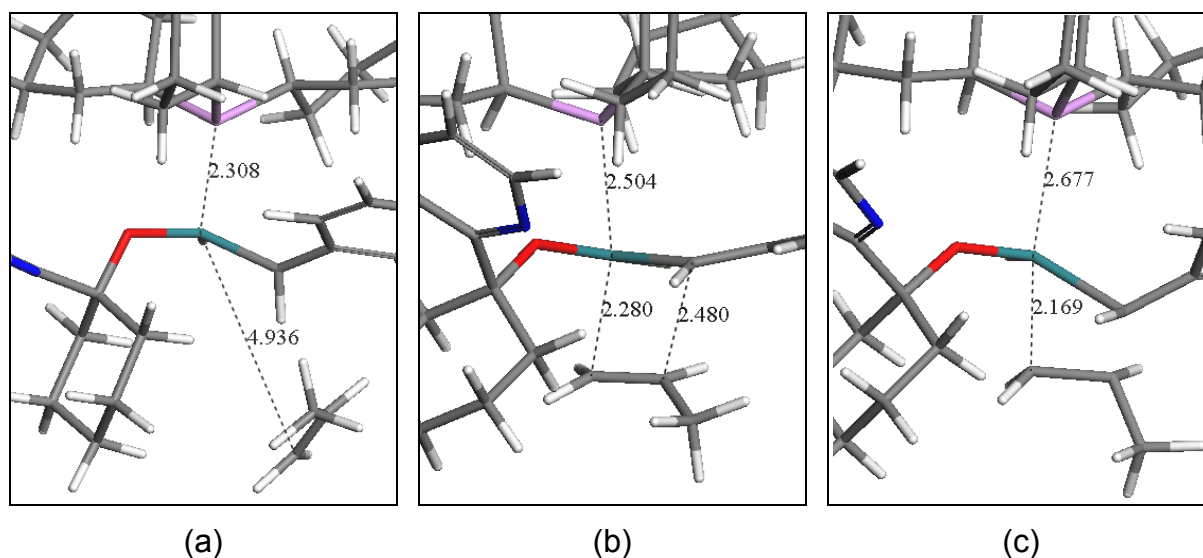


Figure 5.5: Diagrams illustrating that as propene approaches the ruthenium centre *trans* to the phosphine ligand, the phosphine to ruthenium bond length increases.

When no open coordination sites are available, and an associative mechanism is considered, the propene approaches *trans* to the chlorine. (Figure 5.6) This is the only possible approach to the metal centre since the pyridine ring occupies the position *trans* to the phosphine ligand. The attached propene lies on the equator of a distorted octahedron resulting in a considerable lengthening of the ruthenium chlorine bond. (Table 5.3) (See for example, structures 6, 8, 15 and 16 in Table A-4) This was the same approach for diethyl Gr1 precatalyst with the hemilabile ligand studied.

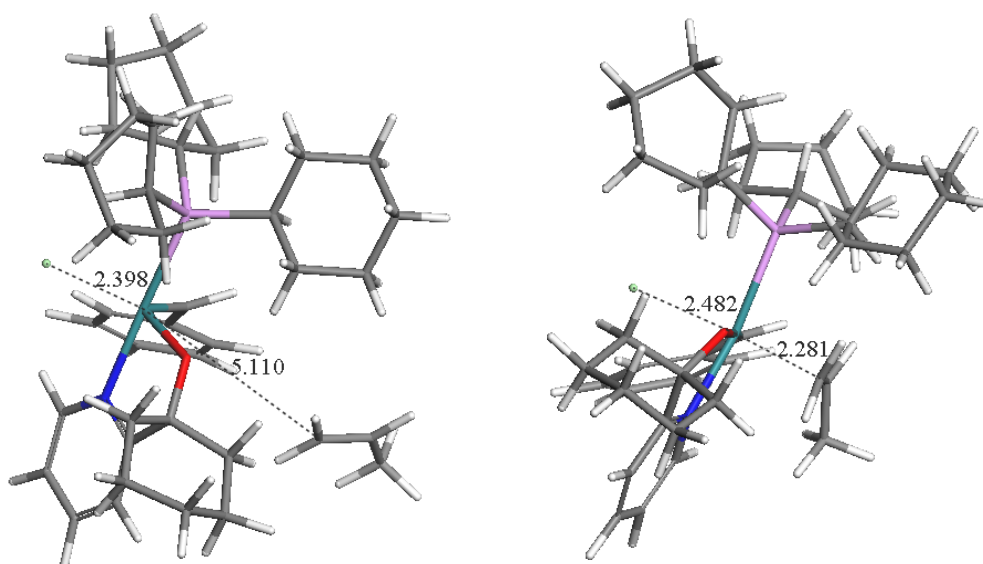


Figure 5.6: Diagrams depicting the changes in chlorine to ruthenium bond length as the propene attaches *trans* to the chlorine ligand in the closed Cy-Gr1 precatalyst

LUMO-HOMO graphics gives us a picture of how orbitals change during the propene approach and how interaction takes place between precatalyst and substrate.

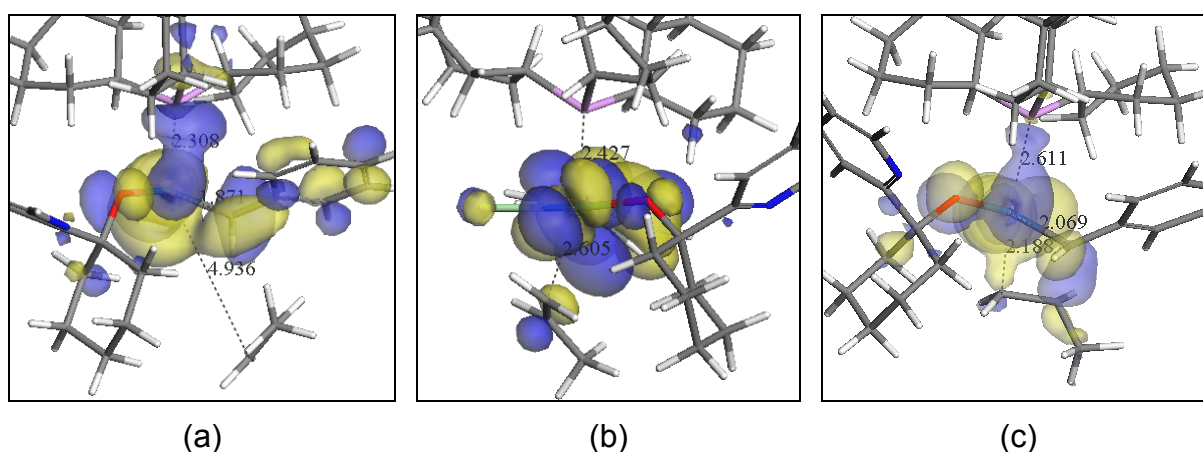


Figure 5.7: Diagrams depicting the LUMO orbitals as the propene attaches *trans* to the phosphine ligand in the open Cy-Gr1 precatalyst.

In graphic (a), we see that the LUMO is spread out over the precatalyst while the substrate is still relatively far away. With the approach of the propene (bottom left of graphic (b)), the phosphine to ruthenium bond has lengthened and the LUMO is

more concentrated over the metal. This could be as a result of electron density shifting away from the metal centre towards the ligands due to repulsion by the π electrons of the propene. In graphic (c), the LUMO extends towards the phosphine and over the propene.

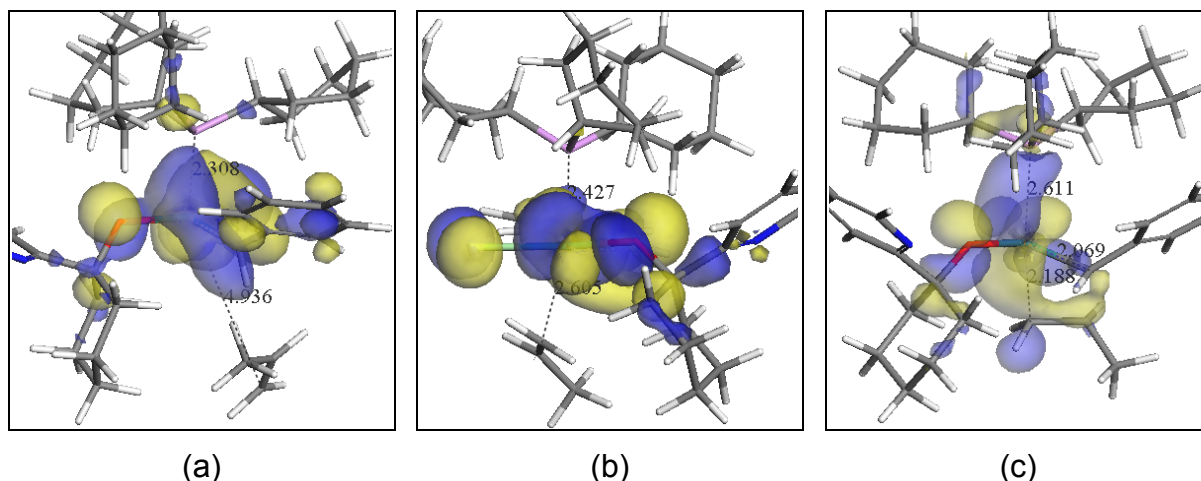


Figure 5.8: Diagrams depicting the HOMO orbitals as the propene attaches *trans* to the phosphine ligand in the open Cy-Gr1 catalyst.

The diagrams in Figure 5.8 show the changes in the HOMO orbitals as propene approaches. As the ruthenium to phosphine bond length increases, so the HOMO orbitals change. Jordaan observed free phosphine during the metathesis of 1-octene in the presence of the Cy-Gr1 precatalyst but it was not determined at which point of the metathesis process the phosphine was dissociated. Aagaard *et al.*¹⁶ also observed a lengthening of the Ru-P bond up to 2.65 Å and proposed that this bond lengthening was critical for metathesis to occur. In diagram (c) of Figure 5.8, however, we can see that the phosphine ligand has withdrawn further from the metal centre. The phosphine ligand could play a major role in the stabilisation of the metallacycle. The HOMO orbitals connect the metal centre, carbene carbon and first and second propene carbons indicating that the propene electrons have also become involved in bonding with the complex.

The diagrams in Figure 5.9 have been rotated to display the best view of the LUMOs. In graphic (a), we see the LUMO spread out over the equatorial region of the precatalyst. What is not visible in these graphics, is the change in geometry of the complex. In graphic (a), the complex has a trigonal pyramidal arrangement of

ligands while in (b) the complex arranges to a distorted octahedron. (view from above P) In graphic (b), the LUMO of propene indicates an empty orbital. (bottom of the graphic) In graphic (c), the propene is engaged in bonding in the metallacycle as can be seen from the HOMO orbitals in Figure 5.10 (c).

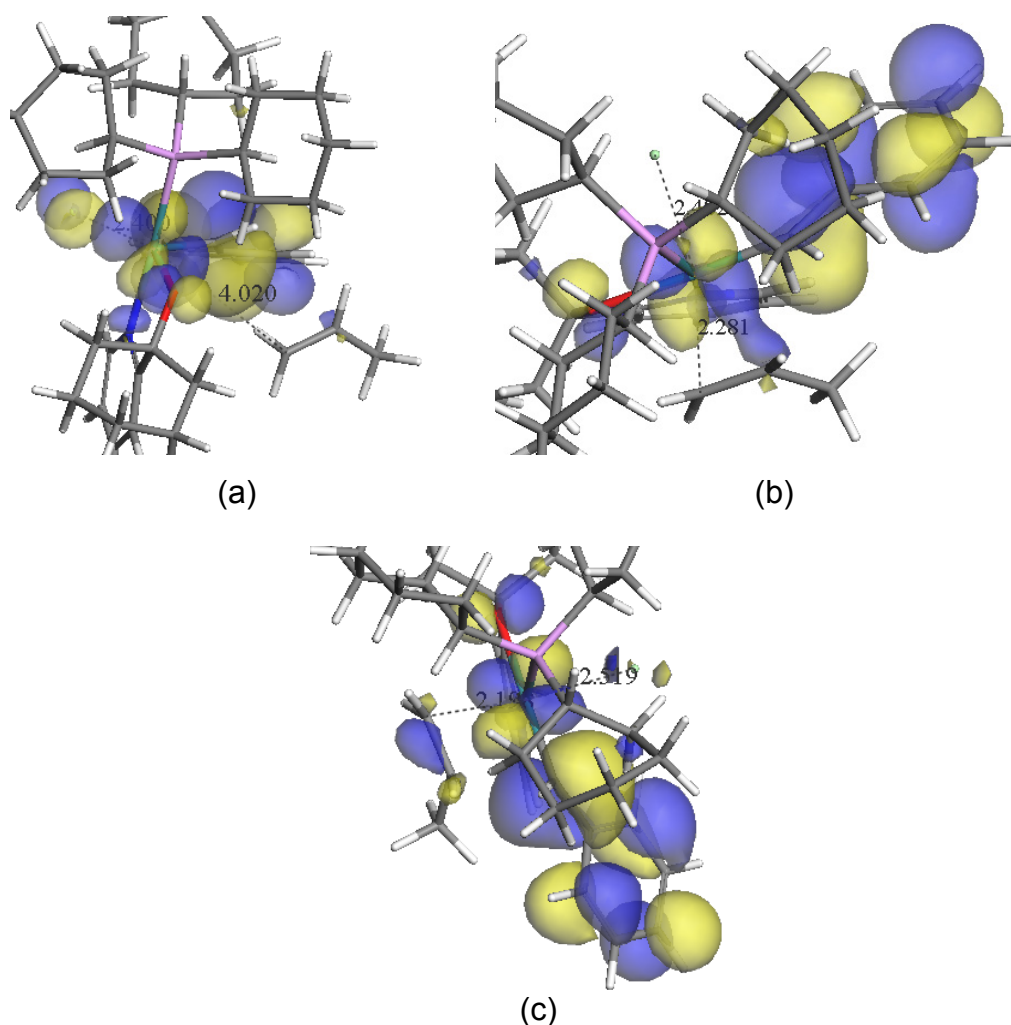


Figure 5.9: Diagrams depicting the LUMO orbitals as the propene attaches *trans* to the chlorine ligand in the closed Cy-Gr1 precatalyst.

The diagrams in Figure 5.10 have been rotated to show the changes in HOMO orbitals over chlorine.

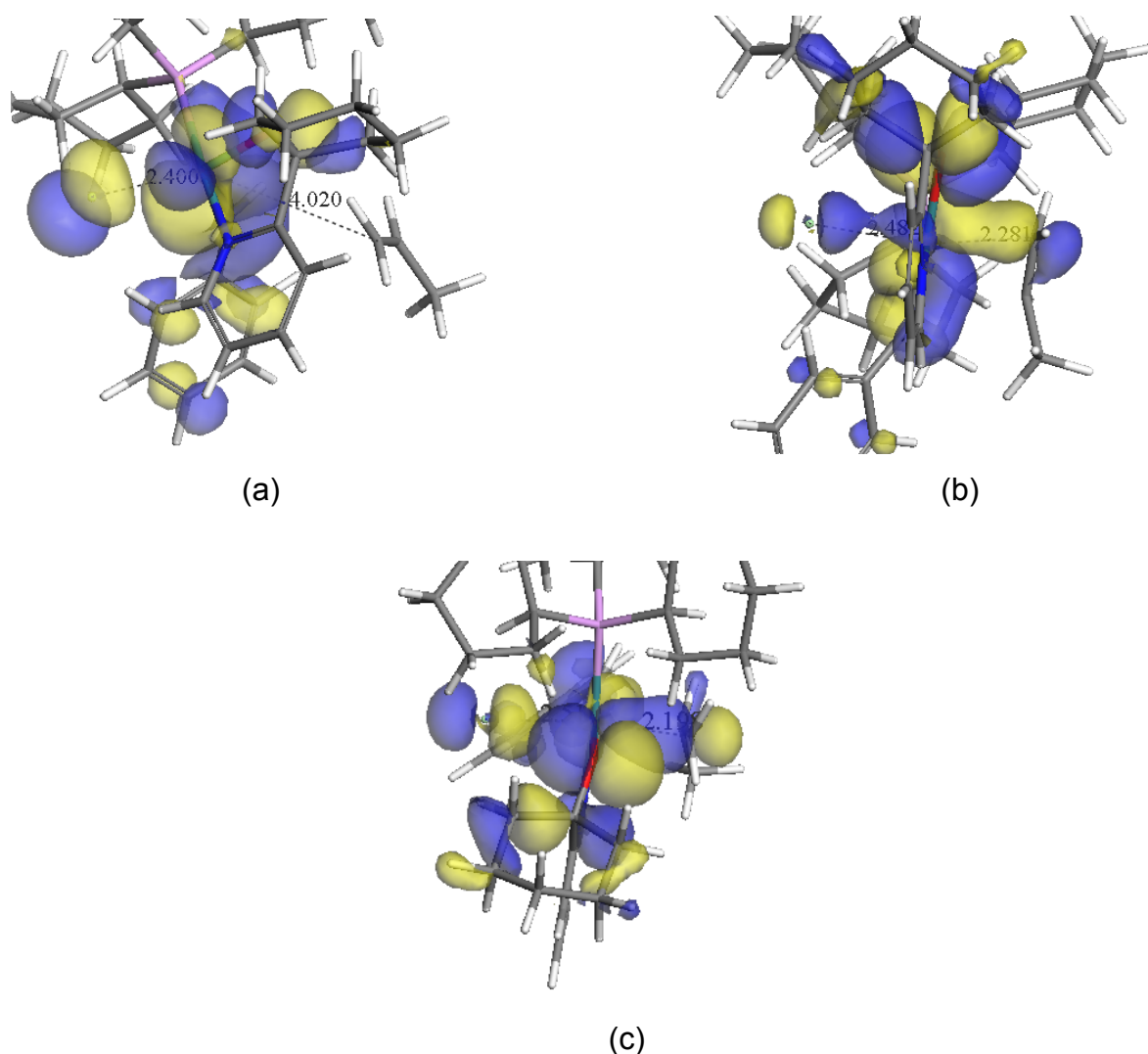


Figure 5.10: Diagrams depicting the HOMO orbitals as the propene (to the right of the graphics) attaches *trans* to the chlorine ligand in the closed Cy-Gr1 precatalyst.

It can be seen from Figure 5.10 that the contribution of the electrons in the HOMO orbitals to the bonding of the phosphine and chlorine ligands varies as the propene approaches. What cannot be seen from this view is the phosphine ligand. In graphic (b) and (c), we see interaction of the propene with the complex.

These changes in bond lengths between ruthenium and chlorine and ruthenium and the IMes ligand were not observed for the incoming of propene to the Gr2-type catalysts with bidentate/hemilabile ligands for the dissociative pathway. (See Table 5.2)

Scanning through the PES scans for the metallacycles of Gr₂-type catalysts with hemilabile ligands, revealed that the approach of propene towards the Cy-Gr₂ complexes with and without the pyridine ring coordinated (Figure 5.11 and Figure 5.12), is in the equatorial region *trans* to the chlorine ligand. This was also the approach for propene in PUK-Gr₂ complexes with hemilabile ligands investigated.

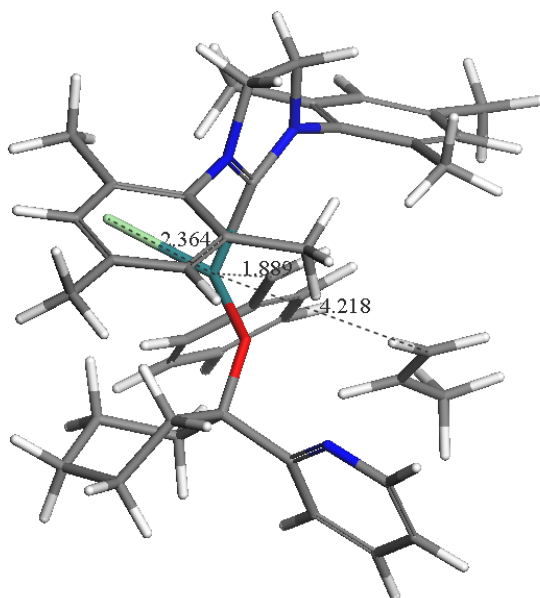


Figure 5.11: The approach of propene to 'open' Cy-Gr₂.

Major changes occurred in only two bond angles of the Grubbs type bidentate/hemilabile complexes. For the associative pathway, the ORuCl angle decreased significantly in most cases. This is because the propene bonds along the equatorial plane of the complex forming a distorted octahedron and forcing the chlorine closer to the oxygen to make room for the metallacycle. (Figure 5.13)

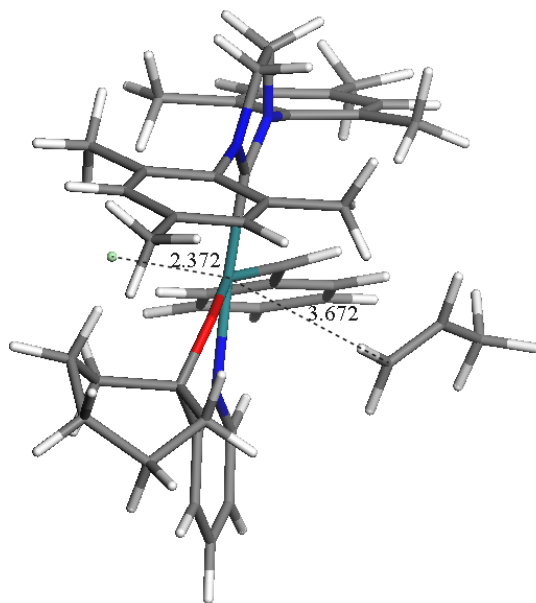


Figure 5.12: The approach of propene to 'closed' Cy-Gr2.

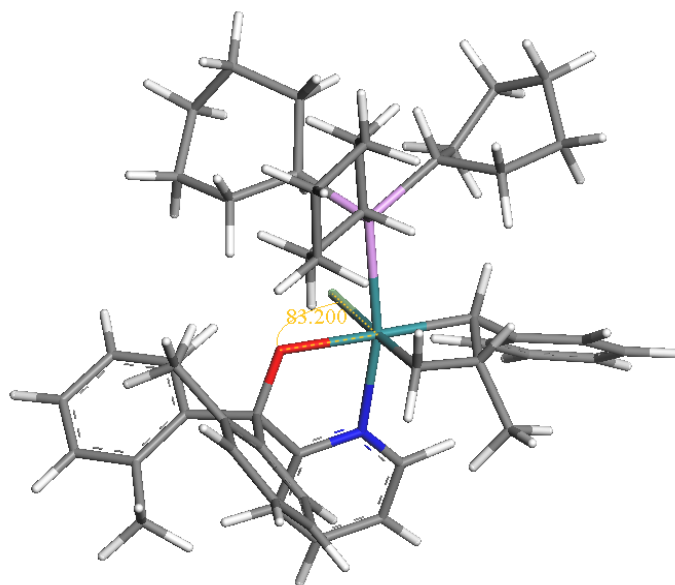


Figure 5.13: Closed complex of a Gr1-type complex with bidentate/hemilabile ligand showing the metallacyclobutane ring on the equator of a distorted octahedron.

For metallacycles of Gr1 precatalysts with hemilabile ligands formed from a dissociative pathway, the CORu angle increases significantly. (Figure 5.14) This is because propene approaches *trans* to the phosphine ligand after a coordination site has become vacant following de-coordination of the pyridine ring. The ligand moves away to prevent steric hindrance of the metallacycle which lies below the equatorial plane. (Table A-9)

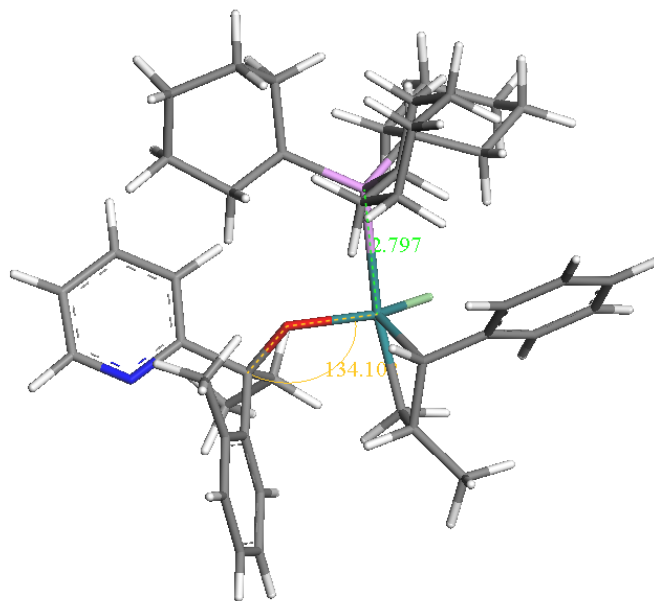


Figure 5.14: Open complex of a Gr1-type complex with bidentate/hemilabile ligand showing the metallacyclobutane ring below ruthenium and large CORu angle.

The PES scans did not reveal any evidence of a concerted mechanism whereby the Ru-N bond breaks as the propene approaches and interacts with the ruthenium centre.

From the PES scans, transition state structures were obtained. The electronic energies obtained for the transition state structures were used to assess the viability of different reaction routes.

It can be seen from Figure 5.15, that when only electronic energy is taken into consideration, the associative pathway for Cy-Gr1 requires a relatively small energy input of 18.13 kcal/mol compared to the 17.95 kcal/mol required for de-coordination of the pyridine ring. However, when corrections are made to the electronic energy

and ΔG is calculated at 298 K, the associative mechanism looks to be a less plausible route for alkene metathesis using Cy-Gr1 since $\Delta G_{298K} = 36.83$ kcal/mol and the Gibbs Free energy remains a low 16.07 kcal/mol for the de-coordination of the pyridine ring. The de-coordination of the pyridine ring is a better alternative to phosphine dissociation with an energy saving of more than 10 kcal/mol. Upon binding of the propene to the 'open' precatalyst, another barrier of nearly 46 kcal/mol is encountered in order to form the 'open' metallacycle. This barrier together with the energy required to de-coordinate the pyridine ring makes this route more energetically expensive than the associative mechanism by 27 kcal/mol. An associative mechanism can be ruled out if one considers Table 5.7, which indicates that at higher temperatures, the de-coordination of the pyridine ring is still the least expensive energetically.

There are very small differences in energy between the 'open' and 'closed' metallacycles at room temperature (3 kcal/mol). This energy difference is less than that required to break a hydrogen bond. Such a small energy difference would certainly satisfy Braunstein's¹ condition for hemilability, suggesting that hemilability is a property of the metallacycle and not the precatalyst. Whether a closed or open metallacycle forms, the pyridine ring will attach or detach easily from its coordination site. It was not observed in the PES scans of the closed metallacycles that nitrogen de-coordinates when the alkene approaches. The Ru-N bond length fluctuated between 2.16 and 2.20 Å. The ΔG value of the 'less PCy₃' metallacycle is lower than the ΔG value of the 'closed' and 'open' metallacycles. The loss of phosphine ligand from these metallacycles would be an exothermic reaction which could explain why free phosphine ligand was observed by Jordaan.¹⁰ No significant lengthening of the Ru-P bond was observed in the PES scans of the closed metallacycle. All that can be concluded with certainty from these results is that metathesis does not initiate with the loss of phosphine from the precatalyst.

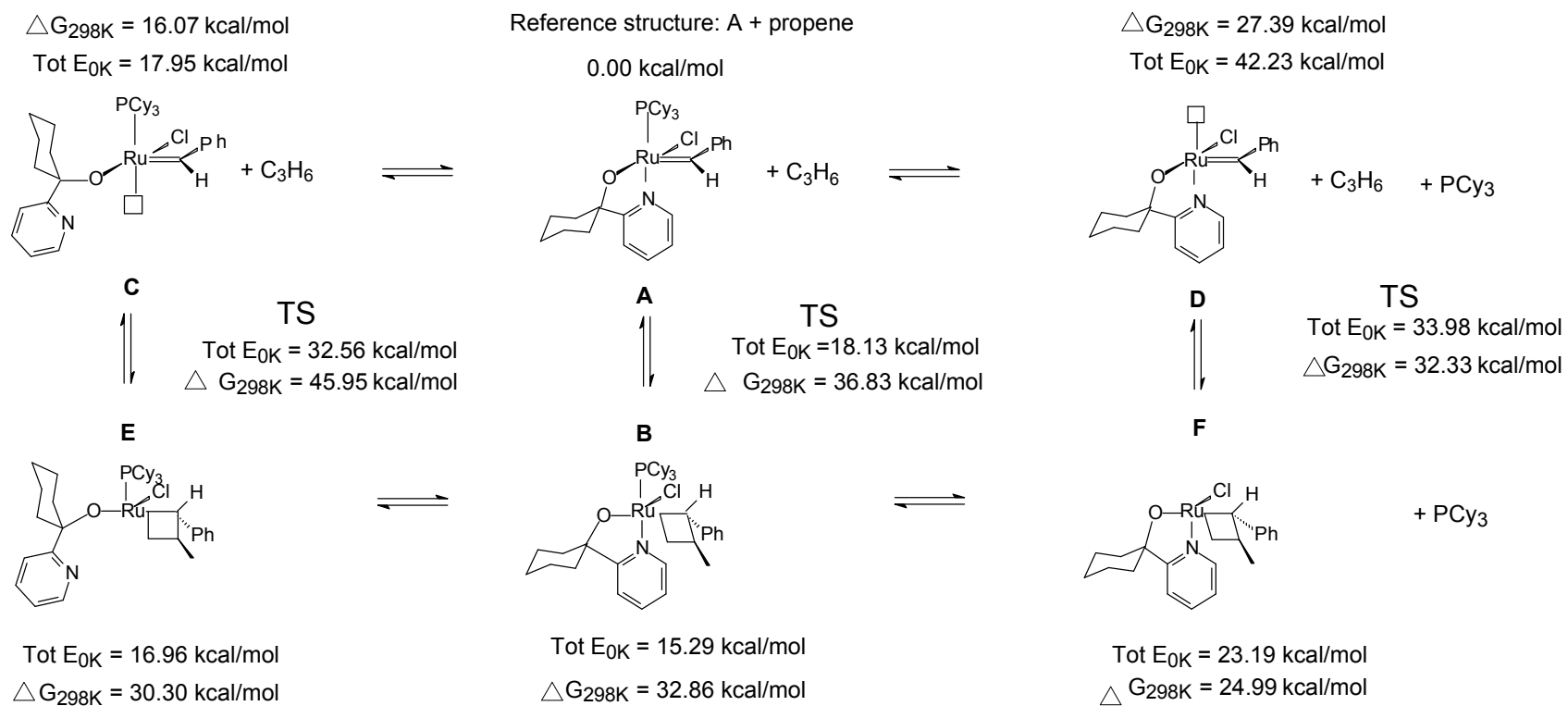


Figure 5.15: Possible reaction pathways for Cy-Gr1.

Table 5.7: Gibbs Free energy values at two different temperatures for the Cy-Gr1 precatalyst complexes.

	ΔG (298 K) (kcal/mol)	ΔG (325 K) (kcal/mol)
Cyclohexyl Gr 1 open precatalyst + C ₃ H ₆	16.07	8.94
Cyclohexyl Gr 1 open metallacycle	30.30	22.71
Cyclohexyl Gr 1 open metallacycle to precatalyst TS	45.95	38.46
Cyclohexyl Gr 1 closed metallacycle	32.96	25.60
Cyclohexyl Gr 1 closed metallacycle to precatalyst TS	36.83	28.03
Cyclohexyl Gr 1 less PCy ₃ precatalyst + PCy ₃	27.39	23.23

When considering dissociative versus associative reaction for Cy-Gr2, it appears that the de-coordination of the pyridine ring to form a 14-electron species is more favourable than the coordination of the propene to the 16-electron complex to form the 18-electron complex by 26 kcal/mol. (Figure 5.16) This would confirm what was observed experimentally by Jordaan *et al.*¹¹ that a variety of open alkylidenes existed during metathesis with 1-octene. The energy barrier required to form the ‘open’ metallacycle, however, is exceptionally high and would make the dissociative pathway more expensive energetically by 52 kcal/mol at room temperature. The ‘open’ metallacycle is lower in energy than the ‘closed’ metallacycle by 13 kcal/mol, so in the event of the associative route being taken, the closed metallacycle could open to form a more stable metallacycle. There was no evidence of this in the PES scan. The HOMO graphics for the precatalyst as well as the ‘closed’ metallacycle, never show good interaction between the pyridine ring and the metal centre. (Figure 5.17(a))

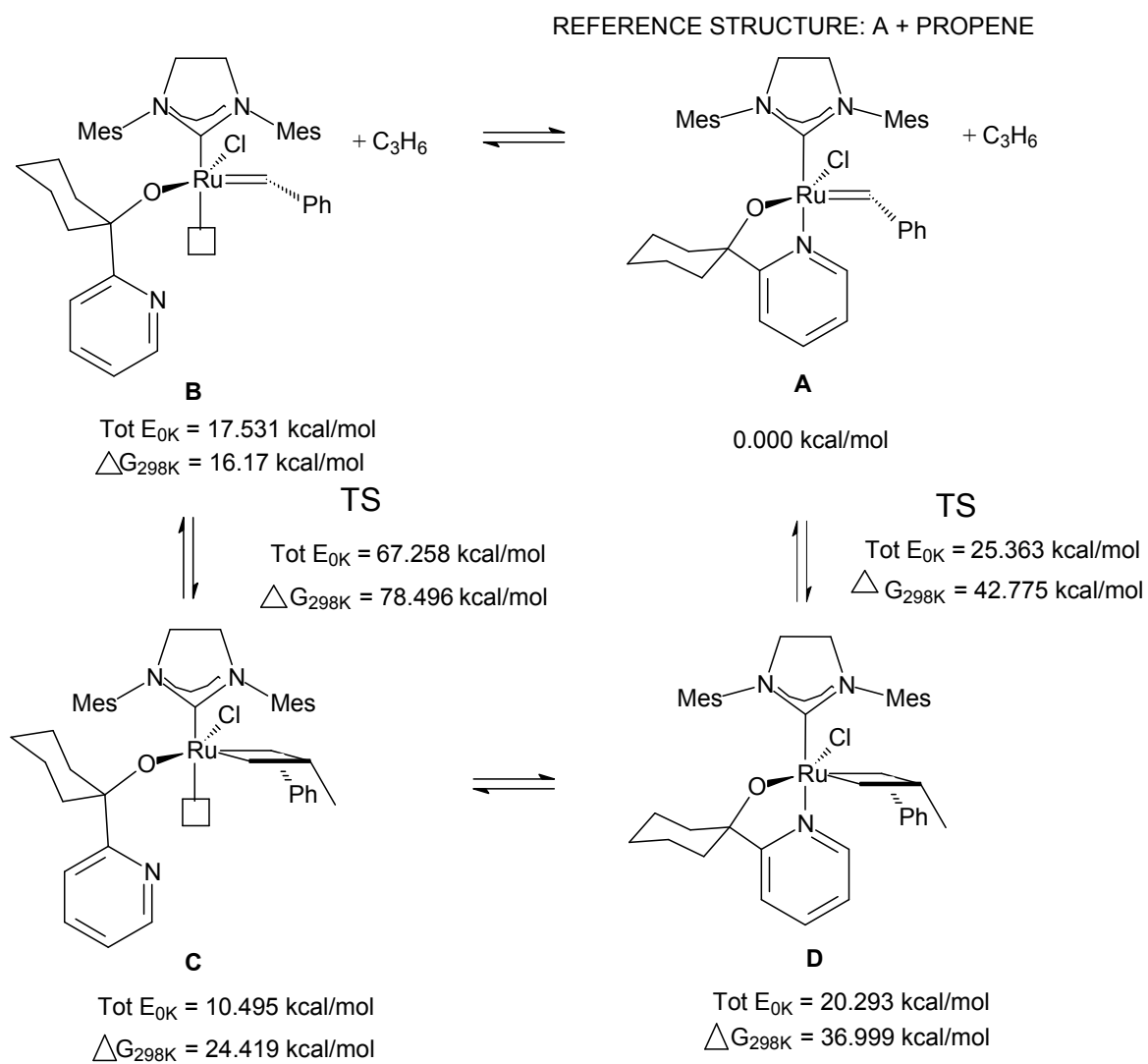


Figure 5.16: Dissociative and associative mechanisms for Cy-Gr2.

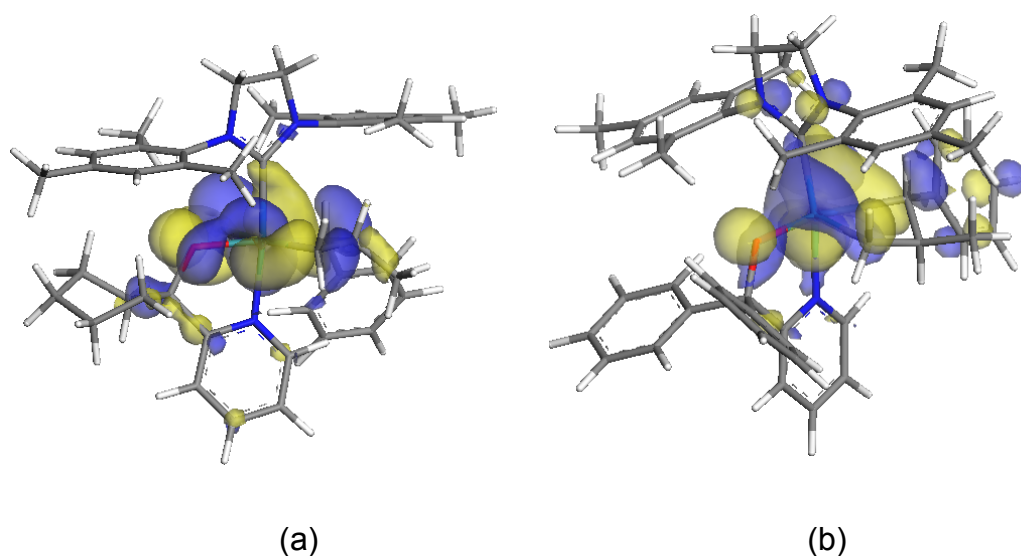


Figure 5.17: HOMO graphics of (a) Cy-Gr2 closed metallacycle and (b) PUK-Gr2 closed metallacycle.

The computational results for Cy-Gr2 were in complete contrast to that observed for PUK-Gr2. The associative mechanism appears more favourable than the dissociative route. (see Figure 5.18) The energy barrier for binding of propene is slightly lower than that for the de-coordination of the pyridine ring. Although the energy barrier for the de-coordination of the pyridine ring is only higher by 1.4 kcal/mol than the associative route, the energy barrier for the formation of the 'open' metallacycle is exceptionally high. The 'open' metallacycle is also higher in energy than the 'closed' metallacycle by 30 kcal/mol. These results indicate that the associative mechanism is very viable for PUK-Gr2. Jordaan¹⁷ observed that PUK-Gr2 had a long lifetime. This could be explained by the fact that the ruthenium centre is being protected by the coordination of the pyridine ring and, hence, decomposition of the catalyst does not occur because there are no open coordination sites. The HOMO graphics appeared different for these two metallacycles. (Figure 5.17)

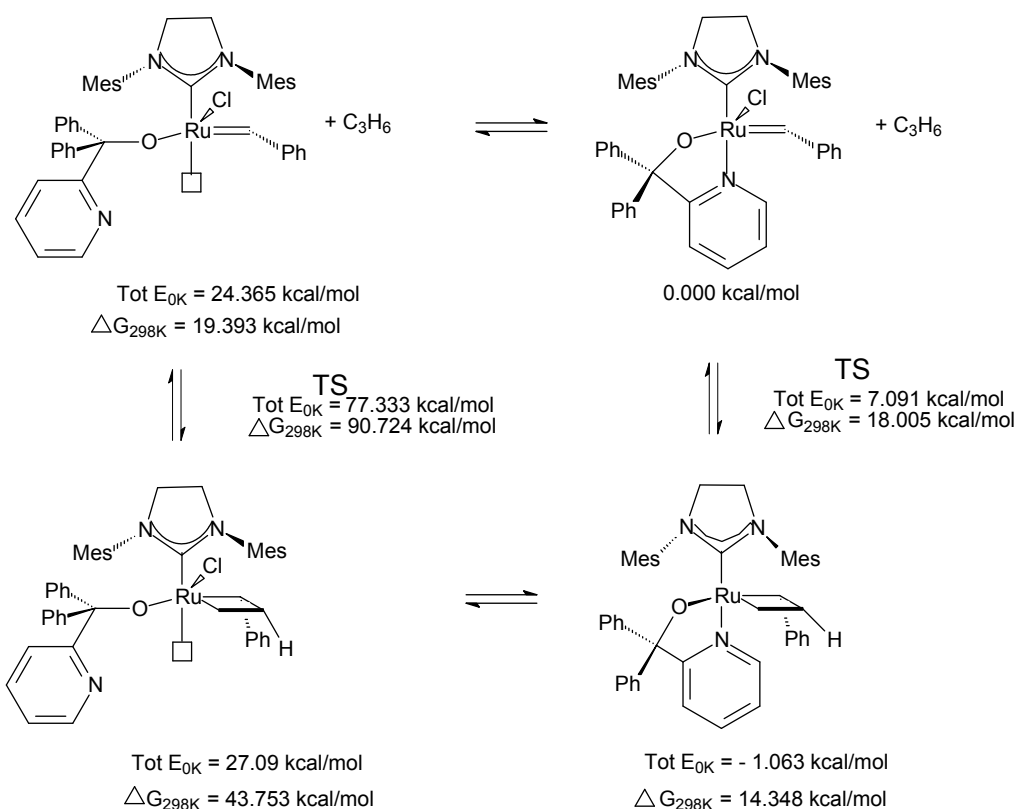


Figure 5.18: Dissociative and associative mechanisms for PUK-Gr2.

5.1.6 Agostic interactions

In a computational study done by Koga *et al.*¹⁸ involving metathesis with ethene and $(\text{PH}_3)_2\text{Ru}(\text{CH}_2)\text{Cl}_2$, the CC bond lengths within the metallacycle were much longer than the typical CC single-bond length of 1.54 Å and the distance between the ruthenium atom and the central carbon of the metallacycle ring was close to the distance between ruthenium and the terminal carbons. There was also considerable deviation of the CCRu and CCC bond angles from the CCC bond angles of 90° in the case of cyclobutane. This was referred to as a nonclassical ruthenacyclobutane structure and was as a result of the presence of agostic interactions. These interactions were believed to facilitate the metathesis process.

Since the goal of this study was to study reaction mechanisms and to determine factors which might influence the mechanism, various Grubbs type catalyst metallacycles were scrutinised to obtain some evidence of agostic interactions to observe any trend that might reveal an influence on reaction pathway. The bond

lengths and angles of various metallacycles within complexes were scrutinised to find differences in the structure of the metallacycles (see Table 5.8).

The following diagram will assist in interpreting Table 5.8:

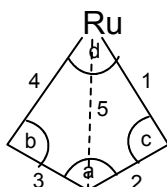


Figure 5.19: Diagram depicting the bond lengths and angles studied and recorded in Table 5.8.

Since the ruthenium atom is large, one would expect the ruthenium to carbon bond to be much longer than a CC bond. This would directly affect the metallacycle structure and cause it to deviate from the cyclobutane ring as an ideal situation for a four-membered ring. If agnostic interactions do play a role in the metathesis mechanism of these complexes, it will be reflected in the ruthenium to carbon (middle) bond. Such interaction will cause large deviations in the bond angles within the metallacycle structure.

Since metathesis with Gr2 is known to proceed via the dissociative mechanism, and the performance of Gr2 is a considerable improvement of previous ruthenium catalysts, its metallacycle bond lengths and angles can be considered to be almost at an 'optimum'.

We can see that the Ru-C_{middle} bond length of Gr2 open metallacycle is considerably shorter than most of the other complexes studied. This bond length does not differ too much from the other RuC bond lengths in the metallacycle. The angles deviate very much from 90°, which should result in considerable ring strain and can also result in the facile cleavage of bonds within the metallacycle.¹⁹ This could be another reason why Gr2 performs better than Gr1, which has a comparatively larger Ru-C_{middle} bond length. Since Gr2 follows the dissociative mechanism, these short Ru-C_{middle} bond lengths would not be unique to catalysts following the associative route.

Table 5.8: Bond lengths and angles within the metallacycle of different complexes.

	Bond lengths in Angstroms						Bond angles in degrees		
	1	4	2	3	5	a	c	b	d
	Ru-C	Ru-C	C-C	C-C	Ru-C _{middle}	CCC	CCRu	CCRu	CRuC
Gr1 Open metallacycle	2.176	2.197	1.520	1.518	2.816	99.59	96.90	97.70	64.11
Gr1 Closed metallacycle	2.304	2.192	1.519	1.504	2.713	98.00	92.51	87.90	60.95
Gr2 Open metallacycle	2.035	1.997	1.621	1.577	2.320	115.91	77.88	77.83	84.52
Gr2 Closed metallacycle	2.248	2.188	1.536	1.503	2.730	96.11	93.57	90.36	61.26
PUK-Gr2 Open metallacycle	2.291	2.175	1.530	1.500	2.856	98.83	100.22	94.62	62.03
PUK-Gr2 Closed metallacycle	2.344	2.172	1.513	1.504	2.811	98.79	98.09	90.93	60.83
Cy-Gr 1 Open metallacycle	2.139	2.169	1.521	1.523	2.711	97.88	92.82	94.04	64.41
Cy-Gr 1 Closed metallacycle	2.149	2.038	1.565	1.598	2.492	112.76	85.63	82.68	77.89
Cy-Gr 2 closed metallacycle	2.116	2.025	1.568	1.610	2.433	114.25	83.19	81.21	80.23
B 15 Open metallacycle	2.330	2.135	1.535	1.499	2.831	99.65	100.85	91.83	62.37
B 15 Closed metallacycle	2.092	2.013	1.616	1.607	2.296	120.56	77.83	75.29	85.97
B 16 Open metallacycle	2.166	2.170	1.531	1.530	2.816	98.96	97.57	97.73	64.91
B 16 Closed metallacycle	2.130	2.014	1.565	1.629	2.418	115.84	82.44	80.17	81.48
B 17 Open metallacycle	2.272	2.178	1.527	1.508	2.816	99.492	98.024	93.619	66.70
B 17 Closed metallacycle	2.122	2.022	1.586	1.608	2.355	119.26	80.01	77.38	83.36
B 18 Open metallacycle	2.168	2.262	1.529	1.5062	2.822	98.94	98.797	94.24	62.74
B 18 Closed metallacycle	2.126	2.023	1.589	1.599	2.387	117.60	81.55	78.51	82.16
B 19 Open metallacycle	2.297	2.156	1.530	1.502	2.829	99.37	99.78	93.17	62.452
B 19 Closed metallacycle	2.116	2.021	1.596	1.599	2.364	118.47	80.62	77.72	83.14

The closed metallacycle version of a Gr2-type catalyst with bidentate/hemilabile ligand (B15: R_1 = Phenyl R_2 = Toly) also has a shorter Ru-C_{middle} bond length and a large CCC bond angle. This particular catalyst was reported by Huijmans³ to be very active. The various metathesis mechanisms for this catalyst have not been explored in great detail in order to determine whether an associative mechanism is viable. The closed metallacycle version of B 17 (R_1 = Phenyl R_2 = isopropyl) also has a shorter Ru-C_{middle} bond length and a large CCC bond angle. This particular catalyst was reported by Huijmans³ to have a long lifetime. This study determined that B 17 requires comparatively larger energy to de-coordinate the pyridine ring. The simultaneous protection of coordination sites by lack of de-coordination of the pyridine ring and possible agostic interactions could make this a good catalyst. The closed metallacycle version of B 19 also has a shorter Ru-C_{middle} bond length and a large CCC bond angle. This particular catalyst was reported by Huijmans³ to be difficult to isolate, possibly due to decomposition of the catalyst. In this study, it was found that the de-coordination of the pyridine ring of B 19 required very little energy and this would suggest that an open coordination site will make the catalyst more susceptible to catalyst decomposition. In this event, a closed metallacycle structure is not achievable. These measurements show that the structure of the metallacycle could be influential in the metathesis mechanism.

5.2 References

1. Braunstein, P., and Naud, F., et al, *Angew. Chem.*, 2001, **40**, 680.
2. Jordaan, M., and Vosloo, H. C. M., *Molecular Simulation*, 2008, **34**, 997.
3. Huijmsmans, C.A.A, ***Modelling and Synthesis of Grubbs type complexes with hemilabile ligands***, MSc-dissertation (North-West University), 2009.
4. Denk, K., Fridgen, J., and Herrmann, W. A., *Adv. Synth. Catal.*, 2002, **344**, 666.
5. Hong, S. H., Wenzel, A. G., Salguero, T. T., Day, M. W., and Grubbs, R. H., *J. Am. Chem. Soc.*, 2007, **129**, 7961.
6. Goodman, J. M., ***Chemical Applications of Molecular Modelling***, The Royal Society of Chemistry, UK, 1988.
7. Gates, B. C., ***Catalytic Chemistry***, Wiley, USA, 1992.
8. Sanford, M. S., Love, J. A., and Grubbs, R. H., *J. Am. Chem. Soc.*, 2001, **123**, 6543.

9. Antonova, N. S., Carbo, J. J., and Poblet, J. M., *Organometallics*, 2009, **28**, 4283.
10. Dulal, C. G., and Jibanananda, J., [Web]
<http://www.ias.ac.in/currsci/feb25/articles23.htm> [Date of access 30/09/2011].
11. Jordaan, M., and Vosloo, H. C. M., *Adv. Synth. Catal.*, 2007, **349**, 184.
12. Sandford, M.S., Ulman, M., and Grubbs, R.H., *J. Am. Chem. Soc.*, 2001, **123**, 749.
13. Adlhart, C., and Chen, P., *J. Am. Chem. Soc.*, 2004, **126**, 3496.
14. Torker, S., Merki, D., and Chen, P., *J. Am. Chem. Soc.*, 2008, **130**, 4808.
15. Dias, E. L., Nguyen, S. T., and Grubbs, R. H., *J. Am. Chem. Soc.*, 1997, **119**, 3887.
16. Aagaard, O.M., Meier, R.J., and Buda, F., *J. Am. Chem. Soc.*, 1998, **120**, 7174.
17. Jordaan, M., ***Experimental and theoretical investigation of new Grubbs type catalysts for the metathesis of alkenes*** PhD-thesis (North West University), 2007.
18. Suresh, C.H., and Koga, N., *Organometallics*, 2004, **23**, 76.
19. Koga, N., Obara, S., Kitaura, K., and Morokuma, K., *J. Am. Chem. Soc.*, 1985, **107**, 7109.

CHAPTER 6: Conclusions

6.1 Introduction

The broader aim of this study was to gain a better understanding of Grubbs type precatalysts with N[^]O-ligands using computational methods. These precatalysts were assumed to be hemilabile based on the studies done by Hermann *et al.*¹ Since these precatalysts were derivatives of Grubbs precatalysts, it was also assumed in previous studies^{2,3} that these precatalysts would follow the dissociative mechanism like their Grubbs counterparts. In an experimental investigation of the metathesis of 1-octene using Cy-Gr1, free PCy₃ was detected but it was not determined at which stage of the mechanism the phosphine ligand was dissociating. The main aim of this study, therefore, was to establish if these catalysts were in fact hemilabile and if the hemilability of these precatalysts served as an initiation step in a dissociative mechanism. For the Gr1-type precatalysts with N[^]O-ligands, the possibility of PCy₃ dissociation also had to be considered. This study also served to explore alternative mechanisms for the metathesis of propene. The results gathered from this study were compared, where possible, with previous experimental studies conducted on Gr1 and Gr2⁴ as well as the Grubbs type precatalysts with pyridinyl alcoholate ligands.^{2,3}

6.2 Computational study of Grubbs type precatalysts with hemilabile ligands

To test the reliability of the computational calculations conducted in this study, computational data obtained was compared to conclusions derived from experimental studies conducted on Gr1 and Gr2.⁴ The associative routes were shown to be less viable for Gr1 and Gr2. HOMO-LUMO energy gaps calculated were able to explain the reactivity of Gr2 relative to Gr1; the greater preference of Gr2 for substrate relative to Gr1 and the rebinding of free PCy₃ to Gr1. HOMO-LUMO energy gaps determined by computational calculations can therefore be used as a tool to predict stability/reactivity of similar precatalysts and preference for competing substrates relative to one another.

Electronic energies of the three possible forms of the Gr1-type precatalysts with N⁺O-ligands, excluded the dissociation of the PCy₃ ligand as the initiation step in a dissociative mechanism. This route was energetically too expensive. The dissociation of PCy₃ ligand was shown to be possible at later stages of the metathesis mechanism during substrate approach and after metallacycle formation.

In most cases, the de-coordination of the pyridine ring to form a 14-electron complex was more favourable than the binding of the substrate to the 16-electron precatalyst to form an 18-electron metallacycle. The energy required to de-coordinate the softly bound N atom was sometimes high and this was shown to correlate with an extended precatalyst lifetime, previously observed in an experimental investigation.³

A strong possibility for an associative mechanism was established for PUK-Gr2. This serves as a caution that one cannot assume that derivatives of Grubbs catalysts will always follow the same mechanism. No evidence of a concerted mechanism was observed.

It was established that hemilability as described by Braunstein *et al.*⁵ might be a property of the metallacycles rather than the precatalysts since large amounts of energy are required to de-coordinate the N-atom of 16-electron precatalysts. In some cases, less energy was required to de-coordinate the N-atom of these bidentate/hemilabile precatalysts than is required for phosphine dissociation with Gr1 and Gr2, in some cases, even more. Although large amounts of data was gathered in this study such as bond lengths, bond angles and Hirshfeld charges, none of these could be correlated to the ease or difficulty of hemilability.

6.3 Recommendations

Further investigations in this field are required. Some recommendations from this study are listed below:

- More precatalysts need to be investigated computationally and experimentally to assess correlation between theory and experiment.
- The alternative mechanisms for more precatalysts needs to be explored computationally.

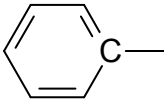
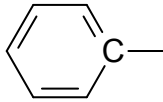
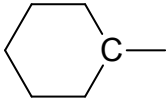
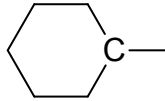
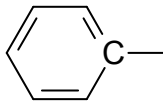
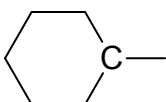
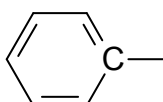
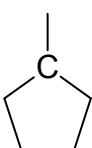
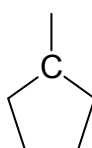
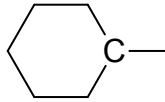
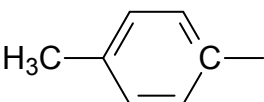
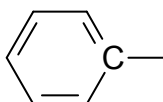
- Structure 21 and 22 were very similar in atomic arrangements but structure 21 gave electronic energies for the 'open' and 'closed', indicating exothermic reactions for both initiation steps, whereas structure 22 did not. These two structures need to be explored further computationally and then experimentally.
- PUK-Gr2 needs to be investigated further experimentally to confirm hemilability and mechanism.

6.4 References

- [1] Denk, K., Fridgen, J., Herrmann, W.A., *Adv. Synth. Catal.*, 2002, **344**, 666.
- [2] Jordaan, M., ***Experimental and Theoretical investigation of New Grubbs type Catalysts for the metathesis of Alkenes***, PhD-thesis (North-West University), 2007.
- [3] Huijsmans, C.A.A, ***Modelling and Synthesis of Grubbs type complexes with hemilabile ligands***, MSc-dissertation (North-West University), 2009.
- [4] Sanford, M. S., Ulman, M., and Grubbs, R. H., *J. Am. Chem. Soc.*, 2001, **123**, 749.
- [5] Sanford, M. S., Love, J. A., and Grubbs, R. H., *J. Am. Chem. Soc.*, 2001, **123**, 6543.
- [6] Braunstein, P., and Naud, F., *Angew. Chem.*, 2001, **40**, 680.

APPENDIX

Table A-1: Groups attached to pyridinyl-alcoholato ligand in Gr1-type bidentate/hemilabile precatalysts according to the template in Figure 4.1.

Structure Number	R ₁	R ₂
1	–H	–H
2	–CH ₃	–H
3	–CH ₃	–CH ₃
4	–CH ₂ CH ₃	–H
5	–CH ₂ CH ₃	–CH ₃
6	–CH ₂ CH ₃	–CH ₂ CH ₃
7		
8		
9	–H	
10		
11		
12	–H	
13		

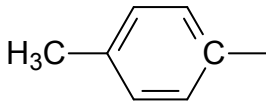
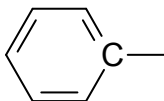
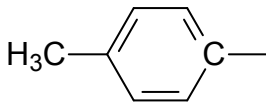
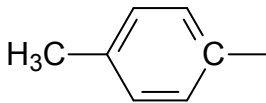
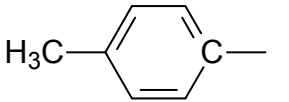
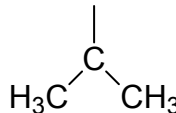
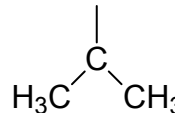
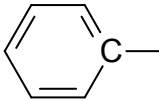
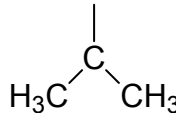
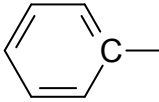
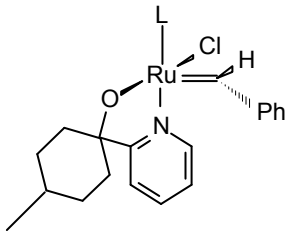
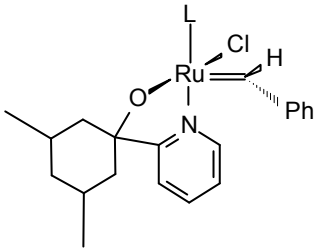
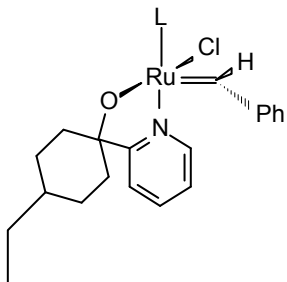
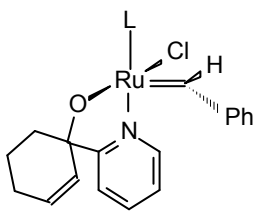
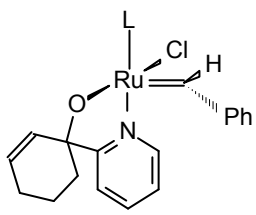
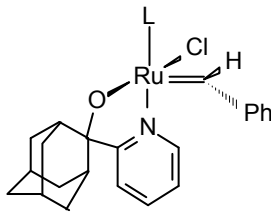
14		CH ₃
15		CH ₃ CH ₂
16		
17		CH ₃ CH ₂
23	H	-CH ₂ CH ₂ CH ₃
24	-CH ₂ CH ₂ CH ₃	-CH ₂ CH ₂ CH ₃
27		
28	-CH ₂ CH ₂ CH ₃	
29		

Table A-2: Groups incorporated into pyridinyl-alcoholato ligand in Gr1-type hemilabile catalysts (L = PCy₃).

18	
19	
20	
21	
22	
25	

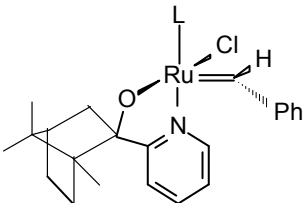
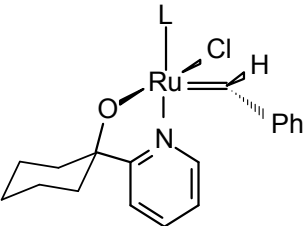
26	 <p>Chemical structure of compound 26: A ruthenium (Ru) center is coordinated by a bicyclic ligand (a norbornene derivative with a methyl group), a pyridine ring, a phenyl group (Ph), a chlorine atom (Cl), and a ligand L. The Ru is also coordinated to a hydrogen atom (H) via a double bond.</p>
Cyclohexyl Gr1	 <p>Chemical structure of Cyclohexyl Gr1: A ruthenium (Ru) center is coordinated by a cyclohexyl ligand, a pyridine ring, a phenyl group (Ph), a chlorine atom (Cl), and a ligand L. The Ru is also coordinated to a hydrogen atom (H) via a double bond.</p>

Table A-3: Groups attached to Gr₂ precatalyst with chelating pyridinyl-alcoholato ligand (L = IMes). Equivalent Gr₁-type catalyst number from Table A.1 and A.2 shown in brackets.

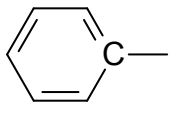
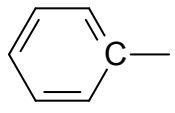
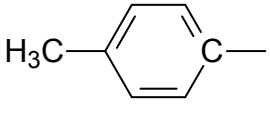
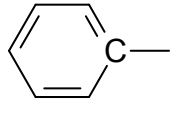
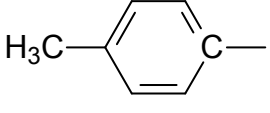
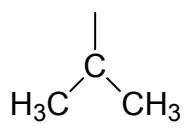
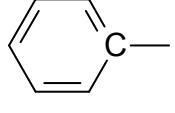
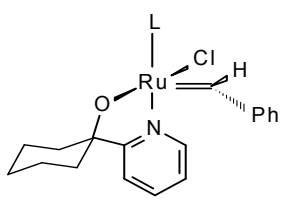
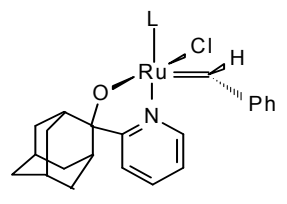
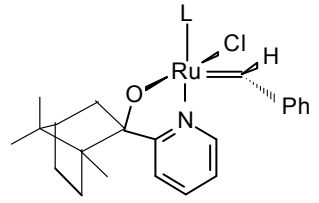
Structure Number	R ₁	R ₂
B-1 (7)		
B-15 (13)		
B-16 (14)		-CH ₃
B-17 (29)		
B-2 (30)		
B-18 (25)		
B-19 (26)		

Table A-4: Electronic energies obtained in kcal/mol of ‘open’ complexes and ‘less PCy₃’ complexes (where applicable) relative to the corresponding ‘closed’ precatalyst.

Structure Number	‘open’ complex	‘less PCy ₃ ’ complex
1	-	44.15
2	16.75	43.67
3	20.30	-
4	15.90	43.84
5	22.40	42.56
6	21.42	42.07
7	-	42.37
8	-	41.56
9	21.06	43.72
10	23.23	42.92
11	22.90	-
12	-	43.72
13	-	43.79
14	-	43.42
15	17.68	43.00
18	17.27	42.18
19	14.36	-
20	17.26	-
21	-68.69	-25.95
22	20.03	42.95
23	17.13	-
24	-	41.57
29	21.25	42.80

30	17.95	42.23
B-1	24.36	NA
B-2	17.53	NA
B-15	14.93	NA
B-16	20.59	NA
B-17	34.86	NA
B-18	17.89	NA
B-19	13.51	NA
“-“ optimised structures were not obtained		

Table A-5: Electronic energies in kcal/mol of ‘open’ metallacycle complexes and ‘less PCy₃’ metallacycle complexes (where applicable), as well as closed metallacycle complexes relative to the corresponding ‘closed’ precatalyst.

Structure Number	‘closed’ metallacycle	‘open’ metallacycle	‘less PCy ₃ ’ metallacycle
1	-	11.028	-
2	-	16.163	-
3	-	20.970	-
4	-	17.277	-
5	-	20.592	-
6	17.153	22.315	24.083
8	17.313	25.200	-
9	-	5.377	-
11	-	15.255	-
13	21.667	-	-
14	-	19.742	-
15	19.848	-	-
16	17.500	13.892	-
17	19.519 (18.128)*	18.608	-
19	-	3.757	-
20	-	19.253	-
23	-	18.034	-
25	-	16.491	-
29	-8.573	17.368	-
30	15.289	16.957	23.193
B-1	-1.063	27.090	NA

B-2	2.293	10.495	NA
B-15	39.818	33.397	NA
B-16	38.442	31.215	NA
B-17	43.788	16.712	NA
B-18	47.596	26.658	NA
B-19	43.213	34.080	NA

Table A-6: Bond lengths around ruthenium centre measured in Å.

Structure		Ru-O	Ru-Cl	Ru-L	Ru to C (carbene)	Ru-N
1	Less PCy ₃	1.980	2.355	NA	1.861	2.015
	Open metallacycle	1.955	2.400	2.361		NA
2	Precatalyst	2.012	2.403	2.388	1.885	2.190
	Open metallacycle	1.927	2.315	2.689		NA
	Less PCy ₃	1.9751	2.356	NA	1.860	2.011
3	Precatalyst	2.008	2.400	2.392	1.887	2.183
	Open	1.984	2.350	2.292	1.880	NA
	Open metallacycle	1.919	2.311	2.682		NA
4	Precatalyst	2.012	2.403	2.390	1.884	2.187
	Open	1.988	2.338	2.296	1.879	NA
	Open metallacycle	1.916	2.306	2.661		NA
	Less PCy ₃	1.975	2.359	NA	1.860	2.008
5	Precatalyst	2.008	2.401	2.397	1.886	2.182
	Open	1.988	2.348	2.277	1.879	NA
	Open metallacycle	1.927	2.312	2.707		NA

	Less PCy ₃	1.970	2.354	NA	1.861	2.006
6	Precatalyst	2.013	2.403	2.396	1.883	2.181
	Closed metallacycle to closed precatalyst TS	2.054	2.578	2.461	2.013	2.203
	Closed metallacycle	1.972	2.657	2.471	2.125	2.186
	Open	1.997	2.348	2.294	1.878	NA
	Open metallacycle	1.930	2.308	2.716	2.116	NA
	Less PCy ₃	1.972	2.353	NA	1.861	2.007
	Less PCy ₃ metallacycle to Less PCy ₃ precatalyst TS	1.948	2.385	NA	1.902	2.084
	Less PCy ₃ metallacycle	1.919	2.392	NA	2.026	2.132
7	Precatalyst	2.013	2.390	2.404	1.886	2.183
	Less PCy ₃	1.969	2.350	NA	1.860	2.015
8	Precatalyst	2.0153	2.401	2.417	1.886	2.164
	Closed metallacycle	1.969	2.674	2.501	2.126	2.179
	Open metallacycle	1.938	2.308	2.796		NA
	Less PCy ₃	1.963	2.349	NA	1.862	2.010

9	Precatalyst	2.013	2.393	2.393	1.886	2.203
	Open	1.988	2.351	2.293	1.874	NA
	Open metallacycle	1.980	2.411	2.351		NA
	Less PCy ₃	1.974	2.353	NA	1.861	2.015
10	Precatalyst	2.015	2.42	2.405	1.884	2.172
	Open	1.999	2.368	2.309	1.883	NA
	Less PCy ₃	1.972	2.359	NA	1.859	2.010
11	Precatalyst	2.004	2.396	2.408	1.886	2.167
	Open	1.989	2.355	2.298	1.884	NA
	Open metallacycle	1.963	2.399	2.370		NA
12	Precatalyst	2.006	2.404	2.397	1.884	2.181
	Less PCy ₃	1.965	2.357	NA	1.860	2.013
13	Precatalyst	2.023	2.418	2.420	1.882	2.176
	Closed metallacycle	2.073	2.582	2.489	2.092	2.189
	Less PCy ₃	1.982	2.357	NA	1.858	2.015
14	Precatalyst	2.010	2.398	2.390	1.886	2.200
	Open metallacycle	1.937	2.312	2.755	2.128	NA

	Less PCy ₃	1.970	2.353	NA	1.861	2.018
15	Precatalyst	2.006	2.398	2.389	1.885	2.200
	Closed metallacycle	2.016	2.599	2.489	2.076	2.198
	Open	2.005	2.358	2.298	1.877	NA
	Less PCy ₃	1.972	2.353	NA	1.862	2.007
16	Precatalyst	2.019	2.396	2.435	1.885	2.173
	Closed metallacycle	2.057	2.578	2.488	2.069	2.175
	Open metallacycle	2.030	2.368	2.406		NA
17	Precatalyst	2.010	2.394	2.427	1.886	2.192
	Closed metallacycle	1.994	2.650	2.482	2.114	2.207
	Open metallacycle	1.932	2.320	2.797	2.119	NA
18	Precatalyst	2.005	2.399	2.398	1.884	2.186
	Open	1.993	2.362	2.299	1.877	NA
	Less PCy ₃	1.965	2.355	NA	1.861	2.006
19	Precatalyst	2.002	2.400	2.399	1.884	2.186
	Open	1.992	2.362	2.301	1.878	NA
	Open metallacycle	1.988	2.379	2.327	2.235	NA

20	Precatalyst	2.004	2.398	2.396	1.884	2.186
	Open metallacycle	1.932	2.310	2.731		NA
21	Precatalyst	2.004	2.400	2.400	1.883	2.189
	Less PCy ₃	1.967	2.355	NA	1.860	2.006
22	Precatalyst	2.011	2.398	2.395	1.884	2.190
	Open	1.999	2.354	2.295	1.884	2.190
	Less PCy ₃	1.973	2.352	NA	1.860	2.011
23	Precatalyst	2.021	2.401	2.390	1.882	2.190
	Open	1.978	2.345	2.290	1.879	NA
	Open metallacycle	1.924	2.312	2.684		NA
24	Precatalyst	2.007	2.405	2.398	1.883	2.174
	Less PCy ₃	1.965	2.354	NA	1.861	2.003
27	Precatalyst	2.007	2.404	2.403	1.885	2.178
29	Precatalyst	2.0119	2.407	2.402	1.886	2.172
	Closed metallacycle	1.997	2.406	2.467	2.274	2.143
	Open metallacycle	1.944	2.303	2.728		NA
	Open	2.009	2.370	2.304	1.877	NA

	Less PCy ₃	1.969	2.359	NA	1.858	2.011
30	Closed	2.004	2.400	2.398	1.884	2.185
	Closed metallacycle to closed precatalyst TS	1.995	2.645	2.460	2.028	2.182
	Closed metallacycle	1.946	2.655	2.473	2.149	2.163
	Open	1.995	2.353	2.296	1.883	NA
	Open metallacycle	1.928	2.312	2.677	2.139	NA
	Less PCy ₃	1.965	2.355	NA	1.861	2.006
	Less PCy ₃ metallacycle	1.924	2.384	NA	2.023	2.149
B-1	Precatalyst	2.035	2.429	2.089	1.883	2.178
	Closed metallacycle	2.003	2.365	2.150	2.344	2.145
	Open	2.031	2.382	2.004	1.874	NA
	Open metallacycle to open precatalyst TS	2.074	2.388	2.096	2.189	NA
	Open metallacycle	2.050	2.438	2.077	2.278	NA
B-2	Precatalyst	2.025	2.428	2.094	1.881	2.181
	Closed metallacycle to	2.020	2.684	2.169	1.978	2.196

	closed precatalyst TS					
	Closed metallacycle	1.955	2.692	2.184	2.116	2.171
	Open	2.000	2.379	2.000	1.877	NA
	Open metallacycle to open precatalyst TS	1.986	2.379	2.061	2.154	NA
	Open metallacycle	1.973	2.408	2.021	2.245	NA
B-15	Precatalyst	2.034	2.425	2.092	1.881	2.188
	Closed metallacycle to closed precatalyst TS	2.069	2.590	2.144	2.007	2.235
	Closed metallacycle	2.015	2.642	2.160	2.092	2.213
	Open	2.039	2.378	2.011	1.876	NA
	Open metallacycle	2.066	2.347	2.047	2.330	NA
B-16	Precatalyst	2.031	2.428	2.088	1.883	2.183
	Closed metallacycle to closed precatalyst TS	2.023	2.676	2.178	1.979	2.211
	Closed metallacycle	1.960	2.688	2.171	2.130	2.189
	Open	2.016	2.365	2.001	1.880	NA

	Open metallacycle	2.000	2.400	2.028	2.166	NA
B-17	Precatalyst	2.033	2.420	2.108	1.883	2.175
	Closed metallacycle to closed precatalyst TS	2.101	2.579	2.151	1.992	2.228
	Closed metallacycle	2.004	2.654	2.159	2.122	2.214
	Open	2.024	2.359	1.998	1.879	NA
	Open metallacycle	2.007	2.414	2.099	2.272	NA
B-18	Precatalyst	2.029	2.426	2.095	1.881	2.191
	Closed metallacycle to closed precatalyst TS	2.049	2.587	2.166	2.004	2.187
	Closed metallacycle	1.962	2.732	2.181	2.126	2.166
	Open	2.011	2.354	2.003	1.882	NA
	Open metallacycle	1.991	2.426	2.051	2.239	NA
B-19	Precatalyst	2.033	2.430	2.104	1.881	2.173
	Closed metallacycle to closed precatalyst TS	2.041	2.613	2.162	2.023	2.191
	Closed metallacycle	1.976	2.698	2.166	2.116	2.193

	Open	2.007	2.375	2.007	1.877	NA
	Open metallacycle	2.020	2.351	2.030	2.297	

Table A-7: Hirshfeld Charges of ruthenium and surrounding atoms in Gr1-type catalysts with hemilabile ligands.

Structure		Ru	O	C*	N	CarbeneC	Cl	P
1	Precatalyst	0.300	-0.242	0.0174	-0.0730	-0.1012	-0.273	0.270
	Less PCy ₃	0.3918	-0.2681	-0.0133	-0.0447	-0.1103	-0.326	NA
2	Precatalyst	0.299	-0.238	0.0255	-0.0728	-0.102	-0.277	0.268
	Less PCy ₃	0.391	-0.263	-0.00580	-0.0442	-0.111	-0.327	NA
3	Precatalyst	0.299	-0.236	-0.070	-0.0718	-0.104	-0.275	0.268
	Open	0.330	-0.219	0.0686	-0.131	-0.119	-0.268	0.298
4	Precatalyst	0.299	-0.235	0.0247	-0.727	-0.101	-0.279	0.268
	Open	0.328	-0.220	0.0263	-0.152	-0.117	-0.267	0.292
	Less PCy ₃	0.391	-0.256	-0.00560	-0.0445	-0.112	-0.326	NA
5	Precatalyst	0.300	-0.231	0.0685	-0.0711	-0.104	-0.261	0.268
	Open	0.334	-0.217	0.0677	-0.131	-0.118	-0.260	0.297
6	Precatalyst	0.300	-0.233	0.0668	-0.0714	-0.102	-0.273	0.267
	Open	0.335	-0.217	0.0673	-0.120	-0.113	-0.256	0.297
	Less PCy ₃	0.394	-0.244	0.0681	-0.0426	-0.112	-0.325	

7	Precatalyst	0.301	-0.230	0.0671	-0.0721	-0.103	-0.270	0.270
	Less PCy ₃	0.395	-0.248	0.0667	-0.0447	-0.1085	-0.316	NA
8	Precatalyst	0.301	-0.231	0.0700	-0.0678	-0.103	-0.269	0.266
9	Precatalyst	0.297	-0.236	0.0223	-0.0725	-0.104	-0.278	0.271
	Open	0.328	-0.218	0.0222	-0.134	-0.117	-0.272	0.300
	Less PCy ₃	0.392	-0.263	-0.00330	-0.0444	-0.109	-0.324	NA
10	Precatalyst	0.296	-0.235	0.0669	-0.0691	-0.0963	-0.270	0.265
	Open	0.322	-0.221	0.0684	-0.128	-0.112	-0.255	0.265
	Less PCy ₃	0.391	-0.244	0.0676	-0.0417	-0.1048	-0.332	NA
11	Precatalyst	0.300	-0.227	0.0707	-0.0707	-0.104	-0.276	0.268
	Open	0.341	-0.219	0.0700	0.133	-0.115	0.239	0.298
12	Precatalyst	0.299	-0.233	0.0261	-0.0725	0.103	-0.277	0.268
	Less PCy ₃	0.393	-0.252	-0.00470	-0.0443	-0.111	-0.325	NA
13	Precatalyst	0.301	-0.232	0.0665	-0.0683	-0.0937	-0.262	0.265
	Less PCy ₃	0.396	-0.240	-0.00350	-0.0419	-0.103	-0.329	NA
14	Precatalyst	0.299	-0.234	0.0685	-0.0724	-0.104	-0.275	0.269
	Less PCy ₃	0.393	-0.252	-0.00470	-0.0443	-0.111	-0.325	NA

15	Precatalyst	0.299	-0.230	0.0653	-0.0727	-0.104	-0.277	0.270
	Open	0.330	-0.223	0.0670	0.135	-0.110	-0.260	0.295
	Less PCy ₃	0.395	-0.256	-0.00460	-0.0431	-0.113	-0.323	NA
16	Precatalyst	0.298	-0.228	-0.0699				0.266
17	Precatalyst	0.302	-0.229	0.0667	-0.0703	-0.104	-0.272	0.269
18	Precatalyst	0.300	-0.233	0.0658	-0.0720	-0.104	-0.273	0.268
	Open	0.324	-0.225	0.0649	-0.127	-0.112	-0.267	0.295
	Less PCy ₃	0.391	-0.252	0.0661	-0.0439	-0.113	-0.326	NA
19	Precatalyst	0.301	-0.232	0.0671	-0.0721	-0.104	-0.273	0.268
	Open	0.323	-0.223	0.0658	-0.127	-0.113	-0.268	0.296
20	Precatalyst	0.301	-0.233	0.0655	-0.0722	-0.104	-0.275	0.269
	Open	0.324	-0.225	0.0643	-0.127	-0.112	-0.267	0.295
21	Precatalyst	0.299	-0.231	0.0623	-0.0725	-0.105	-0.279	0.270
	Less PCy ₃	0.390	-0.254	0.0622	-0.254	-0.113	-0.326	NA
22	Precatalyst	0.300	-0.236	0.0610	-0.0725	-0.103	-0.274	0.269
	Open	0.326	-0.225	0.0622	-0.139	-0.111	-0.266	0.294
	Less PCy ₃	0.392	-0.258	0.0611	-0.0440	-0.112	-0.324	NA

23	Precatalyst	0.299	-0.243	0.0240	-0.0731	-0.102	-0.272	0.268
	Open	0.329	-0.211	0.0254	-0.144	-0.121	-0.271	0.295
24	Precatalyst	0.299	-0.235	0.0683	-0.0723	-0.1035	-0.274	0.267
25	Precatalyst	0.302	-0.229	0.0644	-0.0703	-0.101	-0.263	0.269
26	Precatalyst	0.301	-0.229	0.0644	-0.0703	-0.101	-0.263	0.269
27	Precatalyst	0.301	-0.228	0.0688	-0.0707	-0.103	-0.271	0.267
29	Precatalyst	0.297	-0.232	0.0663	0.0691	-0.100	-0.271	0.267
	Open	0.322	-0.223	0.0683	0.131	-0.105	0.264	0.293
30	Precatalyst	0.293	-0.237	0.0655	-0.713	-0.112	-0.282	0.268
	Open	0.330	-0.221	0.0671	-0.128	-0.114	-0.263	0.294
	Less PCy ₃	0.391	-0.252	-0.00420	-0.0438	-0.113	-0.326	NA
* Carbon connected to O and N in hemilabile ligand								

Table A-8: Hirshfeld Charges of ruthenium and surrounding atoms in Gr2-type catalysts with hemilabile ligands.

Structure		Cl	Carbene C	Ru	O	C ^a	N (pyridine)	L atom
B-1	Precatalyst	-0.254	-0.0889	0.316	-0.244	0.0646	-0.0725	
	Open	-0.255	-0.0937	0.353	-0.239	0.0653	-0.134	0.0408
B-2	Precatalyst	-0.257	-0.0921	0.318	-0.247	0.0666	-0.0736	0.0228
	Open	-0.256	-0.105	0.355	-0.237	0.0651	-0.133	0.0399
B-15	Precatalyst	-0.250	-0.0886	0.319	-0.236	0.0666	-0.0709	0.0192
	Open	-0.269	-0.0927	0.351	-0.236	0.0673	-0.117	0.0432
B-16	Precatalyst	-0.260	-0.0915	0.319	-0.248	0.0683	-0.0739	0.0240
	Open	-0.240	-0.105	0.368	-0.233	0.0673	-0.117	0.0432
B-17	Precatalyst	-0.249	-0.0920	0.319	-0.240	0.0688	-0.0736	0.0229
	Open	-0.262	-0.107	0.364	-0.235	0.0654	-0.130	0.0452
B-18	Precatalyst	-0.254	-0.0891	0.324	-0.236	0.0639	-0.0748	0.0239
	Open	-0.258	-0.113	0.365	-0.228	0.0610	-0.134	0.0451
B-19	Precatalyst	-0.248	-0.0888	0.318	-0.241	0.0661	-0.0738	0.0222
	Open	-0.248	-0.104	0.362	-0.225	0.0649	-0.123	0.0375
^a Carbon connected to O and N in hemilabile ligand								

Table A-9: Angles in degrees around ruthenium centre in Gr1-type catalysts with hemilabile ligands

Structure		ORuP	ORuCl	OCC (pyr)	ORuN	NRu=C (carbene)	CORu	R ₁ CR ₂
1	Precatalyst	93.23	148.70	112.44	77.97	96.32	112.63	106.78
	Open metallacycle	117.79	123.2649	116.05	NA		142.45	
	Less PCy ₃	NA	144.19	111.59	81.60	104.54	112.70	106.98
2	Precatalyst	94.46	148.17	110.53	77.25	96.89	113.78	108.42
	Open metallacycle	93.30	124.24	113.40			130.65	
	Open	96.53	137.01	110.64	NA	NA		
	Less PCy ₃	NA	144.15	109.93	81.25	104.54	113.27	108.42
3	Precatalyst	94.74	145.92	110.08	77.21	97.12	117.34	
	Open	94.42	136.80	108.78	NA	NA	119.53	
	Open metallacycle	89.85	118.25	111.31			135.776	
4	Precatalyst	94.75	148.38	110.84	77.37	96.21	113.75	107.38
	Open	94.99	135.07	111.908	NA	NA	109.670	110.790
	Open metallacycle	91.034	120.341	131.30	NA	NA		
	Less PCy ₃	NA	143.77	110.11	81.30	106.04	114.25	107.54

5	Precatalyst	94.83	145.90	110.12	77.24	96.60	117.45	109.55
	Open	95.71	136.97	109.59	NA	NA	119.66	111.70
	Open metallacycle	92.10	116.54	105.82	NA	NA		
	Less PCy ₃	NA	142.56	109.16	81.31	105.16	115.52	110.19
6	Precatalyst	95.80	147.26	110.24	77.59	98.20	117.03	111.00
	Closed metallacycle	88.62	81.48	111.04	78.92	97.49	119.52	110.55
	Closed metallacycle to closed precatalyst TS	87.90	85.44	111.68	77.89	102.94	119.00	109.14
	Open	94.42	136.43	11.61	NA	NA	118.023	110.38
	Open metallacycle	89.74	116.22	111.85			133.72	109.10
6	Less PCy ₃	NA	142.55	109.07	81.29	105.24	115.31	111.50
	Metallacycle less PCy ₃ to less PCy ₃ catalyst TS	NA	97.99	110.63	80.59	98.27	118.97	110.60
	Metallacycle less PCy ₃	NA	90.54	110.58	80.32	105.17	120.15	111.52
7	Precatalyst	94.972	146.41	110.83	77.44	96.89	120.13	
	Open	94.730	140.82	109.39	NA	NA	121.76	
	Less PCy ₃	NA		109.55	81.27	100.92	117.96	

8	Precatalyst	97.07	145.10	77.78	95.41	119.90	111.63	
	Closed metallacycle	89.47	83.15	109.94	78.32	98.27	121.20	111.11
	Open metallacycle	91.78	126.05	112.85			141.57	109.38
	Less PCy ₃	NA	109.44	81.10	103.34	118.11	112.40	
9	Precatalyst	93.08	144.45	111.51	77.22	96.56	117.26	106.69
	Open	91.74	138.89	113.51	NA	NA	122.95	
	Open metallacycle	93.31	135.15	108.71			114.82	106.67
9	Less PCy ₃	NA	143.32	110.47	81.34	104.11	115.00	107.16
10	Precatalyst	96.23	149.45	108.72	76.77	96.78	116.40	109.30
	Open	97.86	138.10	109.02	NA	NA	123.77	108.26
	Less PCy ₃	NA	144.54	107.51	80.11	102.72	114.50	110.05
11	Precatalyst	94.68	144.70	110.18	77.40	97.12	120.86	114.15
	Open	95.25	136.69	105.68	NA	NA	123.20	114.93
	Open metallacycle		125.71	103.58				112.87
12	Precatalyst	97.79	147.65	110.41	77.03	96.25	114.91	106.99
	Less PCy ₃	NA	144.12	110.10	80.90	102.18	115.56	107.42
13	Precatalyst	95.69	149.38	109.62	77.62	95.86	115.63	111.22

	Closed metallacycle	90.37	84.84	109.09	77.66	99.33	113.71	109.43
	Open	95.39	149.96	109.615	NA	NA	115.51	
	Less PCy ₃	NA	144.27	108.16	80.81	103.08	113.48	111.73
14	Precatalyst	94.197	145.65	110.13	77.40	97.40	117.61	117.81
	Open	93.426	145.70	110.10	77.33	97.95	117.95	117.92
	Open metallacycle	96.75	117.62	33.27			133.04	115.37
	Less PCy ₃	NA	142.59	108.38	81.07	104.44	115.28	118.02
15	Precatalyst	93.07	145.76	109.44	77.06	99.09	117.76	114.02
	Closed metallacycle	85.86	84.81	110.80	78.73	101.83	118.31	113.67
	Open	96.42	139.66	110.57	NA	NA	120.39	
	Less PCy ₃	NA	141.76	108.72	81.28	105.12	115.05	114.33
16	Precatalyst	94.49	146.59	108.82	77.12	97.31	118.16	114.39
	Closed metallacycle	90.51	83.20	109.44	78.19	100.37	117.22	113.70
	Open	89.54	174.40	106.57	NA	NA	108.53	
	Open metallacycle	94.84	131.47	106.43	NA	NA	122.43	
17	Precatalyst	94.66	143.78	109.90	77.27	96.90	117.14	
	Closed metallacycle	86.97	82.79	109.46	78.18	98.30	116.26	112.72

	Open	95.99	135.42	108.209	NA	NA	112.16	
	Open metallacycle	93.56	112.41	105.18			134.102	115.406
18	Precatalyst	94.79	145.34	108.54	76.59	98.04	117.46	
	Open	95.12	138.01	109.83	NA	NA	120.57	
	Less PCy ₃	NA	142.18	107.89	80.66	105.48	115.35	
19	Precatalyst	94.80	145.02	107.81	76.48	97.97	117.58	
	Open	94.37	137.84	109.03	NA	NA	122.36	
	Open metallacycle	94.14	127.42	102.43	NA	NA	118.55	
20	Precatalyst	94.48	145.35	108.52	76.63	98.14	117.38	
	Open metallacycle	95.44	117.43	108.53	NA	NA	134.75	
21	Precatalyst	93.84	145.38	108.91	76.84	97.73	117.72	
	Less PCy ₃	NA	142.40	108.34	81.04	105.26	115.69	
22	Precatalyst	94.37	145.65	109.12	77.14	98.01	116.42	
	Open	97.28	138.04	107.31	NA	NA	117.40	
	Less PCy ₃	NA	142.40	108.29	81.13	105.26	114.53	
23	Precatalyst	95.28	147.03	111.29	77.91	98.59	115.25	107.58
	Open	95.31	135.69	111.04	NA	NA	111.53	

	Open metallacycle	91.98	119.65	112.43			132.09	108.52
24	Precatalyst	95.87	147.51	109.99	77.29	98.53	118.23	113.00
	Open	96.79	137.70	107.72				
	Less PCy ₃	NA	142.39	108.66	80.99	105.15	116.33	113.58
25	Precatalyst	98.45	145.85	107.49	76.26	99.21	117.25	
	Open	97.62	137.88	106.50				
	Open metallacycle	99.62	120.25	107.18			139.80	
26	Precatalyst	98.13	144.66	107.17	76.39	98.77	117.42	
	Open	96.91	139.52	106.81	NA	NA	118.78	
27	Precatalyst	96.44	147.20	108.79	76.89	99.15	118.25	114.93
29	Precatalyst	96.46	146.97	110.03	76.98	96.65	118.02	111.30
	Closed metallacycle	95.72	133.88	109.88	77.63	98.07	120.09	110.37
29	Open	95.82	141.19	109.13	NA	NA	120.85	
	Open metallacycle	95.01	120.36	108.88			133.45	108.79
	Less PCy ₃	NA	144.67	107.89	80.25	102.15	115.88	110.46
30	Precatalyst	94.91	145.26	108.44	76.63	98.41	117.36	

	Closed metallacycle	89.41	79.14	109.74	78.24		121.66	
	Closed metallacycle to precatalyst TS	87.13	84.12	110.19	78.06	102.86	120.25	
	Open	97.54	137.07	106.79	NA	NA		
	Open metallacycle	93.52	120.75	101.60			136.64	
	Less PCy ₃	NA	141.99	107.87	80.67	105.36	115.42	
	Open metallacycle to open precatalyst TS	85.16	162.66	103.08			139.64	
	Metallacycle less PCy ₃		91.77	107.83	79.05			

Table A-10: Angles in degrees around ruthenium centre in Gr2-type catalysts with hemilabile ligands.

Structure		ORuL	ORuCl	OCC (pyr)	ORuN	NRu=C (carbene)	CORu	R ₁ CR ₂
B-1	Precatalyst	97.33	154.84	109.61	77.21	94.55	115.82	110.88
	Closed metallacycle	92.32	103.60	111.27	79.09	98.289	118.90	111.56
	Open	95.83	151.44	108.39	NA	NA	117.91	107.06
	Open metallacycle	100.71	145.27	112.19	NA	NA	120.48	110.95
	Open metallacycle to open precatalyst TS	100.23	144.21	110.62	NA	NA	119.15	110.47
B-2	Precatalyst	94.04	155.52	110.04	77.301	94.19	116.42	NA
	Closed metallacycle to closed precatalyst TS	89.64	82.61	110.84	78.282	99.90	118.67	NA
	Closed metallacycle	93.26	78.05	110.41	78.595	95.56	120.81	NA
	Open	96.61	144.93	110.57	NA	NA	117.80	NA
	Open metallacycle to open precatalyst TS	93.56	131.64	105.91	NA	NA	120.10	NA
	Open metallacycle	94.88	127.70	105.73	NA	NA	118.67	NA
B-15	Precatalyst	97.17	153.97	109.97	77.21	94.67	115.81	111.00

	Closed metallacycle to closed precatalyst TS	90.43	84.78	110.85	77.22	-	119.13	112.71
	Closed metallacycle	89.67	83.19	110.46	78.64	105.98	118.40	113.06
	Open	88.72	151.73	107.95	NA	NA	118.57	108.76
	Open metallacycle	94.26	128.13	108.21	NA	NA	124.74	108.29
B-16	Precatalyst	92.33	157.95	110.10	77.81	95.59	117.07	116.00
	Closed metallacycle to closed precatalyst TS	87.47	82.87	111.31	78.22	-	118.60	116.35
	Closed metallacycle	90.93	78.06	109.37	79.00	92.80	117.24	115.82
	Open	96.97	145.22	110.03	NA	NA	117.36	113.06
	Open metallacycle	103.37	122.74	107.90	NA	NA	117.85	113.03
B-17	Precatalyst	94.14	152.14	110.94	77.67	92.70	119.70	111.62
	Closed metallacycle to closed precatalyst TS	91.95	87.36	110.99	76.10	-	120.80	108.00
	Closed metallacycle	90.34	84.61	110.84	78.09	107.67	120.63	110.03
	Open metallacycle	98.25	133.89	108.64	NA	NA	122.98	114.73
B-18	Precatalyst	93.52	156.14	106.61	75.97	98.76	116.76	NA

	Closed metallacycle to closed precatalyst TS	93.78	84.69	109.49	76.56	-	120.99	NA
	Closed metallacycle	93.15	79.51	109.52	78.03		121.62	NA
	Open	95.12	143.03	106.00			120.82	NA
	Open metallacycle	97.17	132.99	102.20			126.39	NA
B-19	Precatalyst	93.72	153.32	108.69	76.53	95.73	120.29	NA
	Closed metallacycle to closed precatalyst TS	93.64	82.24	110.28	77.64		119.53	NA
	Closed metallacycle	92.73	79.83	109.76	78.14	104.91	120.34	NA
	Open	100.37	143.77	106.79			113.15	NA
	Open metallacycle	97.83	128.37	106.99			116.27	NA
^a Carbon connected to O and N in hemilabile ligand								

Table A-11: LUMO energies of Grubbs type catalysts in eV and calculated HOMO–LUMO gaps between precatalysts and propene.

Structure Number	Precatalyst	$E_{\text{LUMO}} - E_{\text{HOMO}}^*$	Precatalyst less PCy ₃	$E_{\text{LUMO}} - E_{\text{HOMO}}^*$	Open precatalyst	$E_{\text{LUMO}} - E_{\text{HOMO}}^*$
1			-2.905	3.044		
2	-2.548	3.401	-2.883	3.066		
3	-2.519	3.430			-2.628	3.321
4	-2.541	3.408	-2.875	3.074	-2.352	3.597
5	-2.509	3.440	-2.868	3.081	-2.628	3.321
6	-2.513	3.436	-2.871	3.078	-2.567	3.382
7	-2.614	3.335	-2.809	3.140		
8	-2.495	3.454	-2.742	3.207		
9	-2.527	3.422	-2.864	3.085	-2.588	3.361
10	-2.515	3.434	-2.762	3.187	-2.614	3.335
11	-2.440	3.509			-2.637	3.312
12	-2.516	3.433	-2.746	3.203		
13	-2.544	3.405	-2.827	3.122		
14	-2.533	3.416	-2.840	3.109		
15	-2.527	3.422	-2.887	3.062	-2.707	3.242
16	-2.543	3.406				
17	-2.506	3.443				
18	-2.476	3.473	-2.839	3.110	-2.599	3.350
19	-2.454	3.495			-2.589	3.360
20	-2.463	3.486				
21	-2.497	3.452	-2.849	3.100		
22	-2.503	3.446	-2.869	3.080	-2.679	3.270
23	-2.525	3.424			-2.658	3.291

24	-2.503	3.446	-2.841	3.108		
25	-2.505	3.444				
26	-2.473	3.476			-2.626	3.323
27	-2.528	3.421				
29	-2.525	3.424	-2.756	3.193	-2.637	3.312
30	-2.490	3.459	-2.838	3.111	-2.694	3.255
B-1	-2.433	3.516	NA	NA	-2.565	3.384
B-2	-2.415	3.534	NA	NA	-2.487	3.462
B-15	-2.375	3.574	NA	NA	-2.604	3.345
B-16	-2.472	3.477	NA	NA	-2.550	3.399
B-17	-2.450	3.499	NA	NA	-2.575	3.374
B-18	-2.436	3.513	NA	NA	-2.604	3.345
B-19	-2.409	3.540	NA	NA	-2.534	3.415
E _{HOMO} * for propene (substrate in this study) is 5.949 eV						

Table A-12: HOMO-LUMO gaps in electron volts for precatalysts

Structure Number	Precatalyst $E_{\text{LUMO}} - E_{\text{HOMO}}$	Precatalyst less PCy₃ $E_{\text{LUMO}} - E_{\text{HOMO}}$	Open precatalyst $E_{\text{LUMO}} - E_{\text{HOMO}}$
1	-	2.108	-
2	1.703	2.019	-
3	1.726	-	1.892
4	1.702	2.123	2.067
5	1.737	2.116	1.877
6	1.737	2.110	1.918
7	1.811	2.1611	-
8	1.724	2.188	-
9	1.768	2.139	1.91
10	1.628	2.091	1.763
11	1.844	-	1.834
12	1.715	2.139	-
13	1.714	2.108	-
14	1.744	2.116	-
15	1.761	2.118	1.880
16	1.805	-	-
17	1.818	-	-
18	1.773	2.098	1.907
19	1.781	-	1.911
20	1.798	-	-
21	1.779	2.112	-
22	1.768	2.089	1.859
23	1.746	-	2.004

24	1.727	2.112	-
25	1.722	-	-
26	1.759	-	1.857
27	1.704	-	-
29	1.669	2.096	1.901
B-1	1.529	NA	1.887
B-2	1.456	NA	1.792
B-15	1.682	NA	1.819
B-16	1.497	NA	1.701
B-17	1.544	NA	1.730
B-18	1.350	NA	1.731
B-19	1.519	NA	1.786
“-“ optimised structures were not obtained			

